Application of the European Basic Safety Standards Directive in Underground Mines: A Comprehensive Radioecology Study in a Hungarian Manganese Mine

DOI:10.18136/PE.2018.696

AUTHOR

AMIN SHAHROKHI

DOCTORAL SCHOOL OF CHEMISTRY AND ENVIRONMENTAL SCIENCES

SUPERVISOR

DR. TIBOR KOVÁCS (Ph.D.)

INSTITUTE OF RADIOCHEMISTRY AND RADIOECOLOGY

UNIVERSITY OF PANNONIA

VESZPRÉM

2018

Application of the European Basic Safety Standards Directive in Underground Mines: A Comprehensive Radioecology Study in a Hungarian Manganese Mine

Thesis for obtaining a PhD degree
in the Doctoral School of Chemistry and Environmental Sciences
of the University of Pannonia

Written by:

Amin Shahrokhi

Supervisor: Dr. Tibor Kovács (Ph.D.)

I propose for acceptance (yes / no) ……..….
(signature)

The candidate has achieved …… % at the comprehensive exam,

I propose the thesis for acceptance as the reviewer:

Name of reviewer: …..... yes / no
…….
(signature)

Name of reviewer: …..... yes / no
…….
(signature)

The candidate has achieved …..... % at the public discussion.

Veszprém, …….
Chairman of the Committee

Labelling of the PhD diploma ….....

……
President of the UCDH

DEDICATION

Thanks to my loving parents, who guided me to where I am today, who taught me that the best kind of knowledge to have is that which is learned for its own sake, who taught me the way of life and who being my guiding light in the darkness

This thesis is dedicated to my parents for their love, endless support and encouragement

تقدیم به دو فرشته الهی، پدر و مادرم،
که زحماتشان با هیچ واژه ای قابل قدردانی نیست

Amin Shahrokhi

ACKNOWLEDGEMENTS

I would like to express my special appreciation and thanks to my enthusiastic supervisor, Dr. Tibor Kovács, who without his patient guidance, teaching, insightful criticisms and insightful ideas, this dissertation could not have been completed

Thanks to my committee chairmen for their countless hours of reflecting, reading, and most of all patience throughout the entire defence process

Thanks to Dr. József Kaizer, Dr. Janja Vaupotic, Dr. Zoltán Németh, Dr. Edit Tóth - Bodrogi and Dr. Ákos Horváth, the comprehensive exam committee members for their patience time and consideration during exam time

Thanks to Dr. Norbert Kávási, and Dr. Begy Róbert Csaba for agreeing to review and be the references of the current thesis

Thanks to Dr. Miklós Hegedűs for the useful comments as a pre-reviewer of the current thesis, and thanks to all my colleagues in the Institute of Radiochemistry and Radioecology at the University of Pannonia for their help

Thanks to Dr. Tamás Vigh as consultant of the current thesis

TABLE OF CONTENTS

LIST OF FIGURES

LIST OF TABLES

ABSTRACT

The author carried out a comprehensive radioecology study in an underground manganese mine in Hungary, regarding recent changes on European Basic Safety Standard and the new introduced radon dose conversion factor by International Commission on Radiological Protection. The annual integrated averages radon concentration in the whole mine area measured using CR-39 based detector (NRPB) as 824±42, 874±45 and 1050±85 $Bq \cdot m^{-3}$ for years 2014, 2015 and 2016, respectively; Radon concentration during working hours using AlphaGUARD and TESLA measured between 450±65 and 650±83 $Bq \cdot m^{-3}$. The author measured the average dissolved radon concentration in the mine water samples as 3±0.4 $Bq \cdot L^{-1}$, regarding to the low contact surface of water and forced ventilation capacity, this route of entering radon to the mine air is negligible. The areal radon exhalation from mine walls at 5 different galleries using based CR-39 can method (radon accumulation chamber) measured in the range of 0.7±0.1 and 1.5±0.2 $mBq \cdot s^{-1} \cdot m^{-2}$. Using gamma spectrometry (HPGe detector) the black shale, underlayer black shale and carbonate ore show high values of Ra-226 compared to other samples, additionally the highest exhalation rate found from these three rock types. The author found that exactly after mining activity, radon increase dramatically with an average about 5900±420 $Bq \cdot m^{-3}$; Therefore, the ore fragmented during the course of mining operations stated as the main route of entering of radon into the mine air. Using the new developed mitigation system, radon concentration successfully reduced on that specific area to below 300 $Bq \cdot m^{-3}$ with an average of 250±41 $Bq \cdot m^{-3}$. During working hours, the annual average unattached and equilibrium factor measured using SARAD EQF3220 and Pylon WLx, at workplaces where selected miners for dosimetry were mainly worked, calculated between 0.15±0.04, 0.3±0.05 (average of 0.21±0.04) as unattached factor, and between 0.35±0.1 and 0.55±0.2 (average of 0.42±0.1) for equilibrium factor. The annual exposures to radon measured using personal dosimetry between 247±31 and 277±36 $Bq \cdot m^{-3}$ with an average of 261±33 $Bq \cdot m^{-3}$ for 10 miners; The dose conversion factor (DCF) calculated based on the field measurements between 16±9 and 25±10 $mSv \cdot WLM^{-1}$ (average of 20±9 $mSv \cdot WLM^{-1}$). Then, the calculated DCF applied to estimate the effective dose in the range of 5.6±0.7 to 7.6±0.9 $mSv \cdot y^{-1}$ (geometric mean: 6.7±0.9 $mSv \cdot y^{-1}$). The author found in the radioecology point of view, the manganese mining residue can be reused in building material industries (brick production, ceramic industry).

KIVONAT

A szerző egy átfogó radiológiai felmérést végzett el az úrkúti mangánbányában a radonra vonatkozó új nemzetközi ajánlások (EU irányelv – új referenciaszint, ICRP – dózisbecslési paraméterek) miatt. 2014 és 2016 között CR-39 nyomdetektorokat alkalmazva meghatározta a bányában az éves radon koncentrációt, amely rendre 824±42, 874±45 és 1050±85 $Bq \cdot m^{-3}$ volt. Folyamatos mérési módszerrel (ALPHAGuard, TESLA) meghatározta a munkaidőben mérhető átlagos radon koncentrációt (450±65 – 650±83 $Bq \cdot m^{-3}$). A radon lehetséges származási helyét keresve megvizsgálta a vízben oldott radon értékét, amely átlagosan 3±0,4 $Bq \cdot L^{-1}$-nek adódott. Ezt, valamint a kicsi érintkezési felületet a víz és levegő között, valamint a mesterséges szellőztetés mértékét megállapította, hogy a vízből a levegőbe jutó radon mennyisége elhanyagolható. Passzív mérési módszert alkalmazva meghatározta 5 különböző vágatban a bányafalból történő radon exhalációt, amelynek értékei 0,7±0,1 és 1,5±0,2 $mBq \cdot s^{-1} \cdot m^{-2}$ közé estek. A bánya geológiai struktúráját alkotó kőzettípusokat gamma-spektrometriával vizsgálta. Az eredmények alapján megállapította, hogy a fekete pala, fekürétegi fekete pala és karbonátos érc, amelyek a bányászott érc fő alkotói, nagyobb mennyiségben tartalmaznak természetes radioknuklidokat, összehasonlítva a meddőkőzetekkel. Emellett a radon exhaláció értékek is magasabbak. A szerző meghatározta a radon koncentráció értékeket az aktív bányászati tevékenységeket követően a levegőben és jelentősen megnövekedett értékeket kapott (5900±420 $Bq \cdot m^{-3}$). Ezeket figyelembe véve megállapította, hogy a bányalevegőben lévő radon fő bejutási útvonalai a frissen hajtott vágatok. A szerző kidolgozott egy új radon szint csökkentő beavatkozási módszert, amelyet alkalmazva a koncentráció sikeresen lecsökkenthető 300 $Bq \cdot m^{-3}$ alá (átlagosan 250±41 $Bq \cdot m^{-3}$). A szerző meghatározta a bányalégtérben a tapadt és nem tapadt frakció arányát (0,15±0,04 – 0,3±0,05) SARAD EQF3220 monitorral és az egyensúlyi tényezőt (0,35±0,1 – 0,55±0,2) a Pylon WLx alkalmazásával. CR-39 alapú személyi dozimeterrel meghatározta 10 bányász esetében az éves radonexpozíciót (247±31 és 277±36 $Bq \cdot m^{-3}$). A terepi mérések alapján a szerző meghatározta a dóziskonverziós tényezőt (16±9 és 25±10 $mSv \cdot WLM^{-1}$). A saját eredményei alapján kapott paraméterekkel elvégezte a dózisbecslést, ahol az éves effektív dózis 5,6±0,7 és 7,6±0,9 $mSv \cdot év^{-1}$ közé esett. A szerző megvizsgálta a bányában keletkező meddő újrafelhasználásnak lehetőségét radioökológiai szempontból. Megállapította, hogy a visszamaradt agyag felhasználható az építőanyag gyártásban (pl.: téglagyártás).

РЕЗЮМЕ

Автором было проведено комплексное радиоэкологическое исследование подземных разрабатываемых месторождений марганца в Венгрии с учетом последних изменений Европейских Основных Стандартов по Безопасности и недавно введенных коэффициентов перерасчета дозы радона. Ежегодная интегрированная средняя концентрация радона в области месторождения, измеренная с помощью детектора на основе CR-39 (NRPB), составляла 824±42, 874±45 и 1050±85 Бк·м$^{-3}$ в 2014, 2015 и 2016 г соответственно; концентрация радона во время рабочего времени, измеренная AlphaGUARD и TESLA TSR2 равнялась 450±65 и 650±83 Бк·м$^{-3}$. В образцах шахтной воды автором была измерена концентрация растворенного радона, она составила 3±0.4 Бк·л$^{-1}$, вследствие небольшой поверхности соприкосновения и мощности искусственной вентиляции, влияние данного источника на общий уровень радона в воздухе шахты является незначительным. Поверхностное выделение радона шахтными стенами, измеренное в 5-ти галереях методом на основе CR-39 (камера накопления радона), колебалось в диапазоне от 0,7±0.1 до 1,5±0.2 мБк·с$^{-1}$·м$^{-2}$. Гамма-спектрометрия (детектор ОЧГ) темных сланцев, подстилающих темных сланцев и углекислой руды показала высокие значения Ra-226 в этих трех типах пород по сравнению с другими образцами, а также повышенный уровень выделения и эманации. Автор обнаружил, что именно после горной деятельности уровень радона резко возрастает и его среднее значение достигает 5900±420 Бк·м$^{-3}$; поэтому руда, фрагментированная в ходе горных работ указывается как основной источник радона в воздухе шахты. После использования новой разработанной системы снижения концентрация радона на этой территории успешно снизилась и не превышала 300 Бк·м$^{-3}$, средний показатель составлял 250±41 Бк·м$^{-3}$. В рабочее время средний свободный и равновесный коэффициент измерялся с использованием SARAD EQF3220 и Pylon WLx на рабочих местах, где работали отдельные шахтеры для личной дозиметрии, показатели составили 0,15±0,04 – 0,3±0,05 (средний 0,2±0,04) и 0,35±0.1 - 0,55±0.1 (средний 0,2±0,1) соответственно. Ежегодная экспозиционная доза радона, измеренная при личной дозиметрии, составляла от 247±31 до 277±36 Бк·м$^{-3}$, среднее значение - 261±33 Бк·м$^{-3}$ для 10 шахтеров; Коэффициент перерасчета дозы составлял 16±9 - 25±10 мЗв·WLM^{-1}, со средним значением 20±9 мЗв·WLM^{-1}. Эффективная доза рассчитывался в диапазоне от 5,6±0,7 до 7,6±0,9 мЗв·г$^{-1}$ (среднее геометрическое 6,7±0,9 мЗв·г$^{-1}$). Рассматривая результаты с точки зрения радиоэкологии, автор полагает, что остаточные продукты добычи марганца могут быть повторно использованы в производстве строительных материалов (кирпич, керамика и т. д.).

INTRODUCTION

1.1. Basic of Radiation

Radiation is a fact of life, where different radionuclides are inhaled or ingested by the human from the air, food, and water daily. Radiation is often categorized as either ionizing or non-ionizing depending on the energy of the radiated particles; Ionizing radiation is radiation that carries enough energy to liberate electrons from atoms or molecules (enough energy to break chemical bonds), thereby ionizing them. Examples of this type of radiation are cosmic rays, X rays and the radiation emitted from radioactive materials. Non-ionizing is a form of radiation that does not carry enough energy to ionize atoms or molecules (it is located at the low end of the electromagnetic spectrum), including electric and magnetic fields, radio waves, microwaves, infrared, ultraviolet, and visible radiation.

People are constantly exposed to ionizing radiations, which arise from both naturally occurring sources, also called background radiation (e.g. cosmic radiation, solar radiation, internal radiation and radon) and sources with an artificial origin, also called man-made sources (e.g. medical and nuclear medicine; military purposes; consumer products, nuclear power plants; human error and unplanned events such as power plant accidents) on a daily basis.

Exposure to ionizing radiation is divided into three type of exposure situations: 1- Existing exposure situations, which happens when the sources of radiation exist when a decision on control has to be taken; 2- Planned exposure situations, resulting from a planned operation or exposure from a source under a controlled activity where radiological protection can be planned in advance, and exposures can be reasonably predicted; 3- Emergency exposure situations, it happens when exposure arises from an unexpected event and an accident, when control of a source is lost (Unexpected situations that may require urgent protective actions). However, exposure to radiation is categories by itself depending on exposure groups into occupational, public, and medical (International Atomic Energy Agency, 2014; ICRP, 2007).

Exposure to Ionizing radiation can result both cancer and non-cancer health effects on human, each of which differs greatly in the shape of the dose–response curve, latency, persistency, recurrence, curability, fatality and impact on quality of life. For dose limitation purposes, the International Commission on Radiological Protection (ICRP) has classified such diverse effects into tissue reactions known as non-stochastic/deterministic and stochastic effects (cancer/heritable effects). Reducing the risks of stochastic effects needs to

set an effective dose limits that it is based on the detriment-adjusted nominal risk coefficients, assuming a linear non-threshold (LNT) dose response and a dose and dose rate effectiveness factor (DDREF) of 2; However, equivalent dose limits aim to avoid tissue reactions (vision-impairing cataracts and cosmetically unacceptable non-cancer skin changes) and are based on a threshold dose (Nobuyuki & Yuki, 2014). In other words, deterministic effects have a threshold of dose and severity of the effect is dose-related, while, stochastic effects are a probability of an effect increases with dose, does not have a threshold of dose and severity of the effect does not related to dose.

The health risks of exposure to ionizing radiation are well known; Interacting a charged particle with a materials' atom and losing energy causing cellular tissue to become ionized or excited and produces charged water molecules. In other words, exposure to ionizing radiation may produce highly reactive chemically free radicals (e.g. hydroxyl radical), break chemical bonds and damage DNA as result of being directly ionized, or via interacting with free hydroxyl radicals; Figure 1. shows a schematic image of radiation damage to living cells. (International Atomic Energy Agency, 2004).

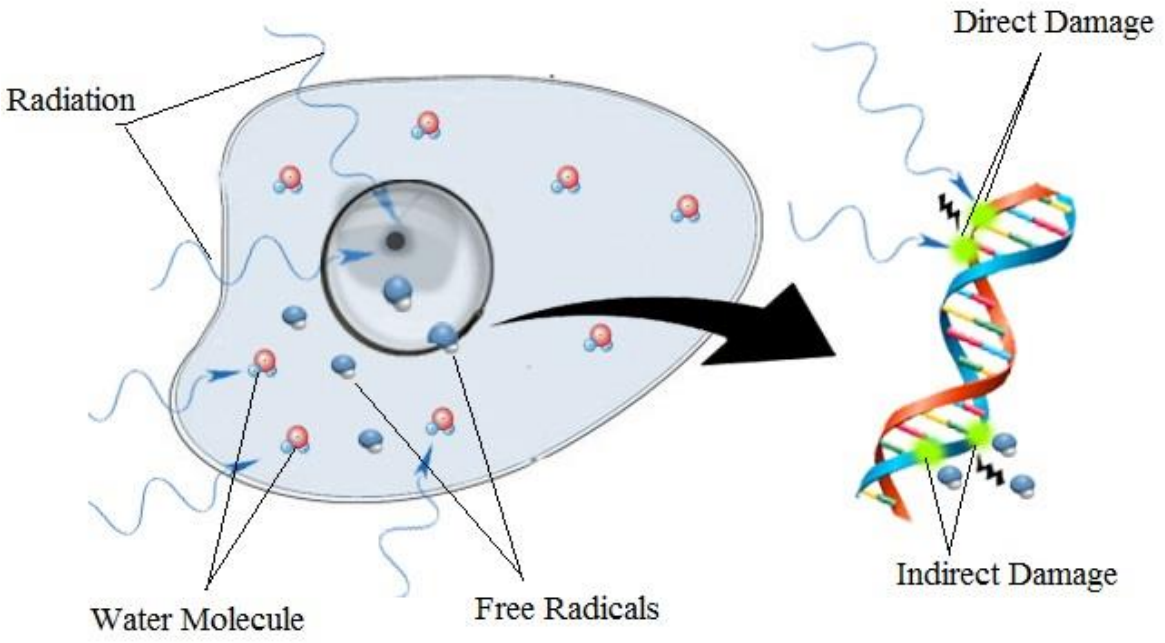

Figure 1- Schematic image of radiation damage to cell

Approximately 80% of human radiation exposure comes from naturally occurring sources, while the remaining 20% branches from man-made sources, while radon is the most significant source of natural radiation exposure to humans; Figure 2. Shows sources and distribution of average radiation exposure to the world's population (UNSCEAR, 2010).

Depending on the type, energy of ionizing radiation and exposure time, the biological effects of radiation may vary from case to case. The risk of biological harm from radiation is the dose that human organs and tissues receive and known as an absorbed radiation dose called "Sievert" (Sv). Radiation toxicity involves exposure to ionizing radiation, most commonly in the alpha, beta and gamma which causes damage at the chromosomal and cellular levels.

On average, human radiation exposure due to all-natural sources amounts to about 2.4 mSv a year, however this amount might be changed to over than 4.2 according to new introduced ICRP radon dose conversion factor (but there is no any valid reference for this value) and it can vary depending on the geographical location and human activity divided into general population and workers.

In buildings (such as dwellings, schools, offices etc.) in addition to the radon from ground, the building materials (mainly bricks, types of cement, gypsum etc.) are a source of radiation exposure by releasing radioactive elements (Rn-222 and Rn-220, decays of radium and thorium) into the air;

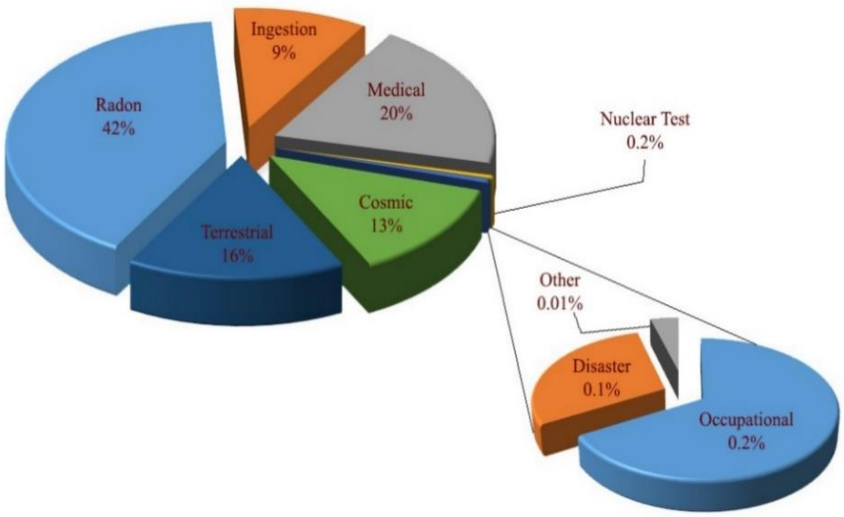

Figure 2- Radiation sources and distribution of average exposure to the population

In workplaces, the exposure source can be divided into natural sources and man-made sources. In underground workplaces (such as mines, caves), addition to the background radiation, workers can encounter both external (gamma radiation from uranium and thorium series, and potassium in the ground) and internal (radon and thoron exhalates from the ground and their decay products) exposure to radiation (Australian Uranium Association and Australia. Department of Resources, Energy and Tourism, 2009; International Atomic Energy Agency, 2014).

External doses occur when the body is exposed to radioactive material outside the body; this is primarily a concern for gamma radiation. Internal doses occur from exposure to radioactive material taken into the body by inhalation or ingestion; this is a main concern for radon and its alpha emitted decay products at workplaces.

The gamma radiation originates mainly from a few decay products of U-238 and Th-232, particularly Pb-214, Bi-214, Ac-228, and Tl-208. Gamma rays are penetrating electromagnetic radiation travelling at great speed. Gamma rays do not have a charge or mass; they are a highly penetrating form of radiation that can cause secondary (indirect) ionizations when their energy is transferred to atomic particles such as electrons. In most exposure scenarios related to underground mining (especially uranium mining and processing), gamma rays may be a concern, the same as radon would be a radiation hazard.

Gamma radiation is the second source of indoor radiation exposure from building materials. It has the potential to increase the risk of cancer by varying degrees for most tissues and organs, however, gamma radiation has a much lower ionizing ability when compared to that of an alpha particle. During mining and processing operations, gamma emitted radionuclides in the ground, waste or tailings can produce a significant gamma radiation hazard in mines, near waste areas or tailings. Additionally, using mining residue – e.g. fly ash, phospho-gypsum, phosphorus slag, tin slag, copper slag, red mud (residue from aluminium production), clay (residue from mining such as manganese mining), residue from steel production – in industries to produce building materials can increase both external and internal indoor radiation exposure from building materials (Kovács, et al., 2017; Council of the European Union, 2014).

On the other hand, Radon with symbol "Rn" and atomic number 86 is a colourless, odourless, chemically inert, naturally occurring radioactive gas fairly soluble in water and organic solvents, and is a decay product of radioactive elements, such as uranium, which are

found in in soil and rock. Rn-220 (known as Thoron) and Rn-222 (known as Radon) are the most important isotopes of radon in view of radiation protection, as only these two isotopes of radon are found in significant concentrations in the environment. "Radon" is used to refer to Rn-222 (a decay product of Ra-226, Figure 3) and its short-lived decay products and, when focuses are specifically on the gas, it is referred to as Rn-222. Radon, as the heaviest naturally occurring gaseous element with a half-life of 3.8, is the most stable isotope among other isotopes of this family and it is a major contributor to the ionizing radiation dose received by the general population from natural origin sources. As radon is chemically inert, it has been used as a tracer in different areas of science, such as environmental studies. Rn-222 exhalates from rocks, soils and building materials (as main sources), and accumulates in enclosed areas e.g. underground mines or buildings. Soil gas infiltration and building materials (mainly productions that use mining residue) are recognized as the most important sources of residential radon; however, water can be another source of indoor radon. (WHO, 2009).

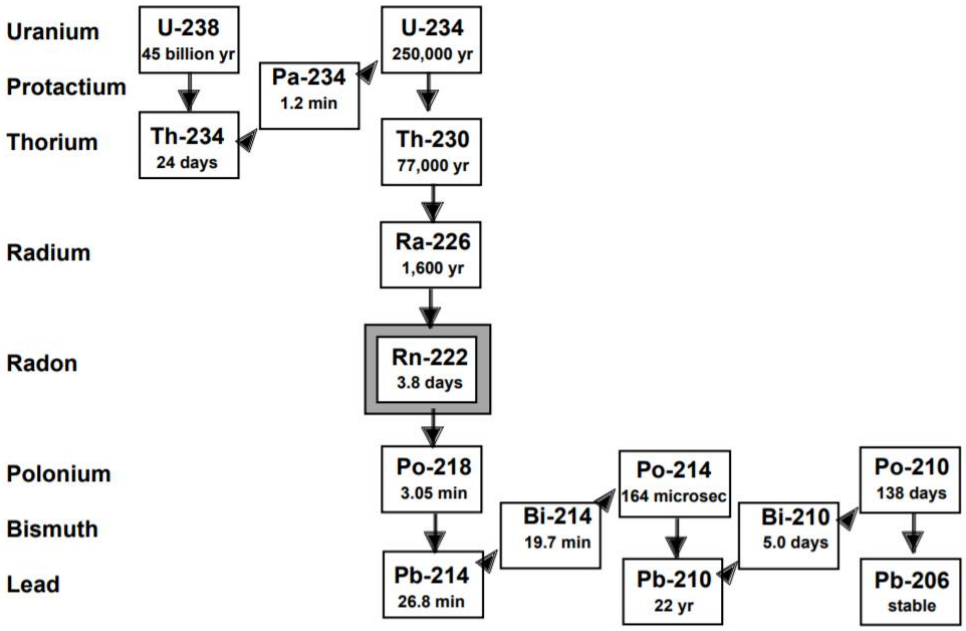

Figure 3- The Uranium decay chain focusing on radon

Radon is a decay product of Ra-226, which is belong to the U-238 decay chain, therefore it seems to be obvious to correlate the ground/soil gas radon concentration with the activity concentrations of uranium and/or radium in the soil. Rnn-222 is the only gas formed during this series, thus, allowing it to move out of the rocks and soils where uranium/radium is typically found into the air.

1.2. Radon & Health Risk

Radon was classified as a human carcinogen by the International Agency for Research on Cancer in 1988 (IARC 1988). Radon is a lung cancer-causing gas, according to the World Health Organization in 2009, with the proportion of related radon-exposed, the lung cancers estimated between 3% and 14%, depending on the concentration of exposure, period of exposure and other committed risk factors; However, radon is not harmful by itself, as its short-lived decay products are responsible for most of the hazard.

Rn-222 is chemically inert, therefore almost all inhaled radon is rapidly exhaled, but short-lived decay products (Po-218 and Po-214) immediately deposit onto the tissue of the lungs, thereby densely ionizing alpha particles emitted by deposited decay products and interacting with biological tissue causing cellular tissue and DNA damage. (Lecomte, et al., 2014; U.S. Environmental Protection Agency, 2003). The atoms of radon short-lived decay products (either radon decay products generated during breathing or inhaled attached and unattached progenies from air) deposit in the bronchial tissue and continue to irradiate the lung tissues for prolonged periods. After alpha decay of radon, the newly generated short-lived radon decay products naturally tend to attach themselves to aerosol particles in the air e.g. dust, water molecules, etc.; This process is known as the "attachment process" and the decayed product after attachment process is referred to as an "attached progeny", if generated short-lived radon decay products remain as a cluster and are not joined with any existing aerosols, they are called "unattached progenies" and described by a parameter known as the unattached fraction; for furthermore details refer to section 1.4. at the current study and Figure 6.

The theory of cancer generally can be expressed as an uncontrolled growth of abnormal cells that have DNA damage, since even a single alpha particle can cause a major genetic damage to a cell via direct or indirect way, and exposure to radon at any level can increase significantly the risk of lung cancer (UNSCEAR, 2012). Regarding to the recent studies, it was indicated that the risk of lung cancer may increase by raising the exposure radon level, i.e. WHO stated that per each 100 $Bq \cdot m^{-3}$ increase radon concentration (on average, over time) the chance of developing lung cancer can increase by 16% (WHO, 2009); Hence, no advised level may exist to assure radon does not have the potential to cause lung cancer below a specific recommended level; For further details refer to Tables 2. & 5. and cited published paper.

Radon-exposure is stated as the second most frequently reported cause of lung cancer, after tobacco smoke; Radon is an inevitable risk factor, thus it may significantly increase the risk of lung cancer among smokers (Tirmarche, et al., 2010); In the other words, in case of lung cancer risk, exposure to radon is inevitable, but smoking is an optional and avoidable factor, meaning "smoking may significantly increasing the risk of lung cancer next to the exposure radon level".

Figure 4. shows a relative risk of lung cancer versus long-term average residential radon concentration based on a European pooling study (Darby, et al., 2005).

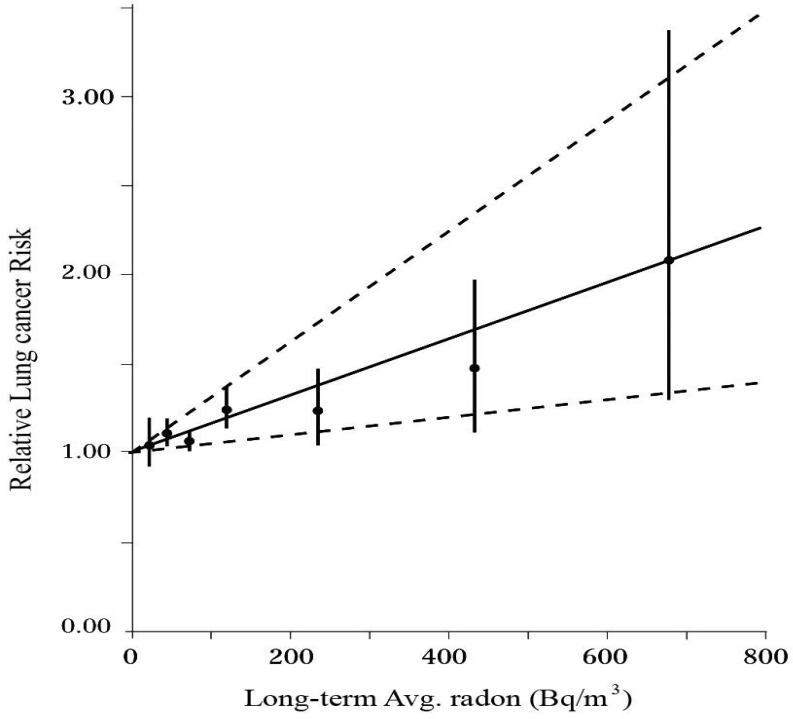

Figure 4- Correlation between radon exposure level and lung cancer risk

From a public health perspective view, low and moderate radon concentrations are the most likely cause of lung cancers, rather than high radon concentrations, as generally fewer people are exposed to high radon concentrations, and exposure to high radon concentration for a long period can generally occur in case of occupational working in caves, underground mines, oil industries etc. To support this fact, a study had been done and indicated an inverse relationship between radon exposure level and the lung cancer rate; It was found that by exposing to moderate cumulative radon, lung cancer rates rose among the miners while it decreased again at high cumulative exposures. It was found that after exclusion of cumulative exposures above 3200 WLM, the lung cancer rate increased

approximately linear with increasing cumulative radon exposure. It could not be by chance as the size of the increment per unit increase in exposure varied by more than a factor of ten between the studies (BEIR, 1999; WHO, 2009). However, other factors also need to be considered for the increase of lung cancer rates, i.e. duration of exposure, breathing behaviour, size of the areole, distribution etc.

It was also found that not only is there an increase in the lung cancer death rate per WLM varied with time since exposure (as the most deaths happened in the period 5-14 years after exposure), but also varied with the exposed person's age, as the death rate due to lung cancer was higher at younger ages (BEIR, 1999; WHO, 2009).

Table 1. shows some risk factor and their contribution towards causing lung cancer among the general population, who are usually exposed to indoor radon (dwelling, office or enclosed publication area) mainly from building materials and the ground (Sethi, et al., 2012).

Table 1- Lung cancer risk factors and their contribution towards causing lung cancer

Risk Factor	Contribution	Lung cancer Relative Risk
Smoke (Tobacco)	92% (Men) 78% (Women)	40
Radon	3% - 15%	2 - 10
Second-hand Smoke	2% - 3%	2
Genetic	1% - 3%	1 - 4

Studies using different modelling systems and risk factors were indicated that radon may cause 3 to 14% of all lung cancers in a single country, all depending on the risk factors such as smoke consumption, as well as the average radon concentration in a country. (World Health Organization, 2009). However, genetics (race) is not widely yet used as a risk factor in epidemiological studies, though it may count as an important risk factor. For example, if we look at Table 2, where the results of two different geographic studies are summarized, the relative increasing lung cancer risk per each 100 $Bq \cdot m^{-3}$ increase is not the same nor as in internal or international group, i.e. the risk between genders in both groups is not equal,

and this difference can even be seen in the same gender of different group; However, to state this idea, it is required to know if all conditions were the same at the time of studying between two groups.

It should be taken into consideration that risk of lung cancer due to radon is different between occupational (such as miners) and public exposure, as miners are generally also exposed to other lung carcinogens, i.e. aerosols, silica, Arsenic, mycotoxins and other hazardous chemical compounds exist on the ore. In addition to this is radon, which is a source of uncertainty in modelling and estimating lung cancer risk not only from the occupational radiation protection point of view but also with applying the epidemiologic studies of miners to the general population (Council National Research, 1999).

Table 2. shows summarized results of some international pooling studies about the risks of lung cancer from indoor radon (Krewski, et al., 2005; Krewski, et al., 2006; Darby, et al., 2005; Darby, et al., 2006).

There is no evidence to show that exposure to radon may have other side effects, such as other forms of cancer, respiratory diseases, or general physical symptoms (Darby, et al., 1995), however, some studies conducted a radon exposure causing diseases other than lung cancer; Harley & Robbins based on An epidemiologic study in Denmark from 1968 to 1994 found a weak, but statistically significant link between radon exposure and acute childhood lymphoblastic leukaemia (Harley & Robbins, 2009); Another study in the USA indicated that exposure to radon could be a significant risk factor for pancreatic cancer in several different American ethnic (Reddy & Bhutani, 2009). Additionally, according to Smith et al., and Řeřicha et al., further studies are required to find out if there is any relation between radon and leukaemia (Řeřicha, et al., 2006; Smith, et al., 2007).

Table 2- Rising the lung cancer relative to an increase of radon every 100 Bq·m^{-3}

based on the European and North American pooling studies (adopted from WHO, 2009;)

Study Based on the European Population				**Study Based on the American Population**			
Risk of Lung Cancer Risk Increase (%) (95% CI*)							
Men (Min, Max)		Women (Min, Max)		Men (Min, Max)		Women (Min, Max)	
11 (4, 21)		3 (-4, 14)		3 (-4, 24)		19 (2, 46)	
Age at lung cancer occurrence (years)							
Under 55	55 to 65	65+		Under 60	60 to 64	65 to 69	70 to 74	75+
~0 (0, 20)	14 (3, 31)	7 (1, 16)		2 (<0, 35)	80 (13, 257)	2 (-5, 28)	33 (1, 102)	-2 (-10, 30)
Smoking Habitat							
Current Smoker	Ex-smoker	Non-smoker	Other	Cigarettes		Smoker	
7 (-1, 22)	8 (0, 21)	11 (0, 28)	8 (-3, 56)	10 (-9, 42)		10 (-2, 33)	
Overlay: increased Percentage based on each 100 Bq·m^{-3} increase							
8 (3, 16)				**11 (0, 28)**			

*CI = confidence interval, p-values less than 0.05 denote statistical significance

1.3. Radon & Underground Miners

As discussed previously, radon as a radioactive gas is an inert gas that can migrate from soils and rocks and accumulate in enclosed areas (i.e. underground mines and caves) however, radon as itself is not a concern; its short-lived alpha emitter decay products are responsible for human tissue damage, as it was found that in the miners, about 40% of all lung cancer deaths may be due to radon progeny exposure, 70% of lung cancer deaths in never-smokers, and 39% of lung cancer deaths in smokers (Lubin, et al., 1995).

Radon presented in the mine atmosphere is almost always prevalent and relatively unavoidable in underground mines, where the source of radon can come from trace concentrations of uranium presents on the ground (ore, host rock, organic material, and soils) or through the exhalation from radon/radium contained groundwater. Therefore, the radon concentration in an underground mine environment mainly depends on emissions of radon from the ore body, broken ore, host rock and underground water.

Radon was the first occupational natural environmental carcinogen gas that identified among miners. Lung cancer has been seen to occur in uranium and underground miners for many years. In the last decades, several epidemiological studies have been done to determine the potential risk factors for underground excavation workers, for the development of irreversible occupational respiratory diseases, such as silicosis and lung cancer (Anjos, et al., 2010). Several studies indicated that exposures to the short-lived progeny of radon significantly increases the risk of lung cancer among miners in uranium and other underground mines (Editorials, 1932; Tomásek, et al., 1994; Saccomanno, et al., 1996; Kreuzer, et al., 2010).

For the first time, it was in the sixteenth century that some signs of increased mortality from respiratory disease among certain groups of underground miners in central Europe were seen, while nobody had any idea and information about the disease and causing reason, nor any evidence of a link between disease and radon concentration in the mines. Finally, in the nineteenth century, it was understood that the disease was, in fact, lung cancer. Radon was introduced as the first suspected primary cause of these cancers in radon-exposed miners, following studies radon's causal role in lung cancer became firmly established in the 1950s, further details about the history of radon, lung cancer and underground miners history can be found in the already published paper elsewhere (BEIR, 1999).

Table 3. shows the summarised results of some studies about the epidemiologic, miners' exposure and the lung cancer rates for different mines (U.S. Environmental Protection Agency, 2003).

Table 3 - Lung cancer rate among the miners in terms of radon exposure

Location	**Mine**	**Miner (Person)**	**Rn Exposure $Bq \cdot h^{-1} \cdot m^{-3}$ (EEC)**	**Lung cancer (Person)**
China	Tin	13,649	182	936
Czechoslovakia	Uranium	4,320	125	701
Colorado Plateau	Uranium	3,347	369	334
Ontario	Uranium	21,346	20	285
Newfoundland	Fluorspar	1,751	247	112
Sweden	Iron	1,294	52	79
New Mexico	Uranium	3,457	71	68
Canada	Uranium	6,895	13	56
Canada	Uranium	1,420	155	39
Australia	Uranium	1,457	5	31
France	Uranium	1,769	38	45

Cohort design has generally been used for modelling and estimation of lung cancer rates related to radon exposure among miners; In cohort design, all miners in a mine are identified during a particular period. Therefore, it is easier to follow up miners over time, regardless of whether they remain employed in the mine or not. The vital status of each miner is established at the end of the follow-up period. If a miner has died, related information i.e. date and reason of death, average radon exposure, age, smoking habitat, medical histories etc. are collected, including the previous primary collected data, and the death rate from lung cancer based on recorded information is calculated. However, there is a problem that the quality of the exposure assessment was low and exposure to radon was usually estimated retrospectively e.g. first years of mining when the exposures were highest, and no radon measurements were performed (WHO, 2009). In the first several studies, simply the influence of smoking on developing lung cancer was not considered as a risk factor due to a lack of evidence, therefore, miners' smoking habits were not questioned when the cohort was set up.

As it shows in Table 5. (EPA, 2016), lung cancer risk for smokers is increased two times greater in each 100 $Bq \cdot m^{-3}$ radon concentration level. Studies show underground miners who exposed to high concentrations of radon during working time, have consistently demonstrated an increased risk of lung cancer for both smokers and non-smokers (Tables. 3). Several studies have been done to indicate the relation between radon exposure and lung cancer among the miners, for instance, Table 5. shows an epidemiological case study on the correlation between Colorado miners' cohorts, radon exposure and cancer death (Leenhouts, 1998).

Regarding the condition of many mines' result in annual exposure to radon progenies, it is of the same order of magnitude as that experienced in a large number of houses around the world e.g. in case of miners if a mine worker had continuous exposure to 1 working level month for a year (WLM_{Annual}) in a mine, this is comparable to exposure over 1 year in a dwelling with a radon concentration of 230 $Bq \cdot m^{-3}$ (Tirmarche, et al., 2012; Axelsson, et al., 2015).

However, the inhalation hazard in mines is principally due to radon ans thoron, though the distribution of aerosol particles in the mine air as a predominant factor on the ratio of attached and unattached fractions cannot be ignored regarding their features of changing the equilibrium factor value, resulting in different dose conversion factor.

On the other hand, results of recent studies show that the remaining radon in enclosed area for a longer period generated higher concentration of radioactive decay products of radon, therefore, a rapid air change can quickly reduce the radon gas concentration from the atmosphere and result in a lower quantity of radon decay products building up, in addition to reducing aerosol concentration. Therefore, the concentration of radon progeny, e.g. within underground mines, depends on the fresh air exchange rate and ventilation (Schroeder & Evans, 1969). Regarding the radon concentration in underground workplaces, Table 4. summarized indoor radon concentration among several different mines.

Table 4- Summarized indoor radon concentration in the different mines

Country	Mine	Indoor Radon ($Bq \cdot m^{-3}$)	Reference
Kosovo	Stanterg (complex mine)	302±20	(Hodolli, et al., 2015)
	Artana (Lead-zinc mine)	191±6	
	Hajvali (Lead-zinc mine)	463±19	
	Badovc (Zinc mine)	527±35	
Pakistan	Punjab (Coal mine)	63±24 - 782±215	(Qureshi, et al., 2000)
	Balochistan (Coal mine)	48±12 - 343±128	
Australia	Gold mine	39 - 59 (49±14)	(Hewson & Ralph, 1994)
	Gold mine	137 - 156 (147±13)	
	Nickel/Gold	20 - 26 (22±3)	
	Nickel/Gold mine	52 - 74 (65±12)	
	Coal mine	86 - 386 (220±150)	
	Coal mine	106 - 166 (136±42)	
	Lead-Zinc mine	30 - 37 (34±2)	
Britain	Coal mine	22 - 518	(Duggan, et al., 1968)
Iran	Robat-Karim (Manganese mine)	1332±236 (no ventilation)	(Ghiassi-Nejad, et al., 2002)
	Venarge-Qom (Manganese mine)	10±2.6	
	Nakhlak (Led mine)	188±74	
	Pabdana (Coal mine)	146 -520 (320)	
India	Godavarikhani (Coal mine)	144 ± 61	(Rao, et al., 2001)
Turkey	Boron mine	51 - 117	(Yener & Küçüktas, 1998)
	Coal mine	31 - 185	
	Chromium mine	10 - 35	

Table 5- Radon exposure and related lung cancer death rate (Colorado miners' cohorts)

Radon exposure (WLM working level months)				**Smoking Habitat** (Cigarettes per Day)									
			Min.-Max. ‣	0		1 – 11		12 – 23		24 – 35		36 – 49	
Min.	Max.	Avg.	Avg. ‣	0		6		18		30		42	
				M	D	M	D	M	D	M	D	M	D
0	49	25		91	1	90	3	96	4	44	0	16	2
50	99	75		82	0	67	1	99	1	40	1	10	0
100	199	150		131	0	113	2	141	8	60	4	19	1
200	399	300		160	0	161	10	237	22	123	10	26	0
400	799	600		141	6	184	13	278	30	126	25	30	6
800	1599	1200		107	9	174	10	228	34	104	24	27	5
1600	3199	2400		84	12	109	16	156	46	69	19	19	5
3200	6400	4800		23	4	24	7	60	18	21	9	7	3
M = Number of Individuals; D = Lung Cancer Deaths;													

1.4. Radon & Dose

As it was explained previously, radiation can cause damage to the human tissues in either direct or indirect way; This potential of impact is measured in terms of time-integrated exposures known as a "dose", e.g. the amount of energy deposited in the body from exposing to radiation is expressed as a dose and can be classified as absorbed dose, equivalent dose and effective dose (Mattsson & Söderberg, 2013); Figure 5. shows a schematic representation of the series of steps from radon exposure to effective dose (Müller, et al., 2016).

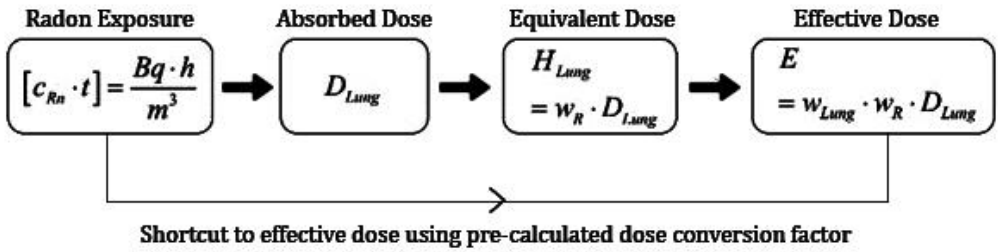

Figure 5- The series of steps from radon exposure to effective dose

The lung absorbed dose (D_{Lung}) is determined by biokinetic models. The lung equivalent dose (H_{Lung}) and the effective dose (E) are obtained by the radiation weighting factor W_R (changed or unchanged) and the tissue weighting factor (W_{Lung}), respectively.

Since radon is the largest contributor to radiation dose from natural sources, therefore, measurements of indoor radon should be performed regularly. A value of about 3 $mSv \cdot y^{-1}$ can be calculated using the latest recommended values published by ICRP as an average annual effective dose to the general population due to inhalation of radon and its progenies (ICRP, 2017).

Occupational exposure to radon and its short-lived decay products is defined as Working Level "WL" and refers to the concentration of short-lived decay products of radon in equilibrium with 3746 $Bq \cdot m^{-3}$ of Rn-222; So that, 1 WL is equivalent to the combination of radon short-lived decay products in one cubic meter of air with the potential of emitting $1.3 \cdot 10^8$ MeV or 20.83 $\mu J \cdot m^{-3}$ ($3.6 \cdot 10^{-3}$ $J \cdot h \cdot m^{-3}$) of potential alpha particle energy; The amount of ionising radiation emitted depends on radon in equilibrium with the decay of its daughters (ICRP, 2010).

Following the previous explanation, if an individual were exposed to 1 WL during a working month of 170 hours which is expressed as a Working Level Month (WLM) a factor of dose calculation. Regarding this, the inhalation doses resulting from the exposure to radon is related directly to the equilibrium factor (the ratio between the concentration of radon and its decay products), and the length of exposure. Received dose of radiation is usually measured in milli-Sievert per year ($mSv \cdot y^{-1}$) as the SI derived unit (ICRP, 2010).

Since the inhalation dose from the exposure to radon is directly associated with the short-lived radon decay products, measuring radon progenies in addition to radon measurement is very important. After radon decays, the freshly formed progeny quickly attaches to existing aerosol particles, thereby giving rise to a consecutive activity size distribution, for more details refer to sections 1.2. at the current thesis and Figure 6.

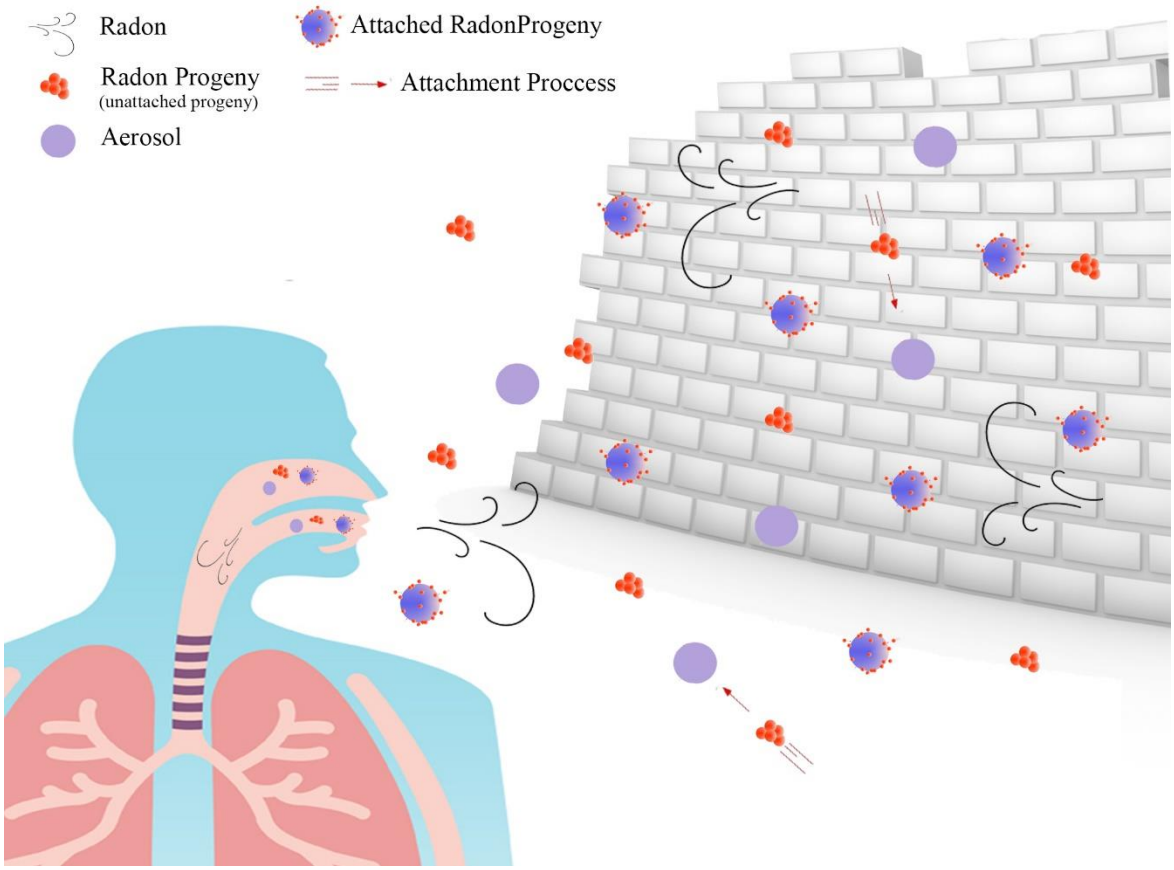

Figure 6- Processes of defining attached & unattached progenies

Calculation of effective dose from inhaled radon and its short-lived decay products follows the same formula for both public and occupational, but the difference is on the value of each parameter of the formula (Figure 7.), i.e. equilibrium factor (F) is an important

parameter on estimating dose, but this value changes depending on the conditions of ventilation, activity, location etc., for example, the equilibrium factor for outdoor, indoor and mine are 0.6, 0.4 and 0.2, respectively; these values are given literally and for a precise assessment it needs to be measured directly, while in some cases obtained value would be either much higher or much lower than given values.

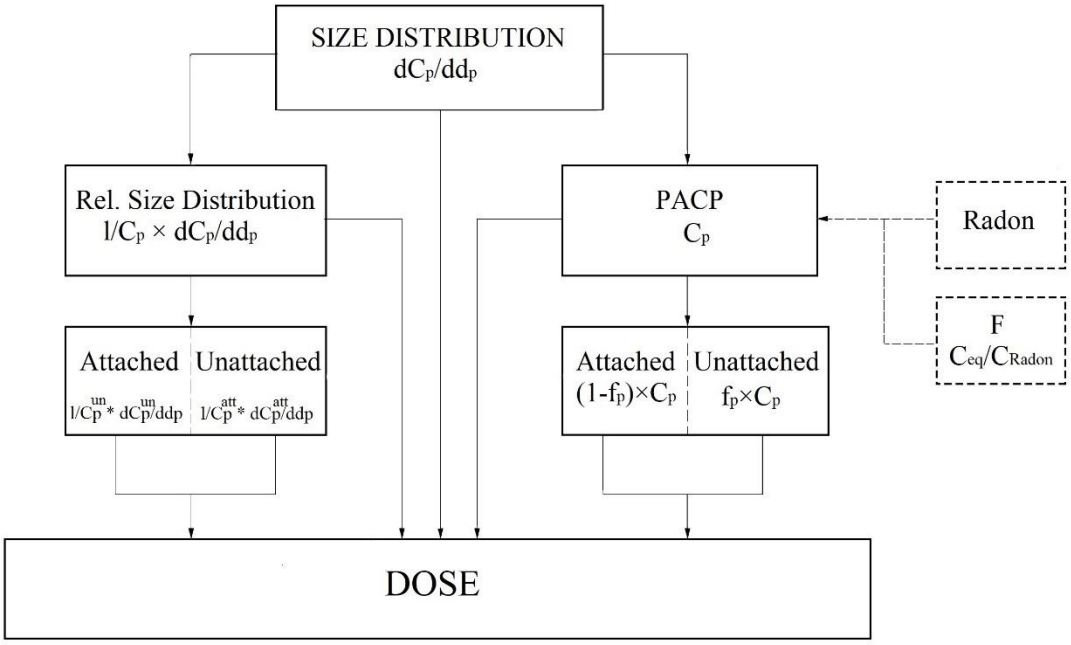

Figure 7- Parameters to estimate the dose from radon short-lived decay products

Another important parameter in dose calculation is unattached and attached factor; These values are used to calculate the dose conversion factor. As equilibrium factor, dose conversion factor is given by some organisations such as ICRP, etc., using epidemiological models (ICRP, 2017); However, these values may differ from the real values and for precise dose estimation it is necessary to calculate dose conversion factor based on field measurements, as it depends on attachment process and attachment process directly depends on environmental conditions; Figure 8. (Ruzer, 2011) shows experimental results of correlation between the unattached fraction of radon decay products and the aerosol surface area measured in these experiments; However, breathing behaviour, based on size distribution of the decay products, plays an important role to estimate dose conversion factor, (Figure 9. - source: Porstendörfer, 1996).

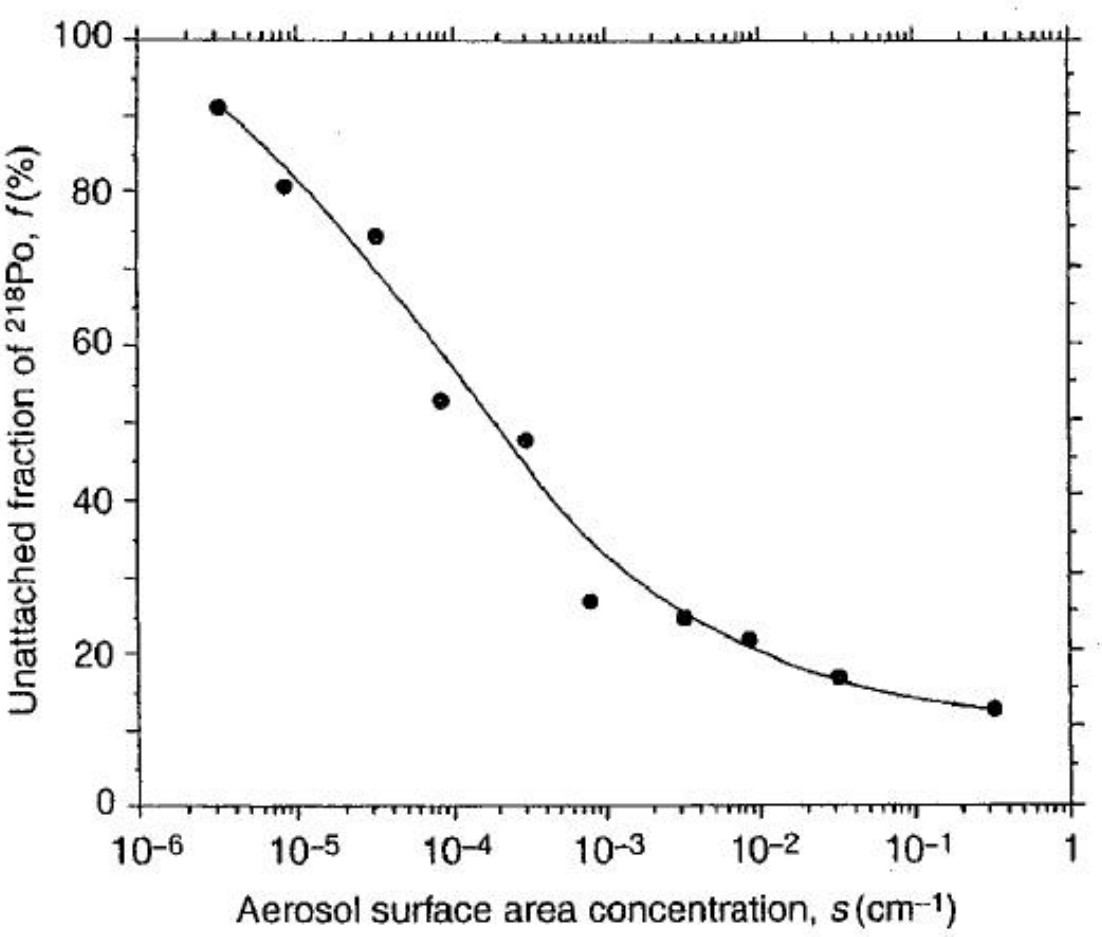

Figure 8- Unattached fraction vs particles surface area

The relation between (a) breathing behaviour and size distribution of the decay products and (b) the dose conversion factor, shows in Figure 9. and further information can be found on the published paper elsewhere (Porstendörfer, 1996). The dose curves show a great dependence on particle diameter with maxima at 1 nm to 5 nm and 4 µm to 10 µm.

Besides the dose conversion calculation, in the view of radiation protection, the ratio between ultrafine/unattached and attached is important as attached progenies (with the site of about 150 nm) may pass through the upper respiratory tract and exit after exhalation; on the other hand, a major part of the ultrafine progenies after passing the upper respiratory tract deposit in the alveoli and subjected to somatic transport processes (Ramola, et al., 2016).

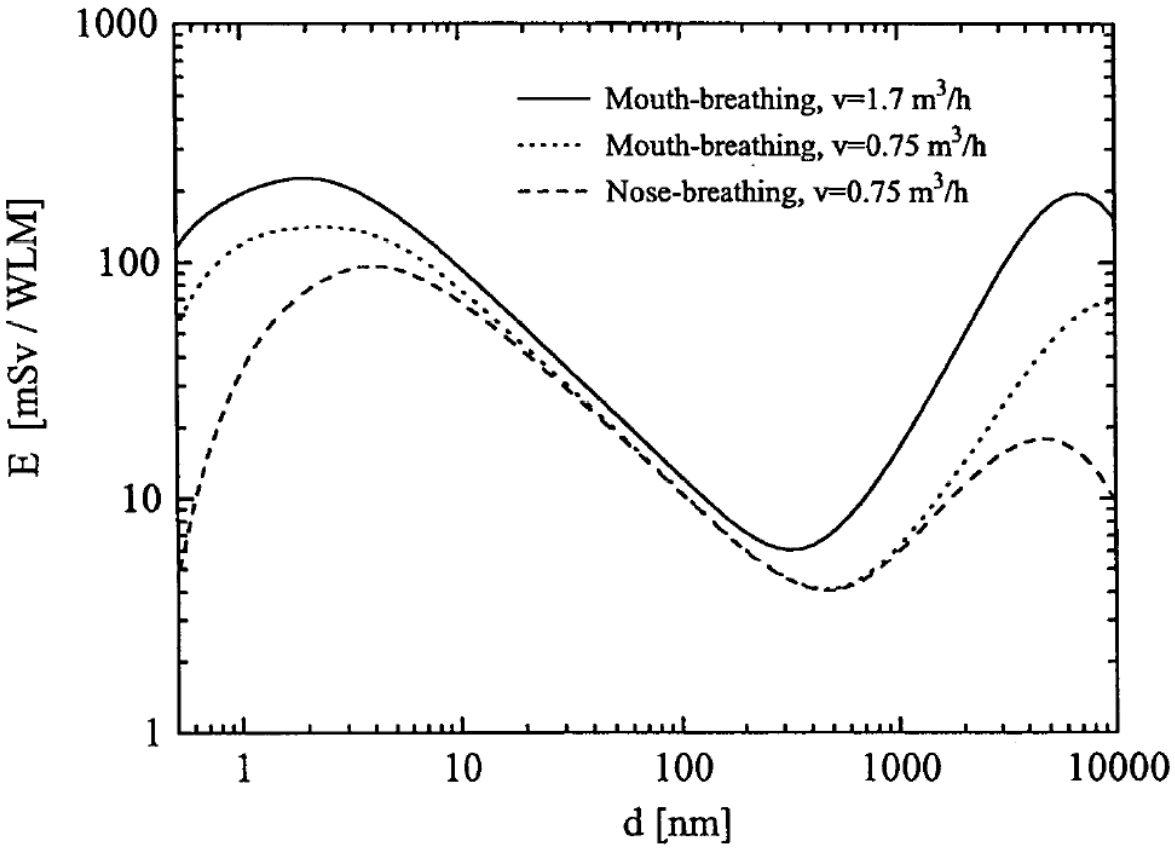

Figure 9- Dose conversion factors based on the breathing behaviour and particle size

Therefore, the equilibrium factor and the unattached fraction, size distribution of the decay products, and breathing behaviour are significant parameters in determining the number of radioactive decay products of radon left in the lungs and estimation of effective dose.

1.5. Radon & Regulations

The potential health risk due to radiation has become a widespread concern by many international organizations in the past and recent years, and prompted the national and international health organisations to establish regular recommendations and recommended dose limits for both workers and the general public for different types of activities, however, due to the importance of radon (as a major source of exposure -both occupational and public- and as a risk factor of lung cancer) outside of dose limit, extra recommendations are issued about accumulation of radon concentration in workplaces and buildings for protection against radon and reducing the risk of lung cancer caused by inhaled radon.

The International Commission on Radiological Protection (ICRP), the World Health Organization (WHO), the International Atomic Energy Agency (IAEA), the U.S. Environment Protection Agency (EPA), the European Atomic Energy Community (EAEC), the United Nations Scientific Committee on the Effects of Atomic Radiation (UNSCEAR) and the Occupational Safety and Health Administration (OSHA) are the well-known organisations that regularly recommend certain interventions concerning the accumulation of radon in workplaces or public area as regulation or suggestion, however, some countries set up their own regulations and recommendation level.

As a major of public health concern due to exposure to radon, the EPA introduced a primary action level of 4 $pCi \cdot L^{-1}$ (~150 $Bq \cdot m^{-3}$), thus, any radon concentration above this level needs mitigation to reduce radon. To find out which level is more appropriate (not only in view of public protection, but also in case of cost-effectiveness) five different radon concentration levels as 2, 3, 4, 8, and 20 $pCi \cdot L^{-1}$ (approximately 75, 110, 150, 300 and 740 $Bq \cdot m^{-3}$, respectively) were examined for preparing the guideline; It was observed, the higher value did not reduce the risk posed by exposure to radon nearly as much as did lower concentration; Therefore, EPA decided to limited the action level ranging between 2 to 4 $pCi \cdot L^{-1}$ (~75 to ~150 $Bq \cdot m^{-3}$); Then, after more examinations, 4 $pCi \cdot L^{-1}$ (~150 $Bq \cdot m^{-3}$) was chosen as action level due to its incrementally cost-effectiveness (the average cost per life saved by using this level of action is about $700,000, the amount, when compared to other government programs and regulations (such as highway safety, air-transportation safety, and occupational safety) is very low) and also EPA believed this level is easily and technically achievable in most of the homes using inexpensive mitigation methods. The action level value continues to be valid up to now and is considered a mitigation when indoor radon

concentrations exceed 150 $Bq \cdot m^{-3}$. Additionally, EPA works on relative-risk projection models to estimate the risk of radon exposure to the public health. For instance, lifetime risks of fatal lung cancer due to radon exposure at 4 $pCi \cdot L^{-1}$ (~150 $Bq \cdot m^{-3}$) was estimated to be $1.6 \cdot 10^{-3}$ and $3 \cdot 10^{-2}$ for individuals of never-smokers and smokers, respectively. The approximate annual of lung-cancer deaths caused by indoor radon for the US population was calculated about 14,000 deaths (National Research Council, 1999).

Meanwhile, the International Atomic Energy Agency, in accordance with the IAEA Safety Standard Series No. GSR Part 3, recommends that radon concentrations should not exceed 300 and 1000 $Bq \cdot m^{-3}$ for the public and workers, respectively.

The International Commission on Radiological Protection (ICRP) is one of the internationally recognised organisations in preparing and drafting recommendations and a source of guidance for radiation protection policies and national's regulations. ICRP basically classified its guidance in two circumstances of exposure: (A) when radiation source is resulting from human activity and increases the overall exposure, which is known as practices; (B) when radiation source exists that calls interventions; Indoor radon in existing buildings due to pre-existing natural sources is an example of interventions. ICRP has recently published two reports about radon and exposure to its progenies; Report 115 "Lung Cancer Risk from Radon and Progeny and Statement on Radon" was published in 2010 focusing on lung cancer risk due to radon and its short-lived decay products' inhalation; a second one was published in 2014 named "Radiological Protection Against Radon Exposure" (Report 126) an updated guidance on radiological protection against radon exposure and control of levels of exposure within dose estimates. Until last year, effective dose arising from radon and its short-lived decay products' inhalation had been calculated using epidemiological approach, but in 2017, ICRP introduced new reference dose coefficients for radon and radon progeny calculated using both ICRP biokinetic and dosimetry models validated for indoor workplaces and mines. The reference dose coefficients following inhalation of radon and radon progeny based on epidemiological approach have been updated several times during a short period until 2017 that the latest value was introduced. For the calculation of doses following inhalation of radon and radon progeny in underground mines and in buildings, in most circumstances, the ICRP recommends a dose coefficient of 10 $mSv \cdot WLM^{-1}$ (3 mSv per $mJ \cdot h \cdot m^3$), Table 6. shows some historical updates on dose coefficient (Marsh, et al., 2017; ICRP, 2017). The reference level value of 300 $Bq \cdot m^{-3}$ is recommended both for dwellings and workplaces.

Table 6- Historical updates on dose coefficient by ICRP

Exposed population	Fatal cancer risk per WLM	Conversion Factor ($mSv \cdot WLM^{-1}$)	Reference
Public	$2.8 \cdot 10^{-4}$	4	Publication 60 & 65
Workers		5	(1991 &1993)
Public	$5 \cdot 10^{-4}$	9	Publication 103 & 115
Workers		12	(2007 & 2010)
Public & Workers	$5 \cdot 10^{-4}$	10	Publication 137 (2017)

Recently, the council of the European Union prepared the new European Basic Safety Standards (EU BSS, Basic Safety Standards Directive entered force on 6 February 2014), and established a new regulation to set the limit on the effective dose for public exposure at 1 mSv in a year and 20 mSv in a single year for occupational. A reference level of 1 mSv per year was applied to indoor external exposure to gamma radiation emitted by building materials (in addition to outdoor external exposure) and building materials should be monitored to assure that the activity concentration index (I) not exceed 1 (Council of the European Union, 2014). EU countries must ensure compliance by 6 February 2018, i.e. Hungary as a member State of the European Union has to establish a national reference level of $\leq$300 $Bq \cdot m^{-3}$ for indoor radon concentration in workplaces by 2018 (Council of the European Union, 2014).

Additionally, it was recommended that the annual average radon concentration should not exceed 300 $Bq \cdot m^{-3}$ at dwellings and workplaces (including underground workplaces where radon concentration may exceed to several thousand $Bq \cdot m^{-3}$) and the dose received from inhaled radon may not be greater than 6 mSv per year, and it was referred to the ICRP to estimate the dose, however, in ICRP-137, based on new epidemiological modelling, the effective dose from radon at 300 $Bq \cdot m^{-3}$ is equal to 4 mSv.

The impact of the new EU-BSS will be important for many EU member states, including Hungary, since it implies for the first time an obligation to develop a regulatory frame to actively work on reducing the radon exposure not only of workers but also of the public, and lowering the reference level for the annual average activity concentration in air

to a maximum value of 300 $Bq \cdot m^{-3}$; However, the new EU-BSS does not include any process or protocol for estimation of dose due to radon, and the precise dose calculations result in significant differences taking into consideration only the activity concentrations.

Table 7. shows the latest recommendations and effective dose limits in both workplaces and public area in terms of dealing organizations.

Table 7 - Radon reference level in workplaces and public area

Organization	Radon Reference Level		Dose Limit		Reff.
	Workers	Public	Workers	Public	
ICRP	≤300 $Bq \cdot m^{-3}$	≤300 $Bq \cdot m^{-3}$	≤ 20 $mSv \cdot yr$-1	≤ 1 $mSv \cdot yr^{-1}$	(ICRP, 2017)
IAEA	≤300 $Bq \cdot m^{-3}$	≤1000 $Bq \cdot m^{-3}$	≤ 20 $mSv \cdot yr^{-1}$	≤ 1 $mSv \cdot yr^{-1}$	(International Atomic Energy Agency, 2014)
CEU	≤300 $Bq \cdot m^{-3}$		≤ 20 ≤ 6 (Rn) $mSv \cdot yr^{-1}$	≤ 1 $mSv \cdot yr^{-1}$	(Council of the European Union, 2014)
WHO	≤100 $Bq \cdot m^{-3}$ Max 300 $Bq \cdot m^{-3}$				(WHO, 2009)
EPA	-	≤~150 $Bq \cdot m^{-3}$	-	-	(U.S. Environmental Protection Agency, 2003)

Workplaces, where radon enters from the ground into indoor workplaces (such as manganese mines, the case study of this thesis), are classified as existing exposure situations and the radon concentration must be set as a reference level (Council of the European Union, 2014). Considering that, it can cause confusions when one compares the dose restrictions (in mSv) with the regulations expressed in activity concentration of radon in the air ($Bq \cdot m^{-3}$), while sometimes occupational are subject to exposure to high dose from radon even when radon concentration is low.

In case of monitoring building materials (as a major source of indoor radon concentration) incorporating residues from industries processing naturally-occurring radioactive material (mining), radon exhalation examination is missing what could be a useful tool to reduce indoor radon concentration.

1.6. Radon Monitor Devices

Radon measurements are divided into categories based on the propose of technique: (A) Passive measurement; (B) Active measurement; The sampling and duration measurement depends on the device used and method may vary over a wide range of grab sampling, time-integrated sampling (short-term (lasting 2 to 90 days), long-term (91 days to a year) and continuums sampling known as real-time radon monitoring, as sample-taken measurement occurs and shows results. However, radon measure devices are also classified differently based on their used method of radon monitoring in addition to other classification, i.e. electrostatic collection of decay products (RAD7, Tesla TSR2, EQF3220), ionizing chamber device (AlphaGUARD), photomultiplier counter and scintillation (Liquid scintillation or scintillation cell), radon absorption (active charcoal), etched track detectors (CR-39, LR115) etc (Baskaran, 2016). Passive radon measurement devices are generally less expensive and are used in most for integrated monitoring of real estate transactions and the output is an average of radon concentration for the whole measurement period, while, active devices are more expensive but are more precise and can give a historical view of radon changed concentration during measurements (WHO, 2009).

As in previous sections, the health risk of exposure to radon was explained and regarding recommendations and legislation, radon prone places should be continuously monitored and measure radon concentration to assure the radon concentration is below the recommended level. Therefore, a long time periodical examination and measurement is necessary to monitor occupational exposure to radon and establish requirements in places such as underground workplaces where radon concentration is high, but it should be in consideration that due to the atmosphere condition within underground workplaces (such as humidity, pressure, temperature etc.) radon monitor devices may be influenced by environmental conditions; So, devices should be comprised parallel to find out an adaptable device base on the workplace condition. However, some devices have been recently introduced on the market which uses high-end technology, effective in the industry as a suitable radon monitor, but needs reported measurement tests to be approved as a reference device for on-site measurement, for example, TESLA recently provided a new radon monitor device (TSR2) with an internal smart central control with ability of connecting to the mitigation system to turn on/off system automatically when radon concentration goes

above/below the set reference value (Figure 10.) that it can save 15%-50% energy consumption in favour of the industry owner.

Figure 10- TESLA radon monitor kit

There are several radon measurement devices that are commonly used to monitor radon concentration at workplaces – depending on environmental conditions – that are divided to two categories: 1- devices that are designed for long-term measurements (such as Alpha track detector); 2- devices that are designed for short-term measurements (Liquid scintillation, activated charcoal, Continuous radon/working level monitor). Each of these devices has variable performance in different environmental conditions which still have not been studied and need to be examined, however, there are several kinds of studies (Shahrokhi, et al., 2015; De Simone, et al., 2016; Moreno, et al., 2013) that have examined some of these devices' performance in variable environmental conditions.

The measurement sensitivity of TSR2 is about 0.15 count·h^{-1}·Bq·m^{-3} (typically) and the range of measuring starts from as low as 5 Bq·m^{-3} up to 65535 Bq·m^{-3} with an uncertainty of 15% at 300 Bq per one hour. Records saving interval (probe) 1- 255 minutes, default 1 hour; Radon concentration results display as: (1) the short-term measurement mode (1 hour running average), and (2) long-term measurement (24 hours running average) (TESLA, 2016).

AlphaGUARD is a battery or net-operated portable instantaneous or continuous radon monitor based on an ionization chamber with high recording storage capacity. In addition to the radon concentration measurement, it also records simultaneously relative humidity, ambient temperature and atmospheric pressure using its integrated sensors. AlphaGUARD due to its high sensibility 0.62 L ionization chamber with the sensitivity of 1 cpm at 20 $Bq \cdot m^{-3}$, very low uncertainty (instrument calibrator error: 3%) and the ability of operating in almost any environment conditions in mines, laboratories and also for complementary investigations in buildings (-15 °C to +60 °C, 800 mbar to 1050 mbar and 0% to 99% air humidity), usually use a reference instrument and calibration equipment in order to perform air, water, soil and exhalation measurements. The range of measuring starts from as low as 2 $Bq \cdot m^{-3}$ up to 2.000.000 $Bq \cdot m^{-3}$ (Saphymo, 2016).

However, AlphaGUARD might be known as a reliable and reference device for measuring radon in almost any environment condition, measuring radon and thoron progeny decay is out of scope of this device and need additional instrument for this purpose. The Pylon WLx is a battery or net-operated portable radon and thoron working level measurement monitor. This monitor uses proven, integrated solid state detector (25 mm diameter) technology to detect alpha particles from radon and thoron progeny decay in a given volume of air. The built in multi-channel analyser circuitry and firmware allows the monitor to calculate radon, thoron, and their progeny in working levels (WL) by sampling a known air volume by the servo-controlled pump through a filter. The radon and thoron progeny in the air sample are collected on a filter that faces a laboratory grade Ion implanted solid state detector. As the radon and thoron progeny decay, alpha particles are released. An alpha particle that strikes the detector releases a quantity of electrons across the semiconductor diode junction. The quantity of electrons released is proportional to the energy of the alpha particle. A multichannel analyser discriminates the radon and thoron progeny. Sophisticated algorithms determine the working level. The detection range starts from 0.001 WL (known as Minimum Detectable Level in one-hour continuous sampling) up to 50 WL (PYLON, 2018).

In Addition to monitoring radon and its short-lived decay products, in some cases, measuring the attached and unattached decay products are of particular importance; SARAD EQF3220 allows measuring the activity concentration not only of radon and thoron gas but also of their decay products (EEC), in relation with the volume of the particles of the aerosol with sampling ultrafine and attached decay products as well as the cluster component within

the range of 20 to 100 nm. EQF3220 is equipped with a 4·200 mm^2 ion-implanted silicon detector for measuring radon/thoron with a detection range between 0 and 10 $MBq \cdot m^{-3}$ and a sensitivity of 3 and 7 cpm/(kBq/m^3) for fast and slow mode, respectively; An attached aerosol sampling head in size of 44 mm in diameter and 100 mm in length with a 2·150 mm^2 ion-implanted silicon detector to able this device measuring attached/unattached (EEC) from 0 to 1 $MBq \cdot m^3$, while the sensitivity of device in case of attached decay products measurement is approx. 600 cpm/(kBq/m^3) (EEC) and for unattached decay products is about 150 cpm/(kBq/m^3) (EEC). Several built-in sensors make this device to simultaneously measure Rel. humidity in range of 0 to 100% with uncertainty ± 2%, temperature in range of -20 to +40 °C (uncertainty ± 0.5 °C), and additional optional air analytics sensors for CO, CO_2, CH4 (SARAD GmbH, 2013).

1.7. EU-BSS and Reuse of Manganese Ore Mining Residue

Over recent years more and more studies have been published on the harmfulness of NORM materials, and there has been no unified recommendation (regulation) on the restriction of their use until recently, yet the European Basic Safety Standard known as EU-BSS (Council directive 2013/59/EURATOM, European Basic Safety Standards) emphasizes the restrictions related to these materials by monitoring the radioactivity index (I) of materials. Additionally, a reference level applying to indoor external exposure to gamma radiation emitted by building materials, in addition to outdoor external exposure, shall be 1 mSv per year.

The importance of the utilization of by-products and residue streams has grown over recent decades due to the concern about the sustainability of the human environment; of course, the use of residues sometimes provides better financial solutions. In recent years, some studies are focused on the utilization of industrial waste residues (e.g., waste glass, concrete waste) in concrete or mortar to improve some (Li, 2008; Gutiérrez, et al., 2015; Sas, et al., 2015a; Kovács, et al., 2017).

Manganese clay is the residue of manganese mining, it is not classified as a by-product as it is listed as a secondary raw material. About 2.8 million tons of the residue of manganese ore mining clay has been deposited on the land surrounding the Úrkút manganese mine. However, in case of reusing of by-product in building material industries, several studies have been conducted mainly focusing on gamma dose; While, measuring only the gamma dose is not suitable as the majority of radiation dose is provided by radon and its progenies (Somlai, et al., 1997; Somlai, et al., 2006). Therefore, it is necessary to include the radon exhalation (as measuring only the radionuclides concentration is insufficient) as a monitoring tool in the processing used in the building industry to derive a useful radon exhalation data; Following recent studies (Kávási, et al., 2012; Sas, et al., 2015a) on utilization of clay as a building material, heat treatment used as a radon exhalation treatment tool in this study.

The quantity and quality of additives usable in building materials have long been set out by strict regulations. The radioactivity of materials usable in building materials is regulated explicitly by the standards of only relatively few countries. However, some have been established for many years: Hungary the regulation setting out the radioactivity limit of building materials has been in effect since 1960 (no. 26/1960 Directive of Hungarian

Ministry of Construction). Due to other major components of manganese clay (Seil & Heiligman, 1928) it is potentially useful in brick productions. Thermal treatment (firing) is the basic treatment method of brick-making and this has implications on the amount of radon emitted.

In this study, in addition to the internal physical features changes, the radon emanation characteristics of manganese clay were measured at different temperatures identifying the optimum firing temperature in order to minimize radon exhalation and provide useful data for later modelling and also for construction companies, and information for authorities on the maximum amounts of additives.

1.8. Background of the Study

The Úrkút Manganese mine was on attention for the first time in middle 2002, doing a regular radioecological measurements along with the new national regulation about radon concentration in workplaces and underground mines. It makes a big opportunity for Hungarian researchers to have some related experiment and studies. Regarding to the properties of the mine as an underground mine, in 2002 the first study was conducted to figure out, if there is a health risk for workers who exposure to radionuclides in the mine during working time based on the standards and regulations at that time; It was indicated that, the only direct potential hazard health can be the accumulated Radon in the air; Therefore, increasing the ventilation rate was suggested as a solution, but increasing the ventilation flow rate to the rate that could guarantee the low radon concentration was not possible due to the Hungarian regulation; On the other hand, increasing the air flow could cause distribution of dust on the mine environment what could cause other health problem. Then, it was suggested to increase the working shifts, as a result, the health risk of exposure to radon could be reduce as workers would expose to radon for a shorter period. Following the first study second one was conducted between 2003 and 2006 focusing on seasonal fluctuations effect on dose estimation and equilibrium factor. The third study had started between 2006 and 2010 about geological role on radon concentration in mine, it was indicated that changes in mining circumstances may cause an increase in radon concentration, and it was found that radon in underground water may not have any influence on the radon concentration in the mine and measuring radon emanation and exhalation of the rhodochrosite and black- shale. Regarding the Tamás Vigh study and suggestion it could be possible to meet the regulation in Úrkút underground mine.

In 2013, Vigh et al., investigated the activity concentration of three natural occurring radioisotopes (U-238, Ra-226, K-40) in black shale (Vigh, et al., 2013).

During years, the average radon concentration was keeping below 1000 $Bq \cdot m^{-3}$ by improving mitigation system in Úrkút manganese mine; However, decreasing working hours and improving mitigation could be a practical solution until 2013 when Europe established a new regulation to keep radon concentration in dwellings and work area below of 300 $Bq \cdot m^{-3}$. According to the timeline of the European Basic Safety Standard, all EU members should apply the requirements by starting 2018. Reducing radon concentration to below the recommended level, can be a new challenge for the work area (such as underground mines

and caves) due to their limitation. Therefore, in this study to follow new European regulation, it was tried to find out the problems and solutions for underground workplaces (Case study: Úrkút manganese mine). The first step to control radon concentration at an environment is to recognize the source of the radon. By following, optimization of ventilation can be other way of reducing the radon concentration, however, a good measurement device and a long-term monitoring are required to plan the best way of reducing radon in workplaces.

In this thesis, it has been tried to apply the EU basic safety on an underground mine as case study manganese mine to be possibility of a guide for other similar workplaces. In the first phase, a regular long-time radon concentration measurements by using passive and active method and difference devices to compare performance of devices under the mine condition and trying a new intelligent system (TESLA TSR2), in the second phase following the last study to get an overview of radon concentration a material analyses have been done to find the main source of radon in the mine. Additionally, a long-term dosimetry was doing and finding the behaver of attached and unattached particles on the received dose by workers based on the radon source. In the third phase it has been tried to develop and optimized ventilation system based on the regulation. In the fourth phase it tried to find attached and unattached rate for working hours and not working hours and the traveling distance of particles and the effect of radon. In the last phase it has been tried to figure out the possibility of reusing by-product of the mine as building material by heat treating and active coal additive treatment.

MATERIALS AND METHODS

2.1. Description and Geology of Úrkút Manganese Mine

Úrkút manganese mine is located near the village of Úrkút in the Balaton upland region of Hungary. Manganese ore extraction from the Bakony Mountains was started in the Early 20th Century (Polgári, 1993; Polgári, et al., 2013).

The Bakony Mountains is an important region for structurally controlled black shale hosted Manganese mineralization of Jurassic age in Hungary. The Úrkút Manganese ore deposit (Úrkút Manganese Formation – ÚMnF) is surrounded by mountains of the Alps and Carpathians in Pannonian Basin and belong to tectonically of the North Pannonian unit (Figure 11.); The Úrkút Manganese is one of the ten largest "black shale hosted Manganese carbonate deposit" in the World (Polgári, et al., 2013)

In geology and plate tectonics point of view, the Csárdahill faults (approximately 800m long sinistral fault and active in the Jurassic and reactivation in the Cretaceous), and the NW-SE Csinger fault (transects the whole Úrkút Basin), are the most important reasons of creation of this region (Polgári, et al., 2004).

The Úrkút manganese mineralization divided into two main units with approximately 40 to 48 meters in thickness. First, Cherty, Fe-rich, Mn-oxide mineralization occurs in varicoloured metalliferous clay stones (overlies on strongly leached limestone); The thickness of this ore is about 6 to 8 meters (Úrkút-Csárdahegy and Eplény); Second, the black shale-hosted Mangenues mineralization happened in a clayey marlstone of Toarcian (Polgári, et al., 2004); Figures 13. (Polgári, et al., 2004) is shown the mineralization geological map of the Úrkút manganese. The formation of the Úrkút manganese ore contains: (a) between 1% and 2% of organic matter; (b) up to 5% of sulphides; (c) a little amount (lower than 1.5%) of phosphorites (Korpás, et al., 1999).

The average values of some selected major and trace element compositions of the Úrkút manganese are given in Table 8. trend form recently published paper (Bíró, et al., 2015).

The largest Manganese mineralization is located in the Úrkút basin and Eplény, where formed by the NW-SE trending block faulting and characterized the late Triassic and Jurassic tectonics of this region, as shown in Figure 11. (Polgári, et al., 2004).

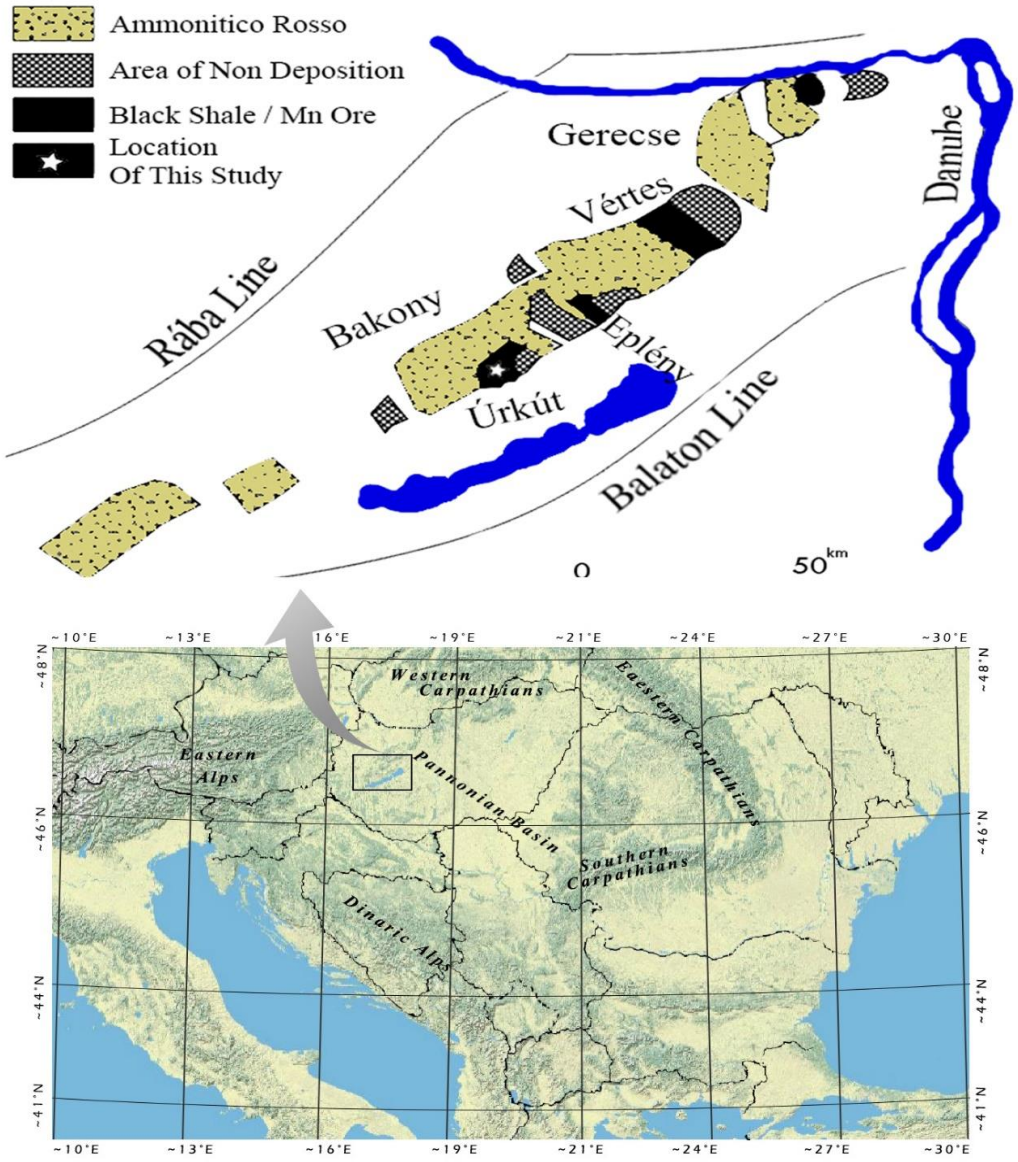

Figure 11- Location of the Jurassic Manganese mineralization of Hungary

As one of the largest Manganese deposit, the Úrkút Manganese mine reserves about 80 million tons of Manganese carbonate ore containing an average of 20-24 wt.% Manganese and around 10 wt.% Iron in an area of about 120 hectares occurred within early Miocene to Middle Miocene by composing of dark-grey to black shale, bioclastic limestone and radiolarian clay marlstone (Polgári, 1993). However, the Úrkút underground mine ore of is composed: (a) primary ore: rhodochrosite by 20 to 30%; (b) secondary ore: pyrolusite, manganite and psilomelane by 40 to 50%; (c) siderite including 5% (Szabó, et al., 1981).

Table 8- The average values of element composition of the Úrkút manganese

	Mn (wt%)	Fe (wt%)	V (μg/g)	Co (μg/g)	Ni (μg/g)	Cr (μg/g)	Th ($Bq \cdot kg^{-1}$)	U ($Bq \cdot kg^{-1}$)	Ce (μg/g)	Nd (μg/g)
Grey Mn-carbonate	20	6	61	266	45	27	8	3	228	56
Black shale	3	6	151	414	105	68	32	5	191	53
Brown Mn-carbonate	28	1	20	454	75	0	8	1	133	29
Brown-grey Mn-carbonate	10	9	80	138	41	39	16	1	128	36
Beige Mn-carbonate	1	6	122	29	45	68	20	2	79	27
Brown-black Mn-carbonate	24	13	61	301	63	15	12	3	162	33
Green Mn-carbonate	16	7	51	155	20		4	1	122	31
Cherty limestone (Mullock)	-	-	-	17	71	-	24	2	41	24
Marlstone (Mullock)	-	-	-	6	79	-	8	1	32	16
Greenish grey calcareous marl (Mullock)	0	3	77	80	35	55	45	4	90	34
Limestone (Mullock)	0	1	39	18	102	20	20	1	33	21

Mining in Úrkút mountains to extract Manganese ore was going on until recently that it was closed in 2017, however, the mine was closed one time before also. Therefore, scientists had a chance to researches and created a great number of geological, mining and scientific data during this period. Over recent decades of mine working, about 2.8 million tons of manganese clay produced after manganese ore processing has been deposited on the land surrounding the mine covering a territory of 20 hectares, however, there is no evidence any influence on mine or environment.

For years, several radioecological studies have been done by focusing on Radon concentration, dosimetry, radiation exposure, the possibility of reusing by-products etc. Nevertheless, a comprehensive study related to the origin of radiation (mainly Radon) as an important factor in point of view of radiation protection, mitigation improvement and the possibility of reusing the manganese mining residue in building industries in the line of national and international health regulations was missing and needed to be completed. The first radon surveys were carried out in 2002, and they continue to be made giving an ever-

expanding database until the present day (Kávási, et al., 2009; Kávási, et al., 2010; Kávási, et al., 2011; Vigh, et al., 2013; Shahrokhi, et al., 2017; Kovács, et al., 2017). Figure 14. (adopted from Tamás Vigh's Ph.D. thesis) is shown a detailed map of the mine.

The mine was operated in one working shift, 8 hours per day and five days a week (business days). About 40 miners, all males with an average age of 44 years old, were working on the mine. The smoking habitat between miners was estimated around 60%, as no official survey was conducted, the valued obtained from director manager of the mine regarding to his knowledge. The average temperature in the mine was calculated at 13±3 °C with an average relative humidity 84±6%, the values was almost constant during the year. In addition to the natural air exchange, a process resulting from difference in the pressure and temperature between underground atmosphere (186 m) and surface by shafts, a central ventilation system was changing mainly the mine environment air during working hours using a vent to blows fresh air into the 6-km-long gallery system (draught between the two shafts by a central fan) with an average air flow of 60,000 $m^3.h^{-1}$ through a canvas or pipes; For those places where using central ventilation was not possible (e.g. blind galleries, faces, galleries under construction, etc.) an auxiliary ventilation was used to exchange the air. The schematic of the system shows in Figure 12. (adopted from Tamás Vigh's Ph.D. thesis).

Since it was not possible to increase the ventilation flow rate due to the workplace regulation and conditions, and the air change functions as partial ventilation and central draught ventilation were not effective enough, a newly developed mitigation system (called mobile mitigation) was used at the active ore production sites. These faces were chosen as they were the location of the most intensive work where involving many workers. The highest radon and its progeny concentration expected there due to low effective natural air exchange rate after working hours.

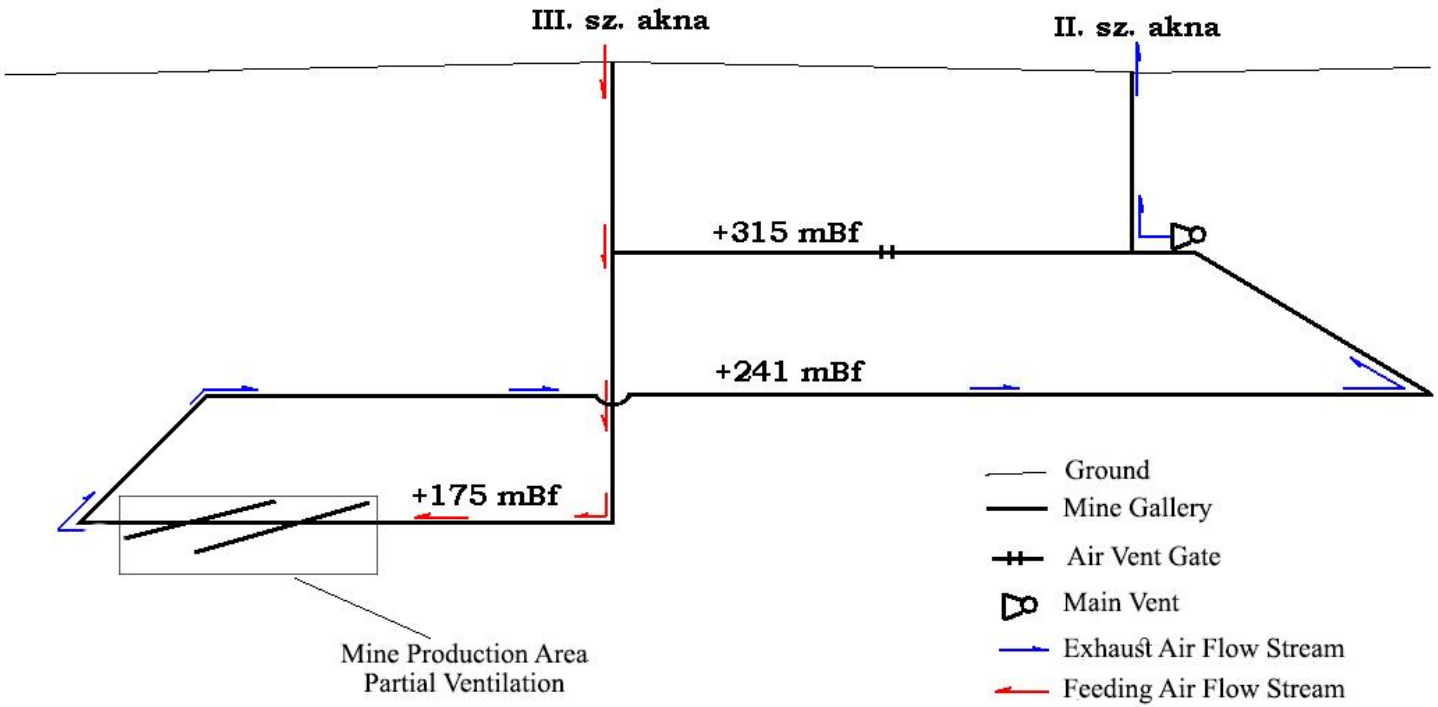

Figure 12- Scheme of Úrkút mine ventilation system

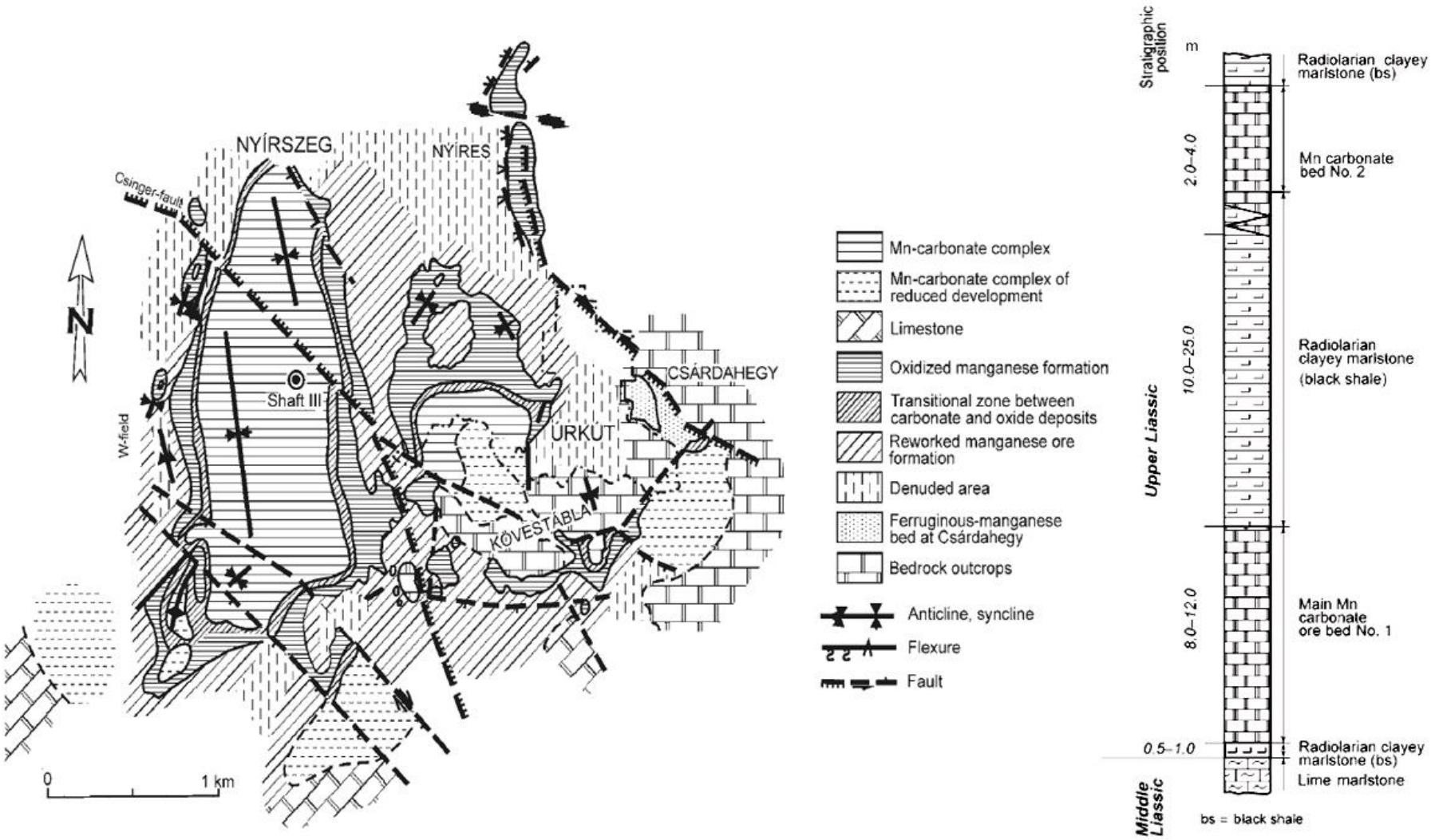

Figure 13- Idealized section and geological map of the Úrkút manganese mineralization

2.2. Radon in Air

This section provides a framework for the selected radon monitor devices which used for radon and its decay products measurements and for developing of the procedures to assure the reliability of radon measurements in the mine air and water. Explaining of various methods for measuring radon, including both passive and active methods, from individual testing to diagnostic measurements to assess radon exhalation form different rocks and layers of the mine. Some methods developed and updated to perform better and accurate results.

Measurement of radon in the air divided into two different methods of passive and active monitoring. Each method has its own advantages and disadvantages reading to the measurement conditions. A passive radon monitoring is an integrated measurement and usually know as a long-term measurement; in this method radon detector is located on the measurement site for a long period (it may start from several days up to several years) and result are observed as an average per period of measurement. On the other hand, an active radon monitoring is a real-time measurement method that uses for a short time measurement. In this method an active radon monitor instrument measures radon concentration per each specific period (can be started from 1 min up to several hours) and real-time result can be obtained during measurements.

2.2.1. Active Monitoring

About 4 places inside the mine were selected as reference locations to measure radon concentration during working and not working hours using several devices including AlphaGUARD and TESLA. The measurements had been done monitoring 4 location, based on 1-hour measurement continually for 5 days, several times in 1 year. However, a special measurement conducted exactly after new mining process like as explosion or digging and cutting wall.

The devices used in this experiment chosen because they involve different measuring methods, namely: semiconductor detector TSR2 (TESLA, Czech Republic) and an ionizing chamber device (AlphaGUARD PQ2000 PRO, Saphymo Gmbh, Germany). AlphaGUARD set up in diffusion mode to conduct measurements over a period of 60 minutes, while Tesla was setting up 60 minutes measurement in slow mode. Figure 14. shows the measurement locations.

The author calibrated the AlphaGUARD using a certified 210.5 L metal chamber (Genitron EV 03209) equipped with an electric fan to ensure internal homogenization (the homogenization of the gas inside the chamber examined using 5 CR-39 placed at three different height levels inside the chamber and standard deviation between each series of CR-39 at different height calculated in the range of 1% to 3% with an average of 1.5%), as an experimental chamber. A certified radon source with 105.7±0.42 kBq radium (Ra-226) (Pylon RN2000A, a passive radon gas source; Pylon Electronics Inc., Canada) supplied a known concentration of radon in the chamber (for more details refer to section 2.2.2. and 2.3.1 at current thesis). The results obtained from measured radon concentration after decay constant correction compared with the radon reference and calibration factor calculated (in case of this instrument calibration factor was ~1). The background of the device was measured in a radon free chamber in 30 minutes measurement cycle for 2 hours, and the mean calculated as 5 $Bq \cdot m^{-3}$, therefore, detection threshold of the instrument estimated to be 5 $Bq \cdot m^{-3}$.

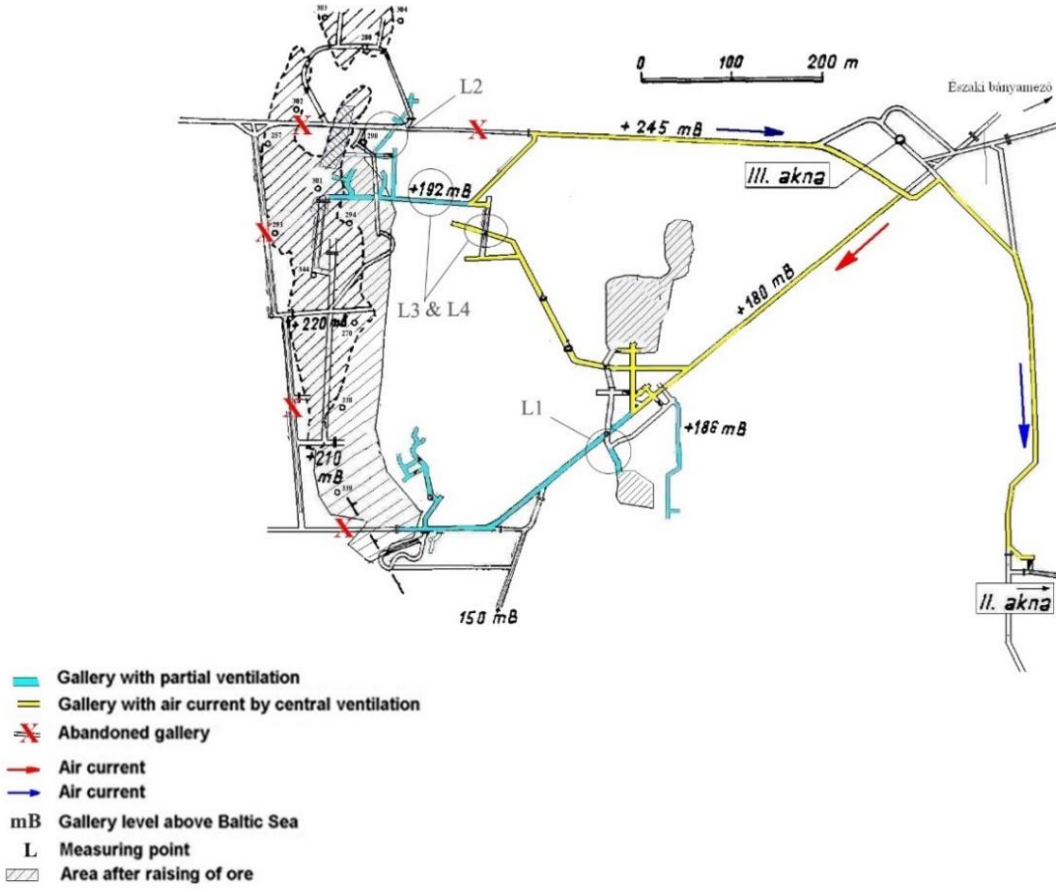

Figure 14-Measurement locations using active radon monitoring

The author involved TESLA TSR2 to its own measurement to check the performance of TSR2 as a newly introduced intelligent radon monitor with ability to connect to the mitigation systems and controlling the system based on radon concentration in the air, resulting saving power consumption. The author calibrated the TSR2 devices based on a certified radon source in two phases. In the first phase the devices where calibrated at the room condition, and in the second phase the calibration factor observed by establishing mine condition (83%±5% relative humidity and temperature of 11 to 14 °C with an average of 13±2 °C). The detectors calibrated using the method as same as the AlphaGUARD calibration procedure. As the devices were new, the background measurement of devices was measured to be under 5 $Bq \cdot m^{-3}$, sensitivity and detection limit based on the manufacture given data are 0.15 count per hour per $Bq \cdot m^{-3}$ and 5 $Bq \cdot m^{-3}$, respectively.

2.2.2. Passive Monitoring

An alpha track detector (ATD) is a small piece of a kind of plastic substrate (generally polyallyl diglycol carbonate (known as CR-39), Kodalpha film type (LR115) or polycarbonate (Makrofol) material) enclosed by radon selective diffusion containers some with possibility of thoron-radon diffusion and some just for radon (Rn-222). The electrically charged alpha particles produced from the decay of radon and its progeny colliding with the surface of the detector caused the chemical bonds of chains to break and producing microscopic areas of damage; These damages are made visible after a chemical etching process and are called tracks. The tracks are made observable by using some special devices like as optical transmission microscope or scanner, and using image analyser software so that they can be counted either manually or by an automated counting device, after subtracting background counts, is directly proportional to the integrated radon concentration in $Bq \cdot h \cdot m^{-3}$ (Shahrokhi, et al., 2016).

In this study a time-integrated passive radon measurment used to detect radon concentrations inside the mine. The detectors, CR-39 based detector (SSNTD, Solid State Nuclear Track Detector, 10×10×0.5 mm) enclosed by the NRPB radon selective diffusion containers (35×30×10 mm), were located in 8 different workplaces of the mine (Figure 15.) and exposed to radon for each period of 3 months (seasonal variation) along 36 months.

After each exposure period, the detectors were sent back to the laboratory of the Institute of Radiochemistry and Radioecology at the University of Pannonia. The detectors evaluated using a developed etching system in the 6 M NaOH chemical solution for 3 hours at 90 °C to reveal the tracks. Two factors of constant temperature and constant solution concentration play the most important role during etching processes. Etching system uses a built-in thermometer and mixer, the temperature of solution keeps constant in whole solution, in such a way that the heating system is cut off when the temperature of solution exceeds 90 °C and the mixer assure same temperature in all solution.

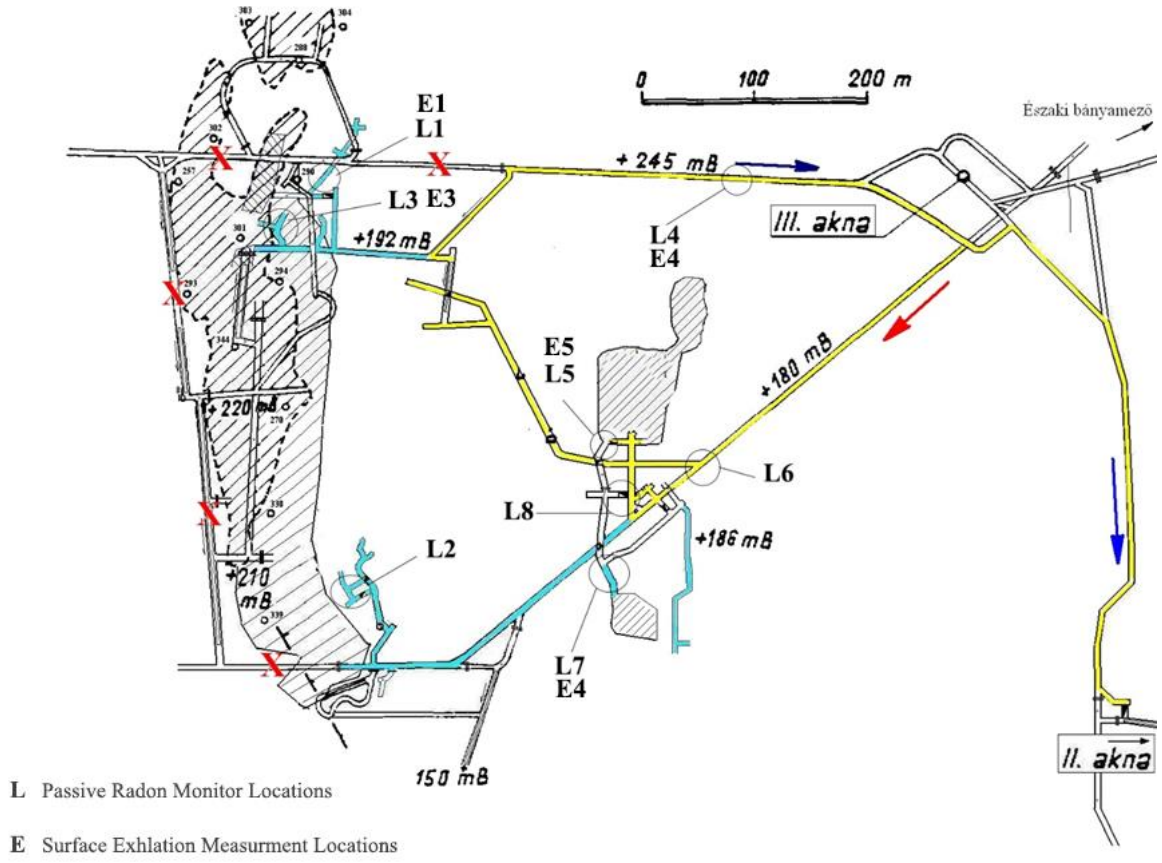

Figure 15- Passive radon measurement locations

Usually, a microscope equipped with a camera, a display, a controlling unit with electro-motors responsible for the precise movements of the microscope lenses and an image analyser is required to evaluate and count the tracks; However, this method has its own cons as: 1- it is taking a long time to count tracks (depending on operator experience can take between 1 to 5 minutes per each detector); 2- Low accuracy and high deviation due to counting repetition and human mistake (mistake on counting, identification error between

track caused by colliding alpha particles and track shapes occurred during etching, focusing, light and dark area); 3- Due to microscope algorithm not all surface of detector can analyse; 4- Different calibration factor per each operator.

Regarding to the mentioned problems in the microscopic method, and due to the lack of information of slide scanner method, a semi-automatic track evaluation system based on slide scan was developed by our researcher group used for this study to make counting the tracks faster and more precise (Bátor, et al., 2015). The detectors after etching process, cleaned with alcohol and placed on the detector holders (detector holder has a capacity of 100 detectors and in each scan 100 detectors can be evaluated) and scanned; Then, the scanned images analysed using an self-developed opensource Image Analyser (IA) software (ImageJ); The recently published paper Bátor, et al., can use as a reference for detailed information about the system and how it works (Bátor, et al., 2015).

The average radon concentration in the mine area calculated using Equation 1. based on the density of tracks on etched detectors (cross-sensitivity to thoron avoided using a radon selective diffusion chamber with a resistance to thoron gas entering the chamber).

$$C_{Rn} = \frac{(N_T - N_B) \times E}{T \times A} \qquad \text{Eq.1.}$$

where C_{Rn} is the average indoor radon concentration ($Bq \cdot m^{-3}$), N_T is the number of total tracks, N_B is the number of background tracks, E is the calibration factor ($Bq \cdot h \cdot mm^2 \cdot m^{-3}$), T is the exposure period (hours), and A is the area in which tracks detected (mm^2). In this calculation, A calibration factor "E" obtained by controlled exposures at a calibration chamber allows conversion from track density to radon concentration using following equation.

The minimum detectable activity concentration calculated using following Equation 2. (Kávási, et al., 2014):

$$MDA = k^2 + 2\,CDA = 2.706 + 4.653\,U_{Bckg} \qquad \text{Eq.2.}$$

And CDA is calculating by Equation 3.:

$$CDA = k_{1-\alpha} \times \sqrt{2U_{Bckg}} \qquad \text{Eq.3.}$$

where α is a certain fraction of a normalized Gaussian distribution (=0.05 for this study), 1−α is the confidence level (=0.95 in this study); k is number of standard deviation,

$k_{1-\alpha}$=1.645 for the confidence interval (CI) of 0.95 and U_{Bckg} uncertainty of the background activity concentration ($Bq \cdot m^{-3}$).

The author calibrated the detectors using a certified leak-free metal radon chamber (Genitron EV 03209, Volume: 210.5 L) and a certified radon source (Pylon RN2000A, a passive radon gas source) supplying a known concentration of radon to the chamber; The Pylon RN2000A source (calibrated in DURRIDGE Company Inc.) was supplied with a removable cap which is used to seal the container or radon gas to completely disperse when the cap is removed. The solid radium, covered by the aluminium container, continues to emanate radon gas at a constant rate following the standard growth rate (DURRIDGE Company Inc., n.d.). Table 9. is summarized the given official data related to the source used in this study by producer.

Table 9- The specifications of the radon source (Pylon 2000A) used in this study

2000A Specifications	
Parent nuclide	Ra-226
Date of manufacture	1998. August.11
Nominal activity	105.7 kBq
Activity Tolerance	0.4% (0.4 kBq)
Daily Emanate Radon	110310.7 Bq

The outlet of the source is electronically controlled, and 24 hours before starting the experiment opened to release the accumulated radon in the container.

The concentration of radon inside of the chamber calculated based on the radon mass transfer as:

$$R_s = \left(\frac{f\ A_{Ra}\ (e^{-\lambda_{Ra}\ t_{Ra}})}{V_{stp}}\right)(1 - e^{-\lambda_{Rn}\ t_{Rn}}) \qquad \text{Eq.4.}$$

Where R_s is radon concentration in the calibration chamber, f is radon emanation fraction from the source, A_{Ra} is activity concentration of source (Ra-226 Activity kBq), λ_{Ra} is the decay constant for radium, λ_{Rn} is the decay constant for radon, t_{Ra} is the time interval from the source creation date to the starting measurement date, t_{Rn} is the time interval for the total duration of radon accumulation and V_{stp} is the corrected air volume inside the calibration barrel at standard pressure and temperature (1 bar; 0 °C): using Equation 5.:

$$V_{stp} = \frac{V\ P\ 273.15}{1013.25\ T} \quad \text{Eq.5.}$$

where *p* is the air pressure in mbar and T is air temperature in Kelvin.

Radon concentration inside the chamber monitored during calibration using an calibrated ionizing chamber device (AlphaGUARD PQ2000 PRO), a device that usually use as a reference device in calibration producer (Roessler, et al., 2016).

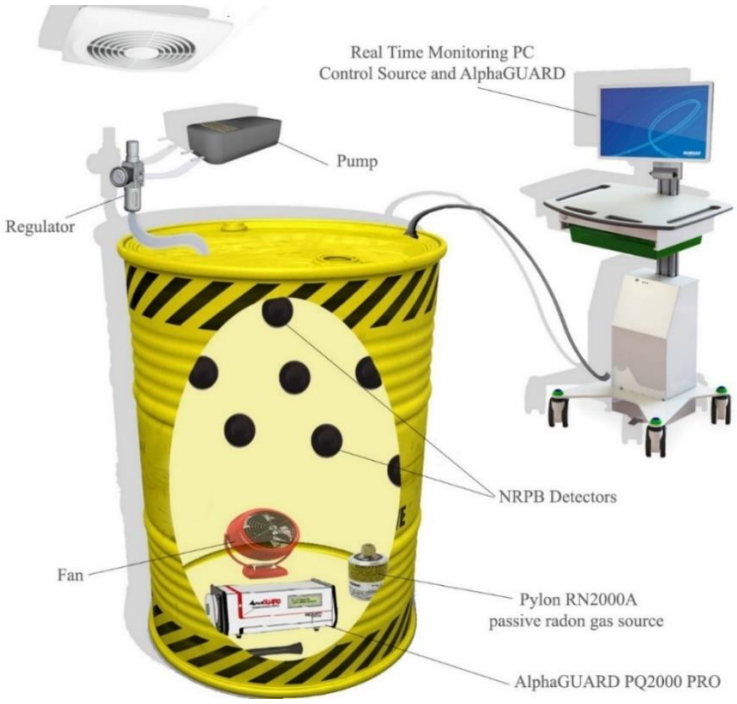

Figure 16- CR-39 Calibration System

AlphaGUARD set up in diffusion mode to conduct measurements over a period of each 30 minutes. The calibration factor "E" is given by Equation 6.:

$$E = \frac{R_S \times T \times A}{N_{net}} \quad \text{Eq.6.}$$

Where T is exposure time, N_n is the net tracks after etching.

The measurement error estimated with following Equation 7. (Bing, 1993):

$$\sigma = \sqrt{(N+B)/(N-B) + E_m} \quad \text{Eq.7.}$$

where N is the total number of counted tracks, B is background in tracks cm^{-2} and E_m is the relative deviation of reading results. For more detailed about uncertainty calculation and calibration refer to Kávási, et al., 2014 and Mansy, et al., 2000.

The repeatability of the measurements tested for track density evaluation on 10 repeated measurements including 20 detectors per each measurement while all detectors exposed in the same conditions. Three difference radon concentration conducted as: low (300 $Bq \cdot m^{-3}$), moderate (2 $kBq \cdot m^{-3}$), high (10 $kBq \cdot m^{-3}$) and an addition mode of high to low concentration, e.g. exposure started at 5 $kBq \cdot m^{-3}$ and finished at 300 $Bq \cdot m^{-3}$.

During the CR-39 calibration, the air temperature and the humidity monitored (17±2 °C to 25±2 °C and 50%±3% to 60%±3% relative humidity) to keep the condition as close as possible to the field measurement. However, this conditions were not exactly same as the underground mine, several studies (Homer & Miles, 1986; El-Sersy, et al., 2004; Yonggang, et al., 2009) are found that environmental conditions do not have any influence on CR-39, as an example, the author was involved in an intercompression radon measurements using two different types of detector (including NRPB and Raduet, CR-39 based detector and RAMARN a Kodak film based detector), finding the results of the involved detectors were in the same range (Műllerová, et al., 2016); Additionally the author compared the CR-39 based detectors' result by an active radon monitor using AlphaGUARD in three different places (thermal baths) with humidity over 85%, and found that humidity did not have influence on NRPB and Raduet, the results of one location is shown in Figure 17. (taken from Shahrokhi, et al., 2016).

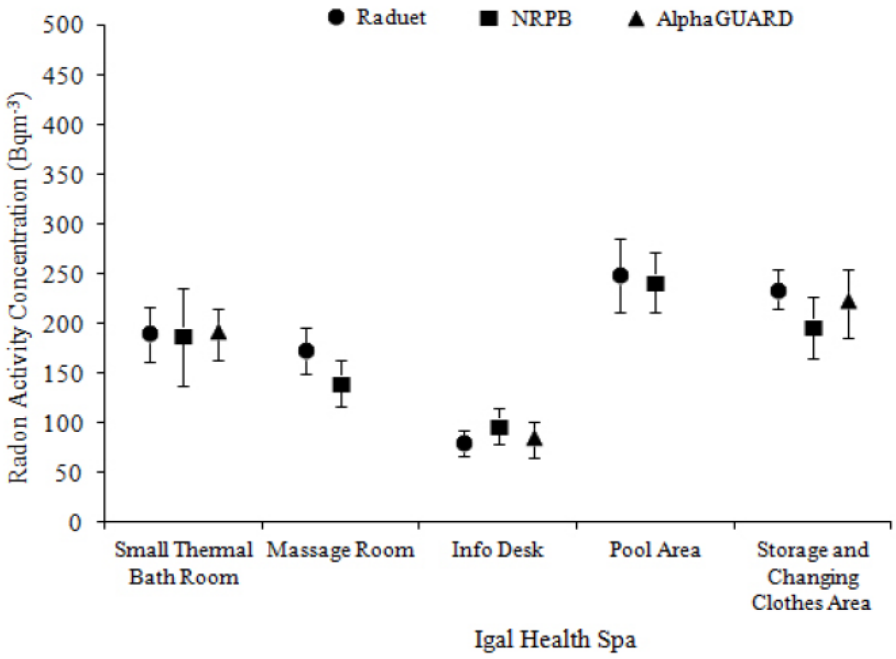

Figure 17- The performance of the three different radon detectors in Igal Health Spa

2.3. Gamma Spectrometry, Radon Emanation & Exhalation

Continuing Tamás Vigh's PhD thesis that studied on two types of rocks from the same mine (Rhodocrolitis and Black shale) and regarding to the his continues investigation suggestion, as “studying on more types of rock to clarify the contribution of different rock in radon exhalation as a tool for controlling the radon concentration in the mine”, 6 different rock types were collected from mine for gamma spectrometry and areal radon exhalation measurements, in addition to the in-situ radon exhalation measurements.

This section of study due to the importance of the topic as a part of the aim of the thesis, finding the source of accumulated radon in the mine air, and due to some limitation divided into two phases.

In the first phase, a measurement carried out to directly estimated the radon exhalation from mine walls. In the second phase, 32 samples (including 6 most abounded type of rocks) from the active area of the mine's walls were collected and transferred to the laboratory of the Institute of Radiochemistry and Radioecology at the University of Pannonia by the manager of the mine for specific aeric radon exhalation; In addition, a gamma spectrometry used to identify and quantify of radionuclides in the rock samples. The quantity of Ra-226 in the samples can help to get an overview of radon exhalation from surface of materials; The quantity of K-40 was measured as it is common in point of radioecology survive and it may help to make a glimpse of the difference in the ingredients of the rocks when there is a high variation of Ra-226 between the rocks of same family type.

Radon atoms formed from Ra-226 inside of the solid grains may not be directly released into the atmosphere due to their low diffusion coefficients. However, when radon atoms escape into the interstitial space between grains, they may be released to the surface.

The release of radon atoms from the material to the atmosphere takes place by the following series of processes: a) Emanation: the process of movement of radon atoms from solid mineral grains to the interstitial space between the grains. b) Transport: the process of diffusion and advective flow causing movement of the emanated radon atoms through the material to the surface and c) Exhalation: the process of movement of radon atoms from the surface of the material to the atmosphere (Nazaroff, et al., 1998). Figure 18. shows a perspective of radon emanation and exhalation process from a material that contains radium.

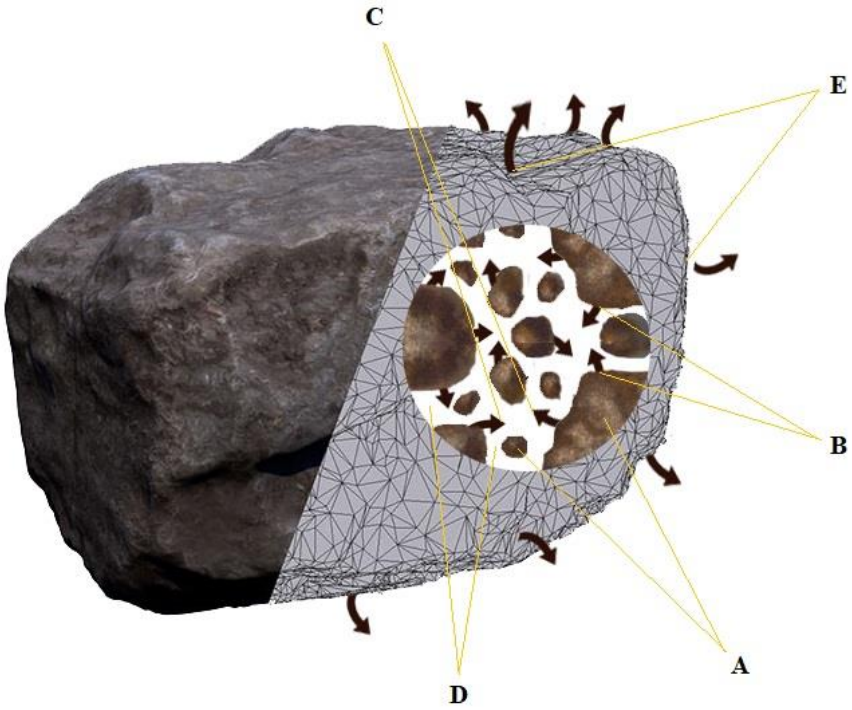

Figure 18- Megascopic of radon emanation, diffusion and exhalation process;

A: Grains; B: Radon Emanation; C: Diffusion (transfer) to pores; E: Exhalation from surface;

Radon emanation is a process of moving the generated radon atom inside the grain to the pores (intergranular space) of the material. In this a fraction of radon atoms are decayed before releasing to the intergranular space. When radon atoms emanated to pores due to its properties as a gas, it can diffuse through the pore and reach to the surface of the material while some atoms are decayed during this time; Radon transport in porous materials is described by the following multiphase time dependent radon diffusion Equation 8 & 9.

$$\beta \frac{\partial C_a}{\partial t} = D_b \nabla^2 C_a + \left(\frac{K \nabla P_{(x,y,z)} \nabla C_a}{\mu}\right) - \beta \lambda C_a - R \rho_b \lambda E \qquad \text{Eq.8.}$$

$$\beta = (1 - m + Lm)\varepsilon + \rho_b K_a \qquad \& \qquad D_b = \beta D_e; \qquad \text{Eq.9.}$$

However, diffusion rate depends on the several internal features of the material, for instant, in the precisely of this study, other experiments done to figure out how heating can influence on the pores structures of Manganese clay and reducing the radon exhalation (Kovács, et al., 2017); and, same result was obtained by Zoltan et.al. for red mud sample (Sas, et al., 2015b). In the last phase, radon atoms after reaching to the surface of material due to the diffusion and convection, exhalate as a gas phase.

2.3.1. Gamma Spectrometry

A high-resolution gamma ray spectrometer, equipped with an ORTEC GMX 40-76 HPGe semiconductor radiation detector by relative efficiency of 40%, used to evaluate all gamma emitting components, both by quality and quantity through the detection of the amplitude and energy level of the emitted gamma photons from isotopes, and hence determining the specific activities of the radionuclides (Th-232, Ra226 and K-40) in the rock samples. The detector was covered with a 20-centimetre thickness of lead shield and a layer of nickel all around to decrease the natural background rate. Data and detected gamma rays analysed by Aptec MCA Multichannel Analyzer software. The activity concentration of radionuclides ($Bq \cdot kg^{-1}$) calculated using Equation 10.:

$$A_X = \left(\frac{1000\ N}{T_c\ P_\gamma\ \varepsilon\ M\ S}\right) \qquad \text{Eq.10.}$$

where A_x is activity concentration of specific radionuclide in time of sampling ($Bq \cdot kg^{-1}$), N is net count rate of photopeak, T_c is expressed as live counting time (second), Pγ is probability of gamma ray transition via the specific energy, ε is the counting efficiency at specific photo-peak energy, M is the sample mass (Kg), t is time interval between sampling and measuring (day), $t_{1/2}$ is half-life of radionuclide calculated, S is decay correction factor ($= e^{-\lambda t}$) and λ is decay constants calculates using following Equation 11.:

$$\lambda = \frac{Ln(2)}{t_{1/2}} \qquad \text{Eq.11.}$$

To determine the activity concentration of Ra-226, Th-232 and K-40, following energy peaks, regards to their sufficient discrimination of gamma ray energy, used (IAEA, 2007; Somlai, et al., 2008):

- Determination of Ra-226 activity concentration by average of energy peaks of: (1) Pb-214: 351.9 keV with 0.3534 emission probability, and (2) Bi-214: 609.3 keV with gamma emission probability of 0.451.
- Measuring of the activity concentration of Th-232 by the average of Th-228 and Ra-228 activity; Th-228 concentration determined using energy peaks of: (1) Pb-212: 238.6 keV with 0.436 probability of gamma emission, and (2) Tl-208: 583.2 keV by emission probability of 0.3055. Ra-228 concentration determined by energy peaks

of Ac-228: 911.1 and 969.1 keV with emission probability of 0.277 and 0.166, respectively.

- The activity concentration of K-40 directly via its energy peak at 1460.82 keV with a gamma ray emission probability of 0.107.

Background contribution measured for an empty Marinelli container with the same geometry of standard and sample container for 200000 seconds and each sample counted for 100000 seconds. Equation (5) and (6) show the calculation of uncertainty and Minimum Detectable Limit of measurement in accordance with given data by Aptec analyzer software.

$$MDL = (\sigma^2 + 2\sigma(\sqrt{2B}))/t \qquad \text{Eq.12.}$$

where MDL is minimum detectable for photo-peak energy, σ is uncertainty, B is background rate under photo-peak ROI and t live counting time.

Respective uncertainties were determined according to the statistical uncertainties of the peak areas provided by the Aptec analyzer software.

$$\sigma = (2\sqrt{C + B}/C) \qquad \text{Eq.13.}$$

where σ is uncertainty, C is net sample count rate under photo-peak ROI (cps) and B is net background rate under photo-peak ROI (cps).

Energy calibration performed using three closed standard sources totalling five experimental points corresponding to the peaks: (1) Cs-137 by two energy peaks of 32.19 and 661.9 keV; (2) Co-60 with two energy peaks of 1173.2 and 1332.5 keV; (3) Am-241 with 59.5 keV energy peak (IAEA, 2007). Figure 19. shows an example of full energy peak efficiency in function of gamma ray energies as a typical efficiency for High-purity Germanium detectors.

To ensure the quality of the analysis, a certified soil standard, provided by the International Atomic Energy Agency with a known activity concentration of various radionuclides, used to validate the gamma spectrometer measurements. The author followed the internal QA protocol standard, prepared in the Institute of Radiochemistry and Radioecology at the University of Pannonia, and also to get a representative sample, a huge amount of the sample sieved and homogenizing (ASTM E300, sampling standard of solid materials, was followed to prepare representative sample). The laboratory regularly takes part in intercomparing projects to keep its own quality assurance updated.

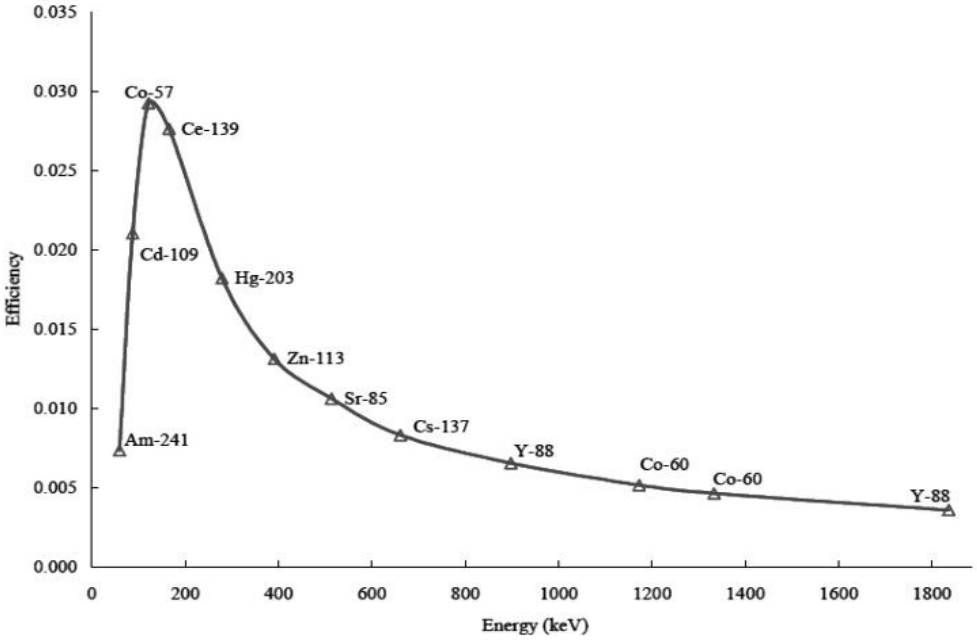

Figure 19- The gamma spectrometry efficiency graph

2.3.2. Determination of Radon Emanation Factor

In the fact, the physical behaviour of radon in ore, rocks and soil is characterized by an emanation coefficient. As explained in previous section radon emanation may express as entering of the radon atoms from the grains that contain Ra-226 to the pore spaces of the material. The amount of the escaped radon atoms per the total number of generated radon atoms from the radium known as the emanation factor.

The emanation process can be divided into components of alpha recoil and diffusion. Regarding to the results from previous studies (Nazaroff, 1992; Nazaroff, et al., 1998), the diffusion coefficient of radon in the grain of the materials can be very low between $1 \cdot 10^{-30}$ and $1 \cdot 10^{-68}$ $m^2 \cdot s^{-1}$ by the relative diffusion length of $1 \cdot 10^{-12}$ to $1 \cdot 10^{-31}$ m; Therefore, it can be considered that alpha recoil is the main component of emanation. Radon atoms generated by the alpha decay of its parent nuclide (radium), recoil with an initial energy of 86 keV; however, just radium atoms within the recoil range from the grain surface can produce radon atoms with the possibility of being emanated to the pore spaces (Sakoda, et al., 2011). Even if radon atoms release from radium-bearing grains, not all can be regarded as emanated radon as some may contained inner pore space, or absorbed on the inner surface, or stayed

on the surrounded area by other grains, or collide with a neighbouring grain, more details can be found published study (Figure 20.) (Sakoda, et al., 2011).

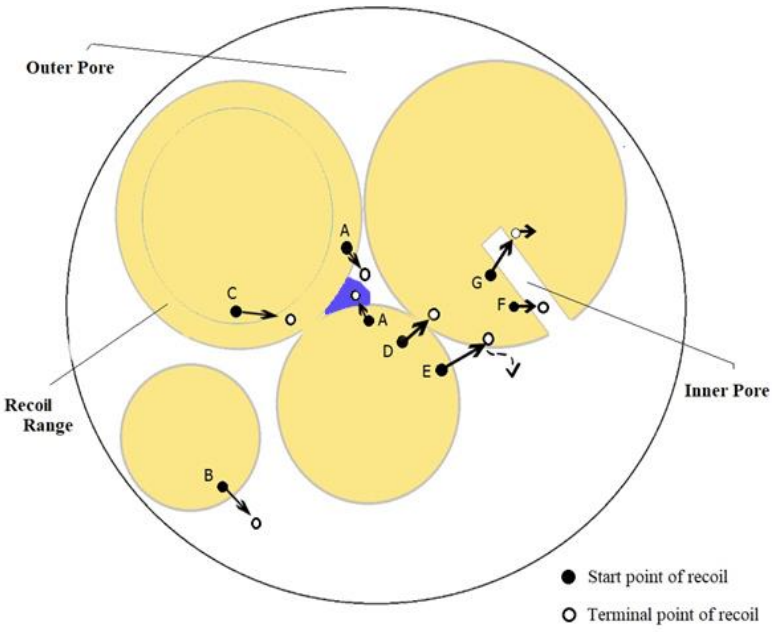

Figure 20- Microscopic scheme of radon emanation phenomenon and probability.

Points (A), (B), (E) and (F) present as emanation Points; And Not emanation as (C), (D) and (G). If radon cannot diffuse out into outer pore spaces, such as happening on points (A) and (F), should not be regarded as being emanated. Arrows following terminal points of recoil represent diffusion process, which are not to scale.

Two factors of radium distribution and grain size are play the important role in radon emanation. If assuming that radon is not embedded into an adjacent grain, the radon emanation fraction (F) from aspherical grain can be expressed as follows (Sakoda, et al., 2011):

(A) Uniform radium distribution in the grain

$$Ra \propto V \quad and \quad Rn \propto S \rightarrow F \propto {}^{S}/_{V} \propto {}^{1}/_{d} \qquad \text{Eq.14.}$$

(B) Radium distribution concentrated on the grain surface

$$Ra \propto S \quad and \quad Rn \propto S \rightarrow F \sim constant \qquad \text{Eq.15.}$$

where Ra and Rn are amounts of radium and radon emanated, respectively, V (μm^3) is volume of the grain equal by [(4/3) $\pi(d/2)^3$], S (μm^2) is specific surface area of the grain (=$4\pi(d/2)^2$), and d (μm) in diameter of the grain.

In Figure 21. (retrieved from Sakoda, et al., 2011), a calculated of radon emanation factor in the single-grain model shows the relationship between grain size and radon emanation as line (a); in addition, line (b) shows the behaviour of radon emanation regarding to grain size up to 10 μm.

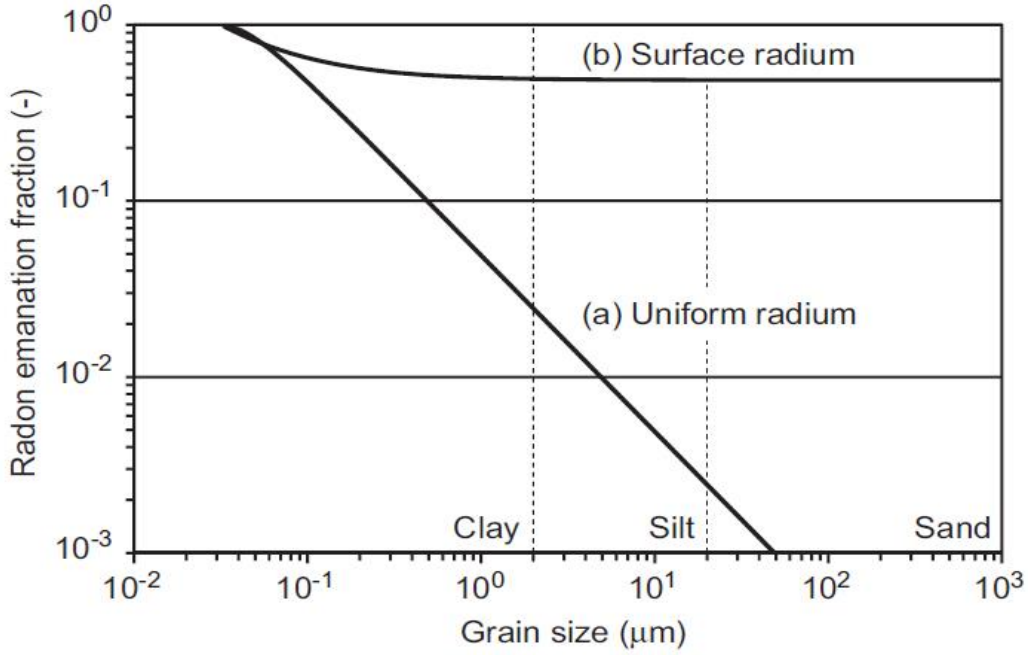

Figure 21- The relation between radon emanation fraction and grain size

Radium is assumed to be distributed (a) uniformly in a spherical grain or (b) on the surface of a spherical grain. As seen in line (a) grains more than 10 mm significantly emanates no radon (disregarding the surface emanation), and in line (b) the radon emanation first decreases by increasing grain size and then reach to a constant rate.

Regarding to the fact that the thickness of the samples was small in comparison to the diffusion length, the radon emanation coefficient could be calculated according to the relation using Equation 16.:

$$f = \left(\frac{E_{Rn}}{C_{Ra}}\right)\left(1 - e^{-\lambda t}\right) \qquad \text{Eq.16.}$$

For quality assuring, the author followed the internal QA standard protocol of the Institute of Radiochemistry and Radioecology at the University of Pannonia was developed by Zoltan Sas (Zoltan Sas's Ph.D. thesis) , however, the institute takes part in intercomparing measurements with other laboratories to keep its QA protocol up to date.

2.3.3. Radon Exhalation

Eventually emanated radon atoms travel through the pores in the material and reach to the surface area. As the surface radon exhalation is on focus in this section, the diffusion process can be assumed to take place in one-dimension along the thickness of the wall towards the surface. Taking that direction as the x-axis, with the origin at the centre of the wall, the diffusion is described by Fick's second law as: (Orabi, 2017a; Orabi, 2017b)

$$\frac{\partial C(x,t)}{\partial t} = D\frac{\partial^2 C(x,t)}{\partial x^2} + g - \lambda C(x,t) \qquad \text{Eq.17.}$$

where C is the radon concentration in the space between grains ($Bq \cdot m^{-3}$), t is the time (s), D is the diffusion coefficient ($m^2 \cdot s^{-1}$), λ (= ln(2) /$t_{1/2}$) is the radon decay constant, and g is the radon production rate per unit pore space ($Bq \cdot m^{-3} \cdot s^{-1}$).

Simplifying the above equation using C as time independent following the concept of a steady state by Equation 18.:

$$C(x) = A_1 + A_2 cosh\left(\frac{x}{l}\right) \qquad \text{Eq.18.}$$

where A_1 & A_2 are constants, and l (= $\sqrt{D/\lambda}$) is the diffusion length as the average distance of transition of the radon atoms during one half-life time.

Solving Equation 7. using Equation 8. and placing 0 on the left side of the equation, A_1 will be equal by g/ λ. Boundary condition can be applied to find A_2 as the concentration of radon inside the wall is much higher than outside: placing 0 as C(L) where L is express as half thickness of the wall, thus $A_2 = -A_1/\cosh(L/l)$. Therefore, simplifying gives Equation 19.:

$$C(x) = \left(1 - \frac{\cosh\left(\frac{x}{l}\right)}{cosf\left(\frac{L}{l}\right)}\right)\frac{g}{\lambda} \qquad \text{Eq.19.}$$

As the radon atoms reach to the surface of the wall, exhalate and enterers to the air, it is known as surface radon exhalation where can be calculated using Equation 20.:

$$E_{wall} = \left|-pD\frac{dC(x)}{dx}\right|_{x=l}, \qquad \text{Eq.20.}$$

where E_{wall} is surface radon exhalation ($Bq \cdot m^{-2} \cdot s^{-1}$), p is the porosity of the material.

Applying Equation 19. into the Equation 20. as a part of the solution and using l = $\sqrt{D/\lambda}$:

$$E_{wall} = pgl \tanh(\frac{L}{l}) \quad \text{Eq.21.}$$

$$g = \frac{a\,\eta\,\lambda\,\rho}{p} \quad \text{Eq.22.}$$

where a is the activity concentration of radium (in this study Ra-226) (Bq·kg^{-1}), and ρ is the material's density (kg·m^{-3}).

Combination two above equations, giving a simple Equation 23. to estimate the radon exhalation from wall:

$$E_{wall} = a\,\eta\,\lambda\,\rho\,l \tanh(\frac{L}{l}) \quad \text{Eq.23.}$$

Surface radon exhalation measurements carried out using CR-39 based can method (radon accumulation chamber method) in size of 6 cm (height) and 11 cm (diameter) covering a total surface of 95 cm^2. The cans were sealed on the surface of the mine wall in 5 different locations, as shown in Figure 15. This method is based on trapping the exhalated radon from the surface and growth inside the accumulation chamber (Figure 22. is shown a schematic of surface radon exhalation measurement using can method). The correlation between accumulated radon and the radon exhalation expresses as:

$$C_{Rn} = \left(\frac{E_{Rn}\,S}{V\,(\lambda+L_{Rn})}\right)\left(1-e^{-\lambda t}\right) \quad \text{Eq.24.}$$

where C_{Rn} is accumulated radon concentration for period of t (Bq·m^{-3}), S is the canister base (m^2), L_{Rn} is leaked radon concentration for period of t, V is the canister total volume (m^3).

Simplifying Equation 24., assuming knowing the accumulated radon concentration in terms of accumulation period, gives Equation 14. to estimate radon exhalation for a specific area:

$$E_{Rn} = \frac{C_{Rn}\,\lambda\left(\frac{V}{S}\right)}{1-e^{-\lambda t}} \quad \text{Eq.25.}$$

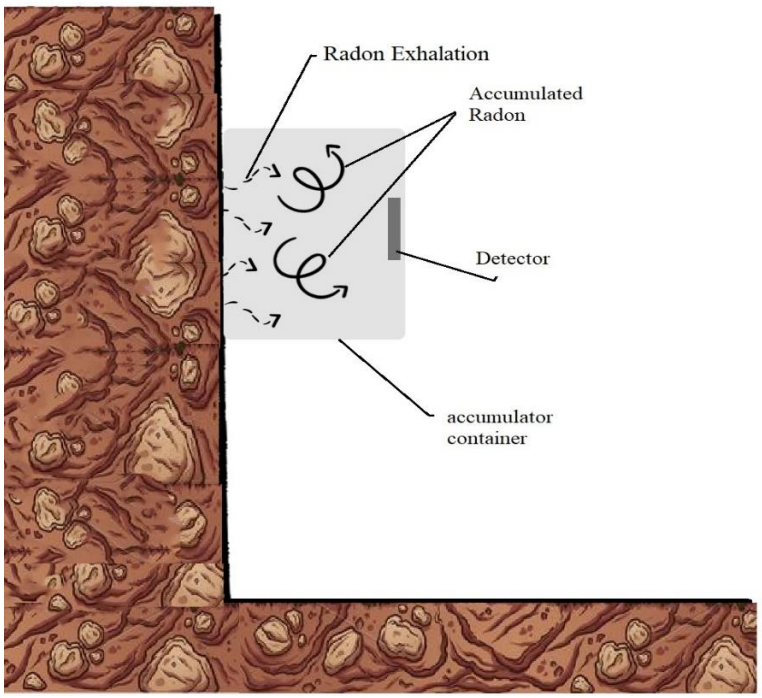

Figure 22- Radon exhalation measurement based on the can method)

In addition to the in-situ radon exhalation measurements, about 32 rock samples of total 6 different kind of rocks (Table 17.) were collected from the mine area for ex-situ aeric radon exhalation. In this method, each sample in three different cylinder length (thickness) with a known surface area (113 cm^2), stored and sealed in a leak proof (leakage rate = < 1%), waiting for a period of 24 to 27 days to accumulate exhalated radon (the condition of the samples was kept in their original condition at the time of sampling). An AlphaGUARD (PQ2000, Saphymo Gmbh, Germany) connected to the chamber as a loop system and pump run for about 15 minutes to reach equilibrium in the system (AlphaGUARD, pump, pipes and container). Then the pump was turned off and waited for 2 to 5 minutes to clear the influence of thoron (Rn-220) and then the measured radon concentration recorded.

The areal radon exhalation from samples determined using Equation 26.:

$$E_{Rn} = \frac{C\,(V_1+V_2+V_3+V_4)\,\lambda}{A\left[T+\frac{1}{\lambda}(e^{-\lambda t}-1)\right]} \qquad \text{Eq.26.}$$

where V_1, V_2, V_3, V_4 are the volume of container, AlphaGUARD, pump and pipes, respectively.

Author followed the internal QA standard protocol of the Institute of Radiochemistry and Radioecology to get more reliable results; Likewise, the institute takes part in intercomparing measurements with other laboratories to assure its own protocol.

2.4. Radon in Water

The drained water in the underground mines can be recognised as a potential route of entry radon to the mine atmosphere. Sometimes water can solve huge amount of radon during passing through the soil and rocks, and then exhalate passing through mine wall or ground. Therefore, due to the importance of the Radon's pathways into the mine, a long-term (two and half years, each month) dissolved radon concentration monitoring in the mine water carried out to not only monitor the behaviour of radon concentration in different seasons but also using a simple modelling calculation to estimate the contribution of the dissolved radon in the water to the radon concentration in the mine air.

To determine the dissolve radon concentration in the water samples, the emanometry measurement method based on water degassing was conducted using RAD7 and AQUA kit. In this method, water sample is degassed using a radon free gas (usually nitrogen gas), dissolved radon in water extracts and transfers to a radon measurement instrument either by gas flow or air circulation (Műllerová, et al., 2016).

8 samples from different parts and collection pools were collected in a glass bottle (250 ml) with a metal cap to ensure any radon leakage and transfer immediately to the laboratory by the mine manager. The author measured dissolved radon concentration in the water samples using RAD7 (Durridge Company, Inc.) with H_2O accessories in the same day of delivery. Before starting the measurement, the RAD7 decontaminated by passing nitrogen gas over the instrument for about 15 minutes to reduce the background and flush the system. A closed loop circuit system was installed between H_2O kit and RAD7, Figure 23. shows the schematic of the measurement system.

The RAD7 set for 30 minutes measurement cycle by changing the pump mode from GRAB to ON. The first 15 minutes recorded results was denied, in order to reaching the equilibrium in the system between the liquid and gas phase. In the other words, when radon degases from liquid phase and transfer to the gas phase, some amount of radon will remain in the water or dissolve again as it's a closed loop system until reach to its equilibrium. The equilibrium ratio of the concentrations expresses as $\propto$ and determined using the von Weigel equation. In the equilibrium condition, a volume of water (V_w) contain as much radon as a volume $\propto V_w$ (air-equivalent volume of the water) (DURRIDGE Company Inc., 2018).

The dissolved radon concentration in the water samples determined using Capture RAD7 data acquisition and analysis software by inserting requested data, based on the following equations.

As the water temperature can influence the radon degassing rate, using correction equation is necessary. Therefore, temperature of water samples during the measurement recorded. Before connecting the water bottle to the RAD7, the system flush with nitrogen gas to eliminate any pre-exciting radon in system. The minimum detection level, based on the RAD7 background, calculated as 0.2 $Bq \cdot L^{-1}$.

Radon concentration in the water samples calculated using the following Equations 27 & 28, assuming where background concentration in recirculating air is negligible (before introducing water, system flushed with nitrogen gas for about 5 minutes) (DURRIDGE Company Inc., 2018) :

$$Rn = C_w\, V_w - \Delta\, Rn \qquad \text{Eq.27.}$$

$$Rn = C_w\, (\tfrac{V_w - V_h}{\alpha}) \qquad \text{Eq.28.}$$

The total equivalent air volume of the system is equal to $V_a + \propto V_w$. The total radon in the system, is distributed by this volume, therefore the concentration in the air loop at equilibrium will be:

$$C_a = \left(\tfrac{Rn}{V_a + \alpha\, V_w}\right) \overset{or}{\Rightarrow} Rn = C_a\, (V_a - \alpha\, V_w) \qquad \text{Eq.29.}$$

substituting for Rn:

$$C_w = \tfrac{C_a\, (V_a + \alpha\, V_w)}{\left(\frac{V_w - V_h}{\alpha}\right)} \qquad \text{Eq.30.}$$

Using a standard RAD7, a laboratory drying unit and typical room temperature, such that $\propto = 0.25$, this would reduce to:

$$C_w = \tfrac{C_a(1.302 + 0.625)}{(2.5 - 0.06)} = C_a\, (0.790) \qquad \text{Eq.31.}$$

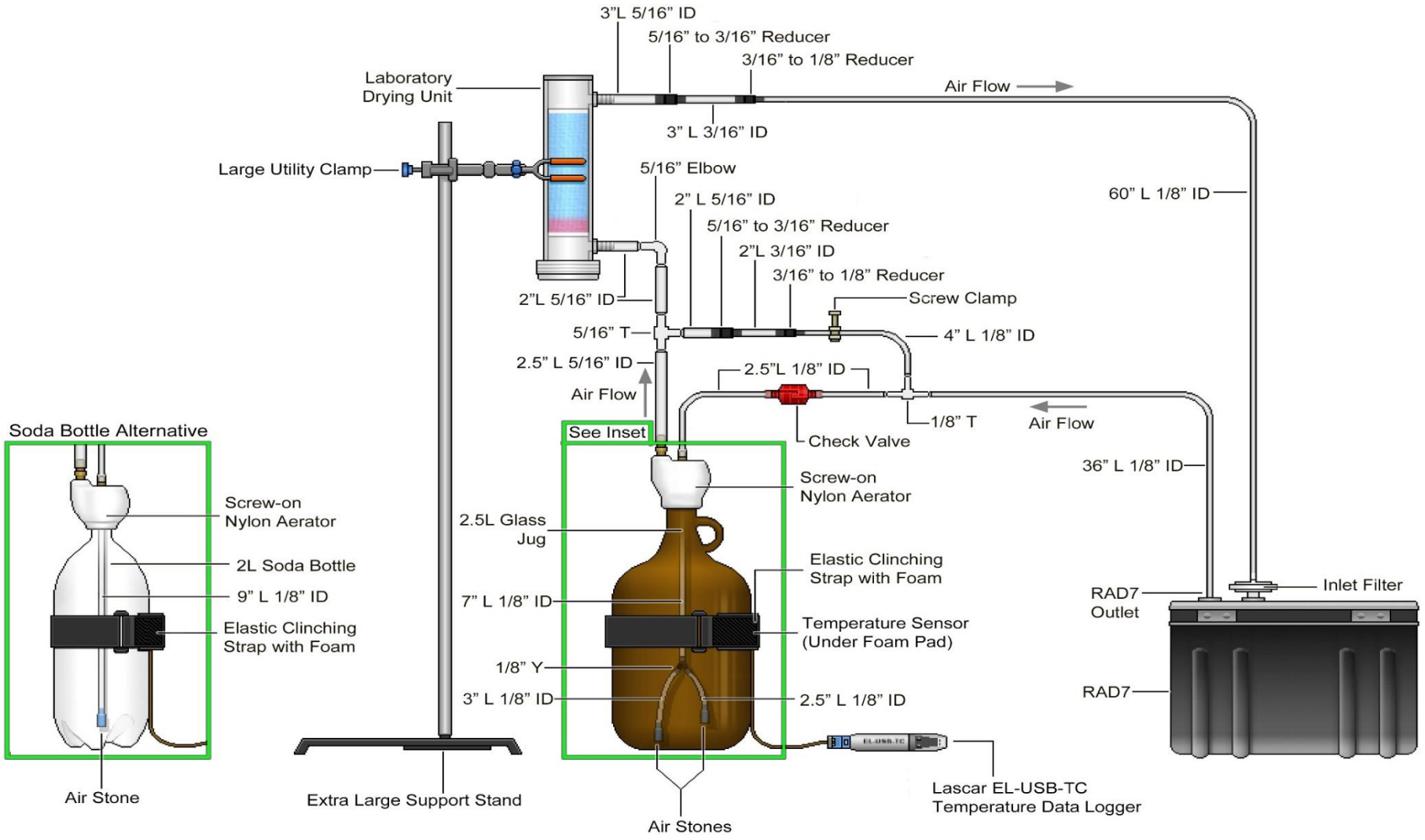

Figure 23- Rad7 radon monitor – Aqua kit to measure radon concentration in water adopted from (DURRIDGE Company Inc., 2018)

Combination above equations gives a simple equation to calculate the radon concentration in the water sample at time of sampling:

$$C_{wt} = \left(\frac{C_a(V_a + \alpha_T V_w) - \left(\frac{V_h}{\alpha_T}\right)}{\varepsilon} \right) \left(1 - e^{-\lambda t}\right) \qquad \text{Eq.32.}$$

where Δ Rn is total radon in system, C_{wt} is original radon concentration in the water at time of sampling, C_w is radon concentration in the water at the time of measuring, C_a is equilibrium radon concentration in system, V_a is total volume of air in the system, V_h is volume of head space in bottle, V_w is volume of water sample in bottle, α_T is equilibrium coefficient from Fritz von Weigel ($= 0.105 + 0.405\, e^{-0.0502T}$) (Weigel, 1978), S ($=1\text{-}e^{-\lambda t}$) is decay correction factor, T is temperature of water at time of measurement, and ε is calibration factor (efficiency) of instrument.

The author calibrated the system using a known activity radon concentration liquid. A diluted solution mixture of desalinated water and liquid Ra-226 used as calibration liquid. 1L homogenised reference liquid concentrated with 6 $Bq \cdot L^{-1}$ of Ra-226 used to calibrate the system. A portion of the reference liquid stored in a 250-ml glass with a radon tight Teflon cap (the glass of the RAD7 H2O kit). Bottle stored for about 29 days to reach equilibrium between Ra-226 and Rn-222. Then using same system of conducted for sample measurement, the instrument calibrated based on the measured dissolved radon concentration in the reference liquid with the known activity concentration. This process repeated 5 times to get a good reputation value.

As the uncertainty contributions are concerned in the laboratory researches, identifying the potential sources of causing errors in an experiment is necessary to get a reliability results. The significant uncertainty contributors for this measurement can name as: system calibration, leakage rate, de-gassing, decay constant, etc. Table 10. shows a list of uncertainty sources for three different measurement methods (Jobbágy, et al., 2017).

Table 10- The comparison of different methods for measuring radon in water

Uncertainty Sources	Gamma spectrometry	Emanometry	LSC
Instrument Efficiency	+	+	+
Radon transfer (de-gassing)	-	+	-
Activity of the Calibration Solution	+	+	+
Calibration Factor	-	+	-
Sample Volume	+	+	+
System Volume	-	+	-
Background Radon	+	+	+
Spectrum Analysis	+	-	+
Leak	+	+	+
Counting Statistics	+	+	+
Uncertainty half-life	+	+	+
Decay Calculation to Reference Time	+	+	+
+ : Applicable - : Not Applicable			

2.5. Radon Exposure & Dosimetry

As it was explained on introduction section, Radon (Rn-222) is well known reason of a high lung cancer incidence in miners. Short-lived radon decay products (Po-218 and Po-214) in the air can be divided into two categories: (1) a fraction that is attached to the existing aerosol in the atmosphere; and (2) a fraction that contains in their origin ionic or atomic form together with those that have grown to small clusters known as unattached fraction (Vanmarcke, et al., 1985); The equilibrium concentrations can calculate directly using these two fraction. From a radiological point of view, radon is not a major source of concern, as the effective dose from the inhalation of radon is low; Mainly, the short-lived radon decay products deposited in the lung tissue deliver dose (Marsh, et al., 2017).

There are two approaches in the dose assessment due to radon and its short-lived decay products: (A) Epidemiological dosimetrist models (e.g. ICRP and EPA); and (B) Realistic dosimetric model calculations approach. While each approach has different results based on the parameter used to estimate the dose, e.g. attached/unattached fraction, equilibrium factor and calculated does conversion factor (DCF). All previous conducted studies about the does estimation in case of Úrkút manganese miners was based on the average accumulated radon concentration in the mine air, however in this study, a long-term dose assessment, using personal radon dosimeters, carried out to specifically monitor the exposure of miners to the radon during working hours.

2.5.1. Radon Exposure

The exposure to radon and its short-lived decay products in the workplaces is dealt with the Council Directive of the European Union 2013/59/Euratom (adopted on 05 December 2013, with a four-year transition period, became enforceable on 06 February 2018). In the Article 54, the annual average radon concentration in air shall not be higher than 300 $Bq \cdot m^{-3}$ in workplaces (Council of the European Union, 2014). Monitoring of the occupational exposure to radon can take several forms, monitoring the radon concentration in the area or with personal dosimeters. Monitoring area radon concentration is highly popular due to its convenience and ease to carry out (as it is the case of EU-BSS). However, when accurate values of the radon exposures are needed, e.g. in epidemiological studies or

dosimetry approach, personal dosimetry can be a choice for not only monitoring the exposure of workers to radon, but also, applying as a tool for health risk assessment.

10 randomly miners, working mainly in the active area of Úrkút manganese mine, were selected for a long-term radon dosimetry. Integrating alpha Track Personal Dosimeter Detectors (PDD) used to estimate the annual average Rn-222 exposure level to the miners. A dosimeter based on diffusion chambers (radon gas selective chamber NRPB) enclosing a Solid-State Nuclear Track Detector (CR-39) used for the current study; The selected miners asked to attached the detectors to their body when start to work and at finishing working time put detector in a radon proof plastic bag and store in a box outside of the mine located on fresh air filter by activated charcoal (it could help to eliminate the background radon disturbance). However, to determine the background, additional detectors (one in the radon proof bag to calculate the background of detectors during preparation, and one without radon proof bag in order to measure the fresh air radon background), were placed on the detector collection box. The background was negligible as the detectors (CR-39) were covered by a plastic film and sorted in an aluminium foil in the fridge. Exactly some hours before sending detectors to the mine, the author removed the plastic films from the surface of each detector, placed on the housing cap and after putting on the radon proof bag, vacuumed the air inside the bag and sealed it. The outdoor background radon concentration in the fresh air measured between 7 to 11 $Bq \cdot m^{-3}$.

Then at end of each exposure period (15 days exposure period in each mont for one year), the average radon exposure per each miner evaluated using same method explained on 3.3.1.1 in this thesis.

Exposure to radon and its airborne decay products is expressed as any combination of short-lived radon decay products in 1 cubic meter of air with the potential of emitting 20.8 μJ of alpha particle energy and shows by WL unit (U.S. Environmental Protection Agency, 1993). Working Level Months is a unit of exposure to 1 WL for 170 hours; Annual radon progeny exposure is calculated following Equation (U.S. Environmental Protection Agency, 2003). In the absence of experimental data on equilibrium factor between radon and its progeny in the representative houses, the EPA recommended value used to estimate annual radon exposure.

$$WLM_a = C_{Rn} \left(\frac{F}{3700}\right) S \left(\frac{H_a}{170}\right) \qquad \text{Eq.33.}$$

where WLM_a is the annual exposure level to radon decay products, C_{Rn} is the average of radon concentration ($Bq \cdot m^{-3}$), F is the equilibrium factor, S is the factor of spending time in workplace, and H_a is total annual hours.

2.5.2. Determination of Attached, Unattached Fraction & Equilibrium Factor

The short-lived radon decay products are positively charged alpha emitted particles and have a high mobility what makes them easily attach to existing aerosol particles in the atmosphere within seconds, forming the radioactive aerosol or known as radon attached progenies.

The unattached fraction of radon progeny determined using Equation 34. (Kávási, et al., 2011):

$$fun = \left(\frac{PACE_{un}}{(PACE_{att}+PACE_{un})}\right) \qquad \text{Eq.34.}$$

where fun is the unattached fraction, $PAEC_{un}$ is the potential alpha energy concentration (PAEC) of unattached radon progeny ($J \cdot m^{-3}$), and $PAEC_{att}$ is the potential alpha energy concentration of attached radon progeny ($J \cdot m^{-3}$).

Attached and unattached fractions of short-lived radon decay products measured using the EQF3220 (SARAD, Germany) supplied with high-end semiconductor radiation detectors and a built-in pump system with sampling head that applies a screen filter mesh grid with 5-nm cut-off size to let complete unattached fraction (< 5nm) deposit on the screen, while, the attached progenies (> 100nm) can pass screen and deposit on the surfaces of the duct and the detector, Figure 24. (SARAD GmbH, 2016).

Measurements done for a period of 5 days in each season with hourly measurement cycle during working hours. Then the unattached fractions of radon progeny calculated using obtained data. The EQF3220 calculates following results: (1) detector filter: EEC and PAEC of the attached fraction of Rn-222 daughters; and (2) Detector screen: EEC and PAEC of the unattached fraction of Rn-222 daughters.

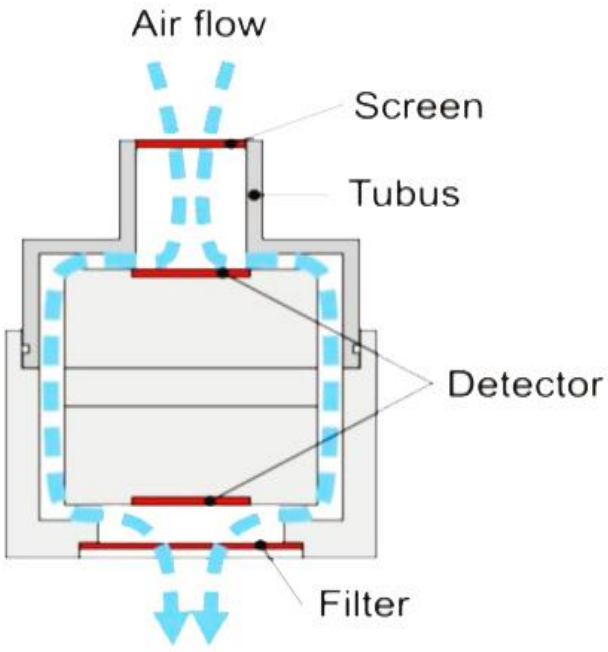

Figure 24- aerosol sampling head installed on SARAD EQF3220

The relative error of the measurement results depends on the magnitude of concentration of the radon and its progeny measured. For concentration above 1000 $Bq \cdot m^{-3}$ the relative error was between 5% and 8% with an average of 6%, and for low concentration (between 200 $Bq \cdot m^{-3}$ and 1000 $Bq \cdot m^{-3}$) recorded around 14% (from 10% to 16%). The device was sending to the manufacture in Germany approximately every year for calibration. The background of the device measured using loop system with a radon free gas chamber (nitrogen gas) for 30 minutes measurement cycle for 3 hours, then the geomean of measured values observed (8 ± 12 $Bq \cdot m^{-3}$) as background value.

Then by using data from SARAD EQF3220, the equilibrium factor is calculated using Equation 35.:

$$F = \left(\frac{EEC_{att} + EEC_{UN}}{C_{Rn}}\right) \qquad \text{Eq.35.}$$

Where F is the equilibrium factor, C_{Rn} is the concentrations of Rn-222, EEC_{att} and EEC_{un} are equilibrium equivalent radon concentrations for attached and unattached progenies, respectively.

Additionally, Pylon WLx (Radon Daughter Element Concentration Measuring) used to measure Simultaneously the radon concentration, radon working level and equilibrium

equivalent concentration (EEC) that can use to calculate equilibrium factor (F) (Shahrokhi, et al., 2017).

2.5.3. Determination of Dose Conversion Factor

As it was mention at the first of this section, there are two approaches in the dose assessment regarding to radon exposure which influence on dosimetry results, e.g. dose assistant based on the epidemiological models which a theoretical per calculated dose conversion factor based on general population are provided for dose calculation, however, in some cases these values are much higher or much lower than the real value due to the factors (these factors can vary from one location to another) that effect on dose conversion coefficient (like as breath behaviour, equilibrium factor and attached an unattached fraction); On the other hand, in case of dosimetric approach, the dose conversion factor is calculated based on obtained related results from field measurements.

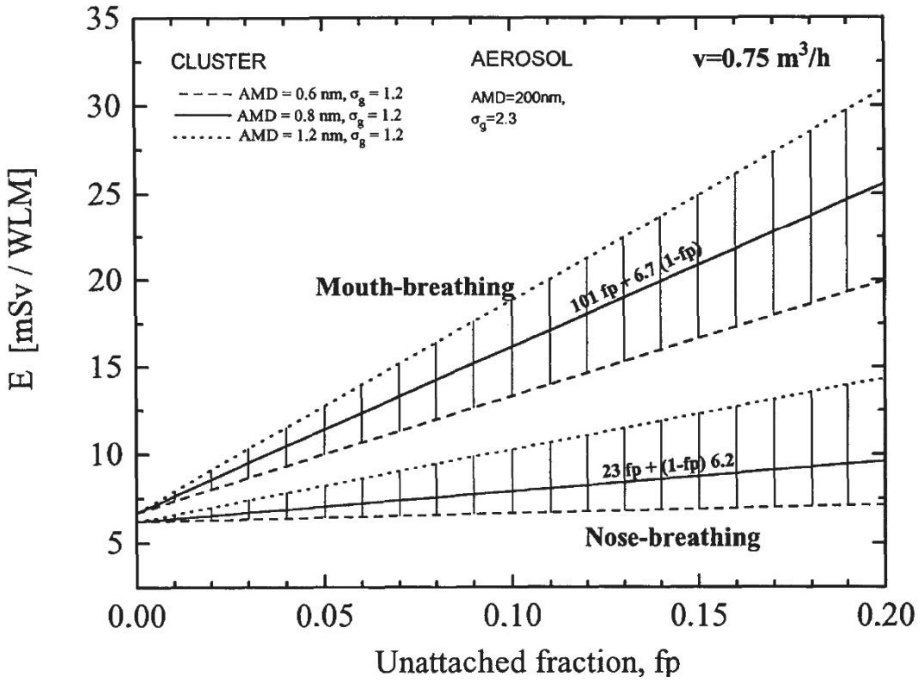

Figure 25- Influence of the unattached fraction (fp) on the DCF (E) (Porstendörfer, 1996)

Thus, beside the given values by some organization, the dose conversion factor can be calculated, based on dosimetric model calculation regarding the results from filed

measurement and depends on the breath behaviour (Figure 25.), using Equations 36. & 37. (Porstendörfer, 1996):

$$DCF_m = 101\, f_{un} + 6.7\,(1 - f_{un}) \qquad \text{Eq.36.}$$

$$DCF_n = 23\, f_{un} + 6.2\,(1 - f_{un}) \qquad \text{Eq.37.}$$

where DCF_m and DCF_n is the dose conversion factor for mouth breathing and nasal breathing ($mSv \cdot WLM^{-1}$), respectively.

According to the results obtained by Bennett et al., breathing behaviour of a heavy physical male worker, e.g. miner, is a ratio of 60% mouth breathing and 40% nasal, therefore, the dose conversion factor for miners can be calculated using the Equation 38.:

$$DCF_{mn} = 0.6\, DCF_m + 0.4\, DCF_n \qquad \text{Eq.38.}$$

where DCF_{mn} is the dose conversion factor for combined breathing ($mSv \cdot WLM^{-1}$).

In this study the author has been tried to use both the dosimetric approach and epidemiological model given by ICRP and EPA to calculate dose conversion factor and prepare a comprehensive comparison between values obtained from dosimetry.

2.5.4. Estimation of Effective Dose

As previously explained, radon by itself is not in concern as almost all inhaled radon is subsequently exhaled; However, the short-lived radon progenies are responsible of any damage to tissues. The rate of change of a j^{th} radon decay product alpha-activity in a compartment i of the respiratory tract at any time is given by the following Equation (ICRP, 1994; Rabi & Oufni, 2018):

$$\frac{dA_c^i(j)}{dt} = F_d(i)\, I_0(j) + \sum_n \lambda_{n,i} A_c^n(j) - \left(\sum_n \lambda_{i,n} + \lambda_j\right) A_c^i(j) \qquad \text{Eq.39.}$$

where $F_d(i)$ is the fractional deposition in the compartment i of the respiratory tract of workers, $I_0(j) = B \cdot C(j)$; where B is the average breathing rate ($1.2 \cdot m^{-3} \cdot h^{-1}$) for workers. C(j) ($Bq \cdot m^{-3}$) is the concentration of the j^{th} radon decay product indoor air, $\lambda_{n,i} = m_{n,i} + S_s$; where $m_{n,i}$ is the clearance rate from region n to region i due to particle transport and S_s is the clearance rate due to particle absorption into blood. The absorption rate of material into blood is the same in all regions of the respiratory tract, except in the anterior nasal passages

(ET_1), where no absorption occurs, and λ_j is the radioactive constant of the jth radon decay product.

Then The equivalent dose in the tissue T of the respiratory tract for a radon decay product jth is given by the Equation 40.:

$$H_T(j) = \int_0^{t'_e} H_T(j)(t)dt \qquad \text{Eq.40.}$$

where t'_e is the exposure time of the tissue T and H_T(j) is the alpha equivalent dose rate ($Sv \cdot s^{-1}$) in a tissue T of the respiratory tract of an individual due to the inhalation of the j^{th} radon decay products given by Equation 41.:

$$H_T(j)(t) = A_c^T(j)(t)\ Q\ K\ (\frac{K_j\ R_J\ S_j}{m_T}) \qquad \text{Eq.41.}$$

where $A_c^T(j)(t)$ is the alpha-activity of the j^{th} radon decay product in the tissue T of the respiratory tract (Bq), Q is the quality factor, which is equal to 20 for α-particles, m_T is the mass of the target tissue T, K_j is the branching ratio, R_j is the range of the α-particle emitted by the j^{th} radon decay product, S_j is the stopping power of the tissue T for the emitted α-particle and k ($1.6 \cdot 10^{-10}$) is a conversion factor. R_j and S_j can be calculated by using the SRIM program using the elemental chemical composition of tissues given in the ICRP publication 66 (ICRP, 1994).

The annual effective dose ($mSv \cdot y^{-1}$) due to short-lived radon decay products to the miners evaluated by using the following equations recommended by ICRP (Equation 42.) recently and using equation suggested by WHO and EPA (Equation 43.) (ICRP, 2017; Marsh, et al., 2017; U.S. Environmental Protection Agency, 2003):

$$E_{ICRP} = DCF\ (1.57 \times 10^{-6})\ \sum_i C_{Rn}\ F_i\ O_i \qquad \text{Eq.42.}$$

$$E_{EPA} = C_{Rn}\ \left(\frac{F}{3700}\right)\left(\frac{T}{170}\right)\ DCF\ =\ WLM_a \times DCF \qquad \text{Eq.43.}$$

where E is annual effective dose ($mSv \cdot y^{-1}$), T is total hours in 1 year. where C_{Rn} annual average radon ($Bq \cdot m^{-3}$). F_i equilibrium factor O_i annual occupancy (h) in location i.

2.6. Manganese Ore Mining Residue

In this study the radon emanation characteristics of manganese clay measured at different temperatures identifying the optimum firing temperature in order to minimize radon exhalation and provide useful data for later modelling and also for construction companies, and information for authorities on the maximum amounts of additives. In total 20 grab clay samples (about 10 kilograms) were taken from the difference part of the depository site, the depository site is marked for environmental monitoring, after removing the 70 cm thick upper layer (from 0 to 40 cm deep).

The relative densities measured using Density Kit and the reference liquid (White Spirit 150/200) with a density of 0.775 $g \cdot cm^{-3}$ at 15 °C. A graduated glass body of defined reference liquid volume (V1) weighed in air and marked as M1; the samples dipped into the holder and placed on an ultrasound wave shaker for 30 min and then the new volume and weight recorded as V2 and M2. Then their density calculated by dividing ΔM by the reference displacement volume (Speight, 2015).

Total pore volumes from 1 nanometre to 15 micrometres determined by combining results from ASAP 2000 gas absorption (Micromeritics, U.S.A) and mercury penetration (Micromeritics, U.S.A) methods.

The porosity features - micro porosity (< 2 nm) and mezzo porosity (from 2 to 300 nm) - and specific surface area calculated by changing the absorbed component of samples in a nitrogen gas tube under specific conditions using ASAP 2000 device (Jobbagy et al., 2009). The surface-adsorbed gases were removed with a vacuum ($p < 0.1$ mmHg) at 100°C for each representative sample (between 1 to 5 grams). Then, adsorption and desorption isotherms for nitrogen gas were measured at the temperature of liquid nitrogen. According to the BET theory (Brunauer-EmmettTeller), the specific surface of the samples was calculated (Brunauer et al. 1938). The macro porosity interval (above 300 nm) of the samples were determined using mercury penetration with the help of a SMH6 mercury; sample, between 1 to 5 grams, was placed in the glass tube and sealed to the instrument and was filled with mercury and the change in Hg level in the capillary was recorded against pressure (0 to 760 mmHg) (Jobbágy et al. 2009).

Gamma spectrometry and radon exhalation measured using same method explained in section 2.3 of current thesis.

RESULTS AND DISCUSSIONS

3.1. Routes of Radon Exhalation into the Mine Atmosphere

To comply with regulations and recommendations such as EU-BSS, firstly it is necessary to find what is the main cause of radon in an area; Then, finding a solution to mitigate radon can be easier by removing the source or using other methods to reduce radon from the origin. Depending on the type of mine, usually the main sources of radon exhalation into underground mine atmosphere (i.e. manganese mine), are: main mine walls, fresh broken ores due to mining activity, backfill tailings and water as usually mining water product dump somewhere near to the mine and leaching from surface precipitation.

3.1.1. Radon in Mine Water

In simple theory, mine water coursing through the soils and rocks (mineralised zones) dissolves exhaled radon from rocks contain Ra-226. However, the solubility of radon in the water on the normal condition is very low, under the enormous pressure of overburden, the solubility of radon increases considerably. As a matter, after mine water pass through bore holes and fissures to the mine wall surface, some part of the dissolved radon due to different pressure is exhalated directly into the mine atmosphere, and a part of remain radon is released to the atmosphere during collection, pumping and transferring processes. As a fact, this route of radon in underground mines are almost solid and cannot prevent to happen and can call as an untreatable source, however, the exhalation of radon from water mainly depends on the total contact surface of water with the air.

To find out the importance and the contribution of the dissolved radon in the water on accumulated radon concentration in the Úrkút manganese mine air, the author planned a long-term measurement (2.5 years) to monitor the dissolved radon concentration in the water samples and estimate the contribution of rich-radon water in accumulated radon concentration on the mine atmosphere.

Tables 11., 12. and 13. present the concentrations of dissolved radon in different mine water samples that were collected from 8 different places of the mine. The statistical analysis for obtained data corresponding to seasonal radon concentrations in mine water samples are summarized in Table 14.

Table 11- Monthly concentration of radon in mine water at sampling locations in 2013

Radon concentration in water samples ($Bq \cdot L^{-1}$)									
Sampling Location		**July**	**Aguste**	**September**	**October**	**November**	**December**	**Min – Max**	**Geomean**
2013	**A-1**	3.6±0.4	3.9±0.5	3.9±0.5	3.9±0.5	4.1±0.5	3.9±0.5	**3.6 – 4.1**	**3.9**
	A-2	0. 3±0.1	0.4±0.1	0.6±0.1	0.3±0.1	0.4±0.1	0.4±0.1	**0.2 – 0.6**	**0.3**
	A-3	2.2±0.2	2.3±0.3	2.5±0.3	2.3±0.3	2.5±0.3	2.4±0.2	**2.2 – 2.5**	**2.4**
	A-4	2.7±0.3	3.1±0.4	3 ±0.4	3 ±0.4	3.1±0.4	3.2±0.4	**2.7 – 3.9**	**3**
	A-5	5±0.6	6±0.7	5.4±0.6	4.9±0.6	4.8±0.6	5.6±0.6	**4.8 – 6**	**5.3**
	A-6	2.1±0.3	2.9±0.4	2.5±0.3	1.9±0.2	2.1±0.3	2±0.2	**1.9 – 2.9**	**2.2**
	A-7	2.3±0.2	2.6±0.3	2.6±0.4	2.9±0.3	3.1±0.4	3.3±0.4	**2.3 – 3.3**	**2.8**
	A-8	3.6±0.3	4±0.3	3.9±0.3	2.9±0.2	3.6±0.3	3.6±0.3	**3.6 – 4**	**3.6**
		$\sum$ ***Annual Geomean***					$\sum$ ***Annual Average***		
		3.2					**3.3**		

Table 12- Monthly concentration of radon in mine water at sampling locations in 2014

Radon concentration in water samples ($Bq \cdot L^{-1}$)															
Sampling Location		**Jan**	**Feb**	**Mar**	**Apr**	**May**	**Jun**	**Jul**	**Aug**	**Sep**	**Oct**	**Nov**	**Dec**	**Min – Max**	**Geomean**
2014	**A-1**	4 ±0.4	3.5 ±0.3	4.2 ±0.5	3.5 ±0.3	3.3 ±0.3	3.6 ±0.3	3.8 ±0.3	3.9 ±0.3	3.6 ±0.3	3.4 ±0.3	3.5 ±0.3	3.6 ±0.3	**3.3 – 4.2**	**3.6**
	A-2	0.5 ±0.1	0.6 ±0.1	0.8 ±0.1	0.5 ±0.1	0.5 ±0.1	0.3 ±0.1	0.3 ±0.1	0.4 ±0.1	0.4 ±0.1	0.4 ±0.1	0.3 ±0.1	0.5 ±0.1	**0.3 – 0.8**	**0.4**
	A-3	2.5 ±0.3	2 ±0.2	2.3 ±0.3	2.8 ±0.4	2.1 ±0.2	2.5 ±0.3	2.4 ±0.3	2.6 ±0.4	2.3 0.3	2.2 ±0.3	2.2 ±0.2	2.6 ±0.4	**2 – 2.8**	**2.4**
	A-4	3.6 ±0.4	2.2 ±0.2	2.8 ±0.3	2.4 ±0.2	2.7 ±0.3	3 ±0.3	2.9 ±0.2	2.6 ±0.3	2.7 ±0.3	2.9 ±0.3	3.1 ±0.4	2.9 ±0.3	**2 – 3.6**	**2.8**
	A-5	4.5 ±0.5	3.5 ±0.4	4.5 ±0.7	4.9 ±0.6	4.3 ±0.5	4.1 ±0.4	4 ±0.4	3.9 ±0.4	3.9 ±0.4	3.9 ±0.4	4 ±0.4	4.7 ±0.5	**3.5 – 4.9**	**4.2**
	A-6	3.2 ±0.4	3 ±0.4	3.1 ±0.4	2.9 ±0.3	2.7 ±0.3	2.8 ±0.3	3 ±0.4	3.2 ±0.4	2.8 ±0.2	2.9 ±0.3	3 ±0.4	3.3 ±0.5	**2.7 – 3.3**	**3**
	A-7	2 ±0.2	2.1 ±0.3	2 ±0.2	2.2 ±0.3	1.8 ±0.2	1.9 ±0.2	2.2 ±0.3	2.3 ±0.3	1.9 ±0.2	1.8 ±0.4	2 ±0.3	2.4 ±0.3	**1.8 – 2.4**	**2**
	A-8	2.4 ±0.3	2.5 ±0.3	2.3 ±0.3	2.3 ±0.2	2.2 ±0.2	2.1 ±0.2	2.2 ±0.2	2.4 ±0.3	2.1 ±0.3	2 ±0.2	2.2 ±0.2	2.3 ±0.3	**2 – 2.5**	**2.2**
$\sum$ ***Annual Geomean***											$\sum$ ***Annual Average***				
2.8											**2.9**				

Table 13- Monthly concentration of radon in mine water at sampling locations in 2015

Radon concentration in water samples ($Bq \cdot L^{-1}$)															
Sampling Location		**Jan**	**Feb**	**Mar**	**Apr**	**May**	**Jun**	**Jul**	**Aug**	**Sep**	**Oct**	**Nov**	**Dec**	**Min – Max**	**Geomean**
2015	**A-1**	4.4 ±0.6	4 ±0.5	4.2 ±0.5	3.4 ±0.4	3.1 ±0.4	2.8 ±0.3	2.7 ±0.3	3.2 ±0.4	3 ±0.3	3.3 ±0.4	3.5 ±0.4	3.7 ±0.5	**2.7 – 4.4**	**3.4**
	A-2	0.8 ±0.1	0.6 ±0.1	0.7 ±0.1	0.6 ±0.1	0.6 ±0.1	0.5 ±0.1	0.4 ±0.1	0.5 ±0.1	0.6 ±0.1	0.6 ±0.1	0.5 ±0.1	0.8 ±0.1	**0.4 – 0.8**	**0.6**
	A-3	2.1 ±0.3	2 ±0.2	2.4 ±0.3	2.1 ±0.3	2.1 ±0.3	2 ±0.2	1.8 ±0.2	1.9 ±0.2	2 ±0.1	2.2 ±0.3	1.6 ±0.1	2.1 ±0.2	**1.6 – 2.4**	**2**
	A-4	3.4 ±0.4	3.2 ±0.4	3.1 ±0.3	3.1 ±0.3	3 ±0.3	2.8 ±0.2	2.5 ±0.2	2.9 ±0.3	2.8 ±0.2	2.7 ±0.2	2.8 ±0.2	3 ±0.3	**2.5 – 3.4**	**2.9**
	A-5	5 ±0.6	3.9 ±0.4	4.7 ±0.5	4.9 ±0.6	4.4 ±0.5	4.3 ±0.4	4.1 ±0.4	4.5 ±0.5	3.9 ±0.4	4 ±0.4	4.2 ±0.5	4.7 ±0.6	**3.9 – 5**	**4.4**
	A-6	2.9 ±0.3	2.4 ±0.2	2.8 ±0.3	2.3 ±0.2	2 ±0.2	2.2 ±0.2	2 ±0.2	2.1 ±0.2	2 ±0.2	2.3 ±0.3	2.5 ±0.3	2.5 ±0.3	**2 – 2.9**	**2.3**
	A-7	2.4 ±0.3	1.9 ±0.2	2.4 ±0.3	2.3 ±0.2	2 ±0.2	1.9 ±0.2	1.6 ±0.1	2 ±0.2	1.7 ±0.2	2 ±0.3	2.1 ±0.4	2.6 ±0.3	**1.6 – 2.6**	**2**
	A-8	4.4 ±0.6	3.4 ±0.4	3.6 ±0.4	3.8 ±0.4	3.7 ±0.4	3 ±0.3	3.1 ±0.3	4.3 ±0.5	3 ±0.3	3.2 ±0.3	3.4 ±0.3	4.2 ±0.5	**3 – 4.4**	**3.6**
$\sum$ ***Annual Geomean***											$\sum$ ***Annual Average***				
2.8											**3**				

Table 14- Statistical analysis of data corresponding to radon concentrations in water

Year	Season	Median ($Bq \cdot L^{-1}$)	Standard Deviation ($Bq \cdot L^{-1}$)	Skewness	Kurtosis	Geometric Mean ($Bq \cdot L^{-1}$)
2013	Spring	-	-	-	-	-
	Summer (July-Aug)	3	1.1	1.2	1	3.1
	Autumns	3	1	0.9	-0.2	3.1
	Winter (Dec)	3.3	1.1	0.9	1.6	3.3
2014	Spring	2.7	0.9	1	-0.1	2.8
	Summer	2.8	0.7	0.4	-1.2	2.8
	Autumns	2.8	0.7	0.3	-1.2	2.7
	Winter	2.9	0.8	0.6	-0.4	2.9
2015	Spring	3.1	0.9	0.5	-0.8	3
	Summer	2.7	0.9	0.8	-0.5	2.6
	Autumns	2.8	0.8	0.3	-0.9	2.7
	Winter	3.2	1	0.2	-1.2	3.1

The standard normal distribution for the specified mean and standard deviation of the monthly measured dissolved radon concentration among the samples per each season are shown in Figures 26., 27., 28., and 29.

It found that the dissolved radon concentration in mine water varies in the range of 0.2 to 5 $Bq \cdot L^{-1}$. The geometric mean of dissolved radon concentration in the mine water samples (obtained from the two and half years of the author results database) determined to be around 3 ± 0.4 $Bq \cdot L^{-1}$; Additionally, it obtained that dissolved radon in the water samples were varied during each month and season, but not in significant deviation; The author investigated the seasonal variation of radon concentration but could not find any tendency. So, it seems there is no seasonal variation in radon concentration in water.

The significant difference radon concentration between sampling point A2 and sampling point A5, considered to be investigated. The author found that the origin of the water sample from point A2 was the fresh water due to condensation process from humidity on the cold surface of the wall and/or capillary rise of rocks moisture, and collected on the

pond; This water contains no radon or very low radon, therefore instead of radon release from water to the air, the radon in the air dissolve in the water; Regarding to this fact, the values of A2 was eliminated from getting average values and other calculation.

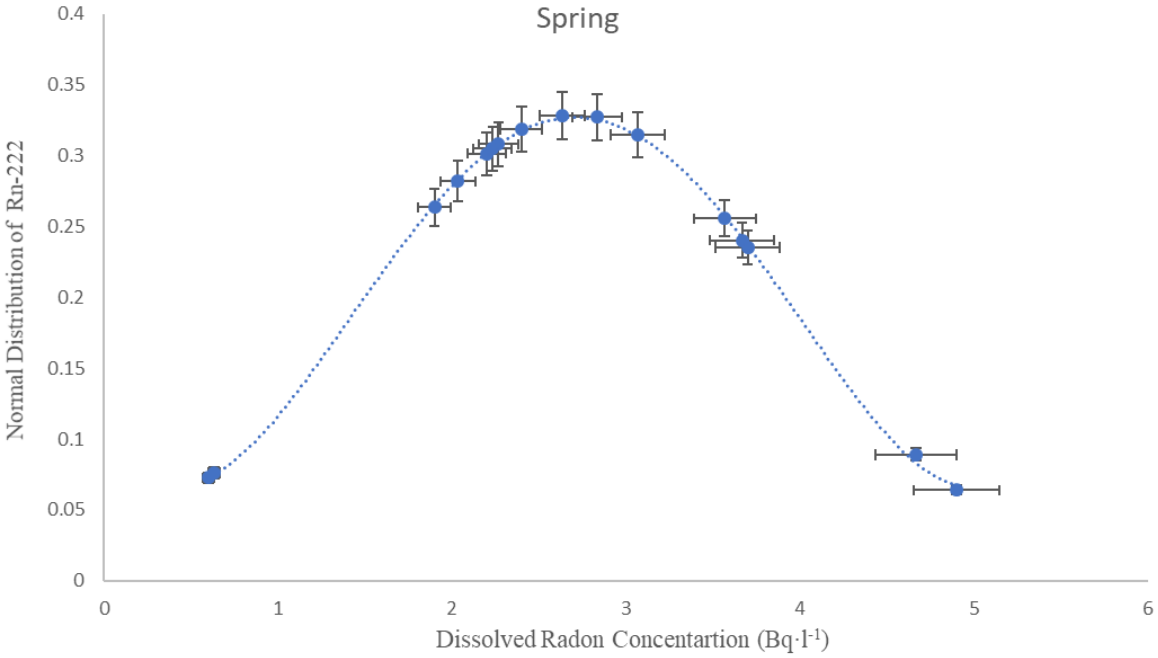

Figure 26- Distribution of radon in the Úrkút mine water samples (Spring)

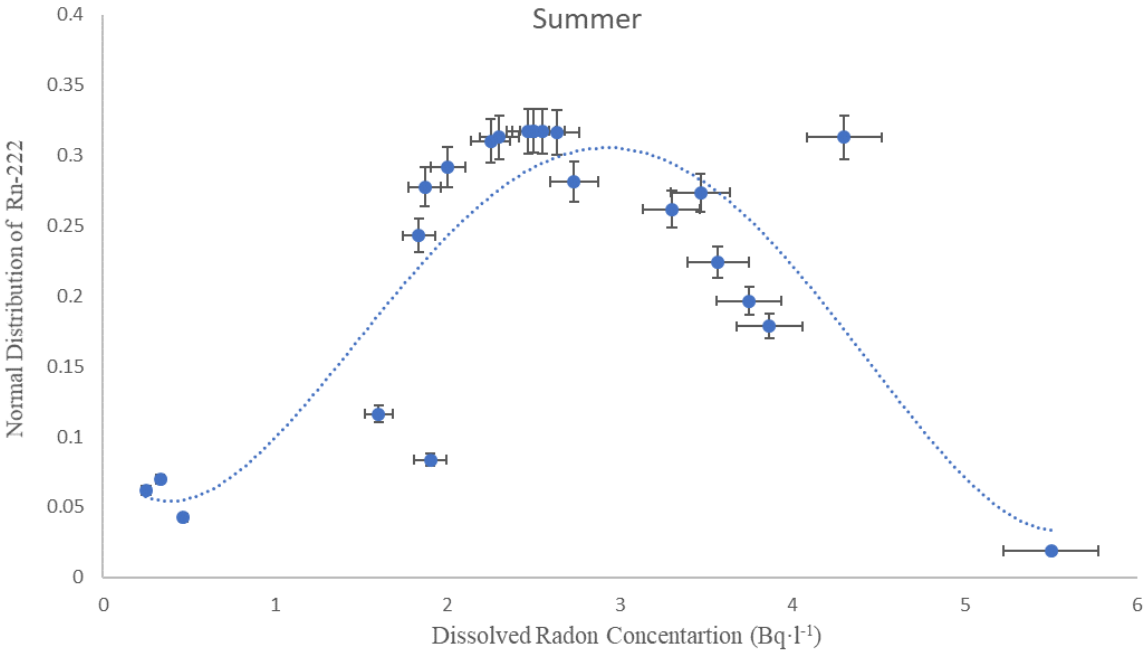

Figure 27- Distribution of radon in the Úrkút mine water samples (Summer)

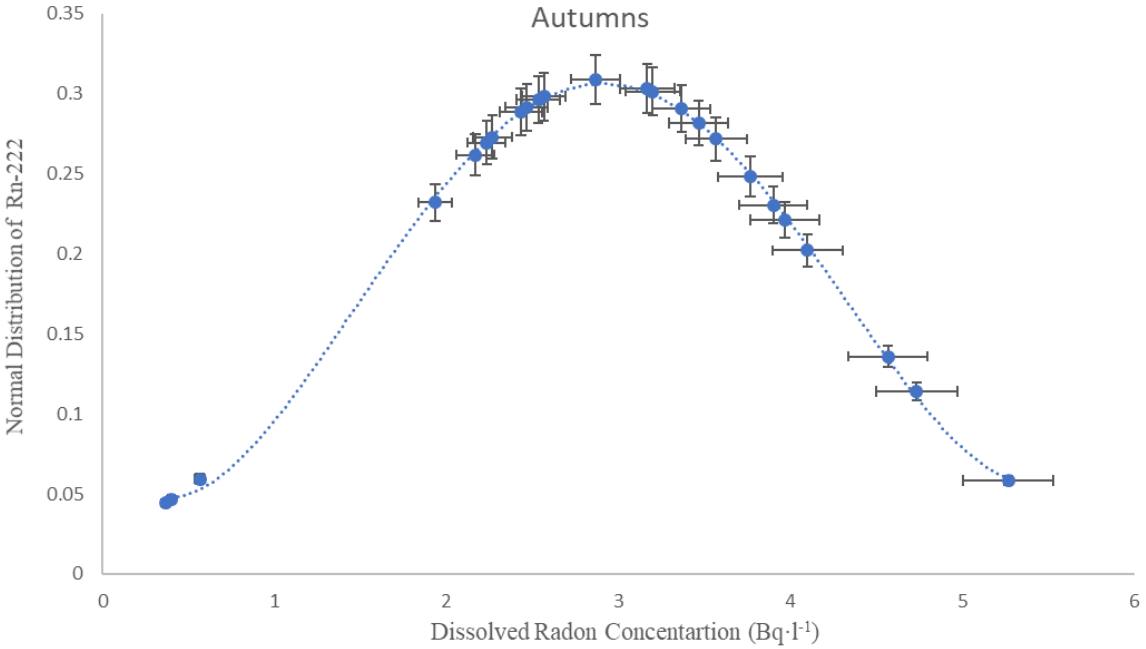

Figure 28- Distribution of radon in the Úrkút mine water samples (Autumns)

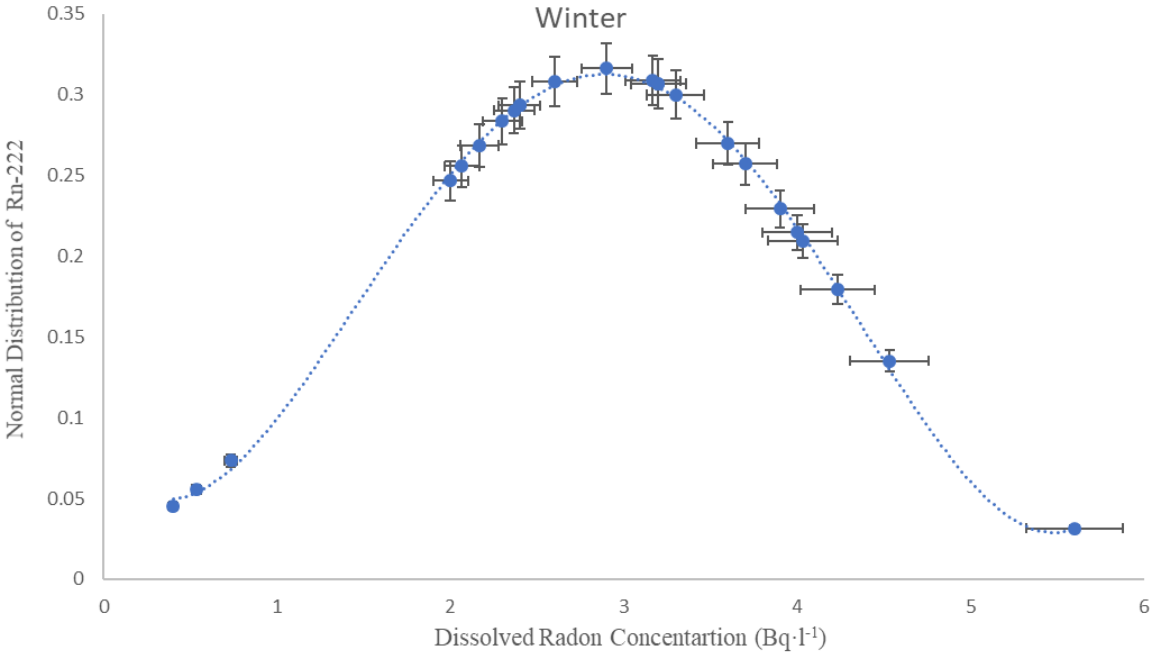

Figure 29- Distribution of radon in the Úrkút mine water samples (Winter)

The concentration of dissolved radon in the water may approach a level much higher than the concentration in the voids filled with air. Since the flow of water from the pore spaces of the material into mine is more rapid than the diffusion process that occurs in dry material, the net transport of radon into a wet mine could be greater than that of the dry mine where the only mechanism for radon transport is gaseous diffusion.

Since the volume distribution concentration of radon in water to air is about 0.3 at normal mine atmosphere, the radon-rich flowing water transfers the radon to the mine air till the radon concentration in air is approximately 3 times more than that of the concentration in water, but as the contact surface of water with the air was low and also by taking the ventilation capacity in consideration, the dissolved radon concentration in the mine water cannot be pointed as the main source of the accumulated radon in the Úrkút manganese mine. To estimate the maximum contribution of dissolved radon to radon concentration in the mine air (in the worst case scenario), a though estimation, using an excel based simple modelling, carried out considering the geometric mean of radon concentration among the waters collected from the mine, assuming the maximum contact surface, based on natural diffusion without forced ventilation, and based on the maximum water volume that transferred from the whole mine to outside. Assuming: forced ventilation is off and radon concentration in water as 3±0.4 $kBq \cdot m^{-3}$ (three years geomean value obtained from current study), the maximum volume of water transferred outside as 3,255,000 m^3 yearly (Tamás Vigh's Ph.D. thesis), and considering a 0.75 transferring rate of radon from water into the mine atmosphere (Khan, 1979), the author estimated a value about 7 $mBq \cdot s^{-1} \cdot m^{-3}$ for radon exhalation from water as the contribution of water in the radon concentration in the mine air; But, regarding the low contact surface (as water transferred regularly from the collected pond in the mine to outside using the pipes) and also considering the force ventilation capacity, practical this value could not happen, therefore, the contribution of dissolved radon in the air radon concentration is negligible. However, water still can be a source of entering radon to the mine air, further studies are necessary to find out the exact contribution of radon concentration in the water to the indoor air radon concentration based on the field measured values. It should mention the radon exhalation from water on the wall surface may be out of this expectation (while the surface radon exhalation from mine wall rocks was measured), however as water can be a route of radon in the mine air, it can also play an important role as a deterrent factor on radon exhalation from the mine wall, i.e., high moisture content can reduce the radon exhalation by trapping radon (refer to section 3.1.2).

3.1.2. Radon Exhalation

One of the major sources of entry of radon into the mine area is by diffusion through the mineral bearing host rock and subsequent exhalation through the mine walls. Radon generated from Ra-226 presented in the rocks on the mine wall diffuse to the surface area and then exhalate to the mine atmosphere. However, the exhalation can depend on ore grade, atmospheric condition and other factors. Radon exhalation can be categorised into two main phases: one, mine wall, it regards to old broken rocks and two, freshly broken ore and wall what occurs due to mining activity; The measurement is described below in two parts as in-situ and ex-situ measurements.

3.1.2.1. In-situ Measurement

The quantitative estimation of the radon exhalation from the wall made by measuring the build-up of radon activity concentration in the accumulation chamber in 5 different mine locations for 4 times measurements (each season one measurement). The geological of the rocks present in the mine galleries consist different types of limestone and marl (Cherty limestone, Greenish grey calcareous marl, etc.) as it is difficult to determine pure rocks due to the mixture of above-mentioned rocks. Detectors sent to the mine manager and placed in the same location were mostly miners were working there for each measurement. At the bottom of the cap, a CR-39 detector was placed. The cap was sealed on the surface of the mine wall. At the time of sending detectors, three detectors kept in the laboratory to evaluate the background. It was letting the exhalated radon accumulated in the cap about one week before determining the surface radon exhalation; These measurements carried out 4 times for 1 year in same locations. Table 15. is summarized the surface radon exhalation from the wall per each location.

The surface radon exhalation, from mine walls, measured to be in the range of 0.7 ± 0.1 mBq·s^{-1}·m^{-2} and 1.5 ± 0.2 mBq·s^{-1}·m^{-2}, with an average of 1.1 ± 0.1 mBq·s^{-1}·m^{-2}. Also, some variation between each period of measuring for same location observed that as it could be as results of precipitation. As results show, the seasons with high precipitation might be a reason that the radon exhalation from mine wall was lower than other seasons and it can be due to high moisture content in the rock and soils that known as a deterrent factor. The historical average precipitation data, for the month that measurement occurred, obtained from the Department of Limnology of the University of Pannonia. The average precipitation

for March, August, October, February was about 33, 62, 53, 32 mm, respectively. Likewise, the monthly average outdoor temperature obtained as 5, 22, 10 and 2 °C, respectively.

Table 15- Surface radon exhalation from 5 different walls location in the Úrkút mine

	Radon Exhalation (mBq·s^{-1}·m^{-2})					
Location	March	Aug	October	February	Min.- Max.	Mean
L-1	1.4±0.2	1.1±0.1	0.9±0.1	1.5±0.2	0.9-1.5	1.2
L-2	1.2±0.2	0.9±0.1	0.8±0.1	1.3±0.1	0.8-1.3	1.0
L-3	1.4±0.2	1±0.1	0.8±0.1	1.4±0.2	0.8-1.4	1.1
L-4	0.9±0.1	0.8±0.1	0.7±0.1	1.1±0.1	0.7-1.1	0.9
L-5	1.1±0.1	1±0.1	0.8±0.1	1.3±0.2	0.8-1.3	1.0

Regarding the results, the surface exhalation varied from each other, in some location, the radon exhalation could reach up to two times higher than the lowest exhalation value in other location. It can be due to rocks mineralization feature on the mine wall. Therefore, to figure out the contribution of different rocks and in continues of the previous study, the author carried out second measurements (refer to section 3.1.2.2) in the laboratory of the Institute of radiochemistry and radioecology at the University of Pannonia.

Following in-situ measurement, interesting results obtained from two different age mine walls measurements; Author conducted a continues radon monitoring (real-time measurement) some days before starting new mining activity. An AlphaGUARD radon monitor device connected to an accumulation chamber to the wall about 70 cm above the floor. Radon concentration was monitored in flow mode with hourly measurement cycle this phase of measurement named as point A (aged wall mine); Another measurement carried out after mine activity on the freshly broken wall in the same the location, named as point B (Fresh broken wall or ore); Measurements continued until released radon reduced up to its origin value at point A. Figure 30. shows the measurement result in the function of time and radon concentration in each point of time marked on the graph.

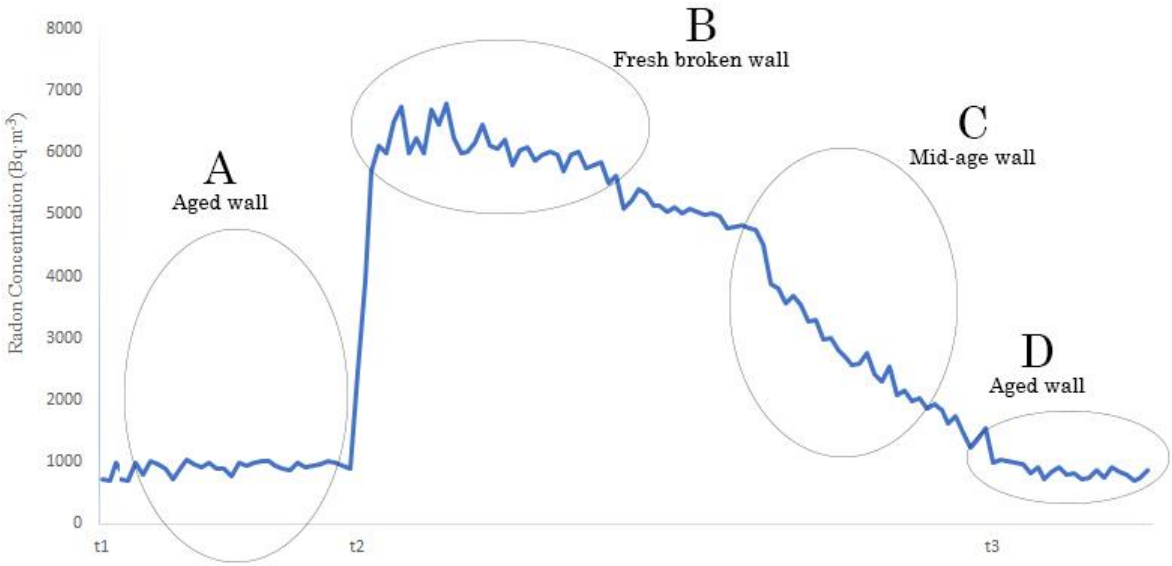

Figure 30- Released radon in function of the age of the broken wall

As shown in Figure 30., the radon concentration in the air directly depends on the broken ore (wall) age; "A" represents radon concentration near the old mine wall with average about 850±125 $Bq \cdot m^{-3}$, exactly after mining activity the radon released from same location with fresh broken wall increase dramatically with an average about 5900±420 "B", these increase dropped down near to 3300±365 $Bq \cdot m^{-3}$ by passing the time and getting aged, finally at point "D" and radon concentration came back to its constant value at point "A". This can be due to releasing trapped or accumulated radon between pores and grains space, when the rock was broken, radon could scape to the air, however, after a period and by aging the broken wall, the radon concentration reduces to it origin value.

This graph can be used as a mitigation management tool to reduce radon concentration at manganese mine or other underground mines; however other measurements such as a recognition of high potential radon exhalation rocks can be useful.

In section 3.2.3. of the current study an explanation of how such this experiment could be used to improve mitigation system resulting a successful reduction on the radon concentration.

3.1.2.2. Ex-situ Measurement

As it was discussed, on section 3.1.2.1. in the current thesis, to estimate the contribution of each type rocks in the radon exhalation, it is necessary to know the radon exhalation rate from each rock. Following of previous study which two types of rocks were examined, in current study, the author carried out an ex-situ areal radon exhalation measurement for 32 collected rock samples of total 6 different most abundant rock types (Table 16.). Additionally, the author used a gamma spectrometry to measure the main radionuclides concentration in each sample. Three main naturally occurring radionuclides (K-40, Th-232 and Ra-226 known as radon parent) considered for gamma emitted measurement using A high-resolution gamma-ray spectrometry, using an ORTEC GMX40-76 HPGe semiconductor detector (refer to section 2.3.1. at the current thesis).

In case of gamma spectrometry, a portion of samples following AQ of the laboratory of the Institute of Radiochemistry and Radioecology at the University of Pannonia, after being transferred to the laboratory, stored at room temperature for several days and dried in a ventilated oven at 90 °C for 24 hours to reach a constant weight. Samples pulverized, sieved to less than 0.3 mm to be same size as the reference material (IEA-375, Soil standard).

Then 500 grams of the homogenized prepared sample (in same by the standard weight) filled into a leak-proof and air-tight Marinelli beaker (same geometry as standard Marinelli beaker) and sealed for 29 days in order to reach secular equilibrium between Ra-226 and Rn-222 and its short-lived decay products before being counted by gamma spectrometry.

The specific peak detection efficiency, determined for K-40, Ra-226, and Th-232 as 1.2%, 2.4%, and 1.4%. Meanwhile, the minimum detectable activity of the gamma spectroscopy, based on the observed data from background measurement, calculated at 23, 0.5, and 0.7 $Bq \cdot kg^{-1}$, respectively. Table 16. shows the concentration of natural radionuclides in the rock samples (dry weight).

Table 16- Concentrations of natural radionuclides in the mine rock samples (Bq·kg^{-1})

					Ra-226	Th-232	K-40	Ra-226	Th-232	K-40
		Ra-226	Th-232	K-40	**Min. – Max.**			**Average**		
Carbonate (Mn ore)	C-1	15±4	7±2	245±40	15 – 18	7 – 25	244 – 245	16	16	245
	C-2	18±4	25±5	244±42						
Underlayer Lime stone (Mullock)	F-1	4±1	6±2	45±9	2 – 6	5 – 8	45 – 102	4	6	75
	F-2	4±1	7±2	62±12						
	F-3	2±1	8±2	84±13						
	F-4	6±2	5±1	102±17						
	F-5	4±1	5±1	83±14						
Dogger limestone (Mullock)	D-1	2±1	6±2	88±14	2 – 3	2 – 7	54 – 95	2	5	72
	D-2	2±1	7±2	95±16						
	D-3	3±1	2±1	66±11						
	D-4	2±1	5±1	54±10						
	D-5	2±1	3±1	58±10						
Black shale (Mn ore)	B-1	18±5	21±6	299±50	9 – 18	15 – 21	266 – 456	12	19	375
	B-2	9±2	16±4	345±60						
	B-3	12±3	15±4	266±45						
	B-4	10±3	16±4	315±54						
	B-5	13±4	20±6	456±78						
	B-6	13±4	18±5	438±74						
	B-7	11±3	21±5	451±76						
	B-8	11±3	19±4	398±69						
	B-9	13±4	20±5	415±70						
	B-10	10±3	20±5	365±62						
Underlayer Black shale (Mn ore)	UB-1	11±3	13±3	255±43	11 – 21	12 – 26	218 – 724	16	19	432
	UB-2	21±6	22±6	345±58						
	UB-3	18±4	26±7	218±38						
	UB-4	20±6	22±5	654±110						
	UB-5	11±3	12±3	724±123						
Puce greenish Marl (Mullock)	R-1	4±1	8±2	66±10	3 – 6	6 – 8	66 – 84	4	7	74
	R-2	3±1	8±2	74±13						
	R-3	4±1	8±2	84±15						
	R-4	5±2	7±2	78±14						
	R-5	6±2	6±2	69±13						

After statistical analysis, it observed that dogger limestone consist the lowest concentration of naturally occurred radionuclides such as Ra-226, Th-232 and K-40 among the other rocks type with an average of 2±1, 5±1 and 72±12 $Bq \cdot kg^{-1}$, respectively; However, underlayer black shale shows the highest values between all of the samples with an average of 16±4, 19±5 and 432±74 $Bq \cdot kg^{-1}$, for Ra-226, Th-232 and K-40, respectively. Additionally, black shale and carbonate ore shows high values of Ra-226 compared to other samples. The concentration of Ra-226 is higher than the mean value in 47% of the samples, while Th-232 was above the average concentration in 44% of the samples. The highest activity concentrations of Ra-226 was found in underlayer black shale.

The normal distribution for the specified mean and standard deviation of the measured radionuclides' concentration among the samples is shown in Figures 31. and 32.; According to the obtained data, most of the K-40 distribution is in the range of ~50 and ~300 $Bq \cdot kg^{-1}$, while the values for Ra-226 and Th-232 are between ~3 and ~15 $Bq \cdot kg^{-1}$ and ~10 and ~30 $Bq \cdot kg^{-1}$, respectively. The highest normal distribution values for K-40, Ra-226, and Th-232 were calculated around 0.002, 0.07, and 0.05, respectively.

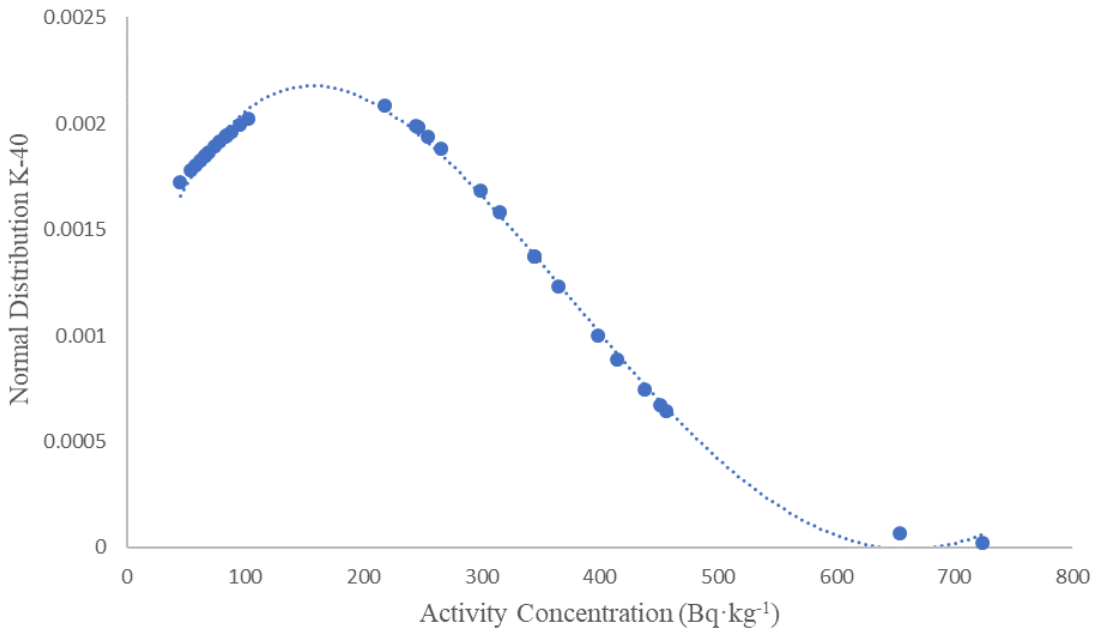

Figure 31- Distributions of K-40 concentration among the rock samples

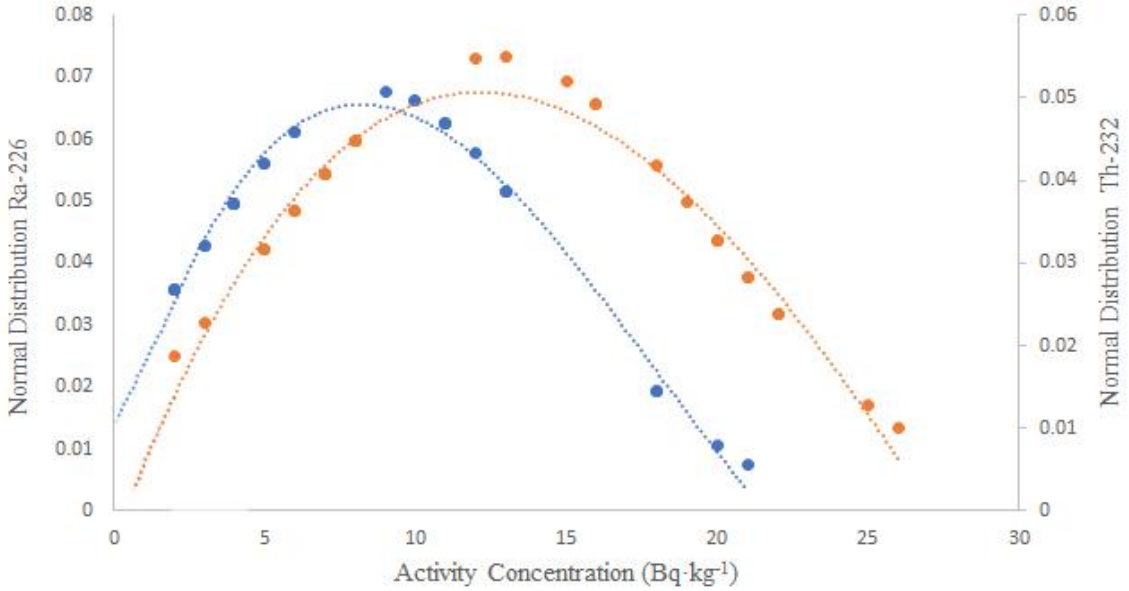

Figure 32- Distributions of R-226 and Th-232 concentration among the rock samples

A compression between the Ra-226 concentrations found in this study with U-238 concentrations from other study (Bíró, et al., 2015) for the same family rocks and the same mine are summarized in Table 17.

Table 17- Comparison of the Ra-226 and U-238 concentration among rock samples

Rock Type	U-238 (Bq·kg^{-1})	Ra-226 (Bq·kg^{-1})
Carbonate Ore	1-3 (1.6)	15 & 18 (16)
Black shale	5	9-18 (13)
limestone	1-2 (1.6)	2-6 (3)
Marlstone	1 & 4	3-6 (4)

Samples in different cylinder length used for measuring the aeric radon exhalation from each rock type in terms of sample thickness; The aeric radon exhalation measurement of prime importance in the determination of contribution of each type of rocks in radon exhalation. Following the accumulation period, the chamber connected to a closed loop system, where in the radon increment was measured by an ionization radon monitor device (AlphaGUARD PQ 2000). The aeric exhalation rates of each sample in terms of thickness are illustrated in Table 18. The overall average values of radon exhalation from samples in terms of their thickness are shown in Figure 33.

Table 18- Areal radon exhalation from rock samples in terms of sample thickness

Sample		Radon Exhalation ($mBq \cdot m^{-2} \cdot s^{-1}$)			Average Radon Exhalation ($mBq \cdot m^{-2} \cdot s^{-1}$)		
		5 cm	10 cm	15 cm	5 cm	10 cm	15 cm
Carbonate ore	C-1	0.41	0.75	1.1	0.37	0.78	1.2
	C-2	0.34	0.81	1.4			
Under layer Lime stone	UL-1	0.04	0.08	0.14	0.03	0.08	0.13
	UL-2	0.03	0.08	0.12			
	UL-3	0.04	0.07	0.14			
	UL-4	0.03	0.09	0.12			
	UL-5	0.03	0.07	0.13			
Dogger limestone	D-1	0.03	0.07	0.13	0.04	0.08	0.14
	D-2	0.04	0.06	0.14			
	D-3	0.05	0.09	0.15			
	D-4	0.04	0.09	0.14			
	D-5	0.04	0.09	0.15			
Black shale	B-1	0.71	1.24	1.51	0.76	1.28	1.54
	B-2	0.69	1.31	1.48			
	B-3	0.7	1.21	1.49			
	B-4	0.75	1.28	1.5			
	B-5	0.81	1.32	1.55			
	B-6	0.75	1.41	1.58			
	B-7	0.76	1.2	1.55			
	B-8	0.77	1.27	1.61			
	B-9	0.91	1.31	1.68			
	B-10	0.78	1.24	1.48			
Under layer Black shale	UB-1	0.69	1.35	1.51	0.76	1.3	1.62
	UB-2	0.74	1.38	1.65			
	UB-3	0.75	1.39	1.65			
	UB-4	0.88	1.21	1.81			
	UB-5	0.75	1.21	1.48			
Puce greenish Marl	R-1	0.04	0.07	0.13	0.05	0.08	0.16
	R-2	.05	0.06	0.17			
	R-3	0.05	0.1	0.15			
	R-4	0.06	0.08	0.18			
	R-5	0.04	0.09	0.16			

Carbonate ore, as was expected, showed the highest aeric exhalation, as it contained highest Ra-226 concentration among the other rock types. Puce greenish marl stone, shows the lowest radon exhalation. It needs to mention that radon exhalation directly depends on the moisture in the grain's pores and has an inverse relationship with grain size (Masahiro, et al., 2007; Harb, et al., 2016).

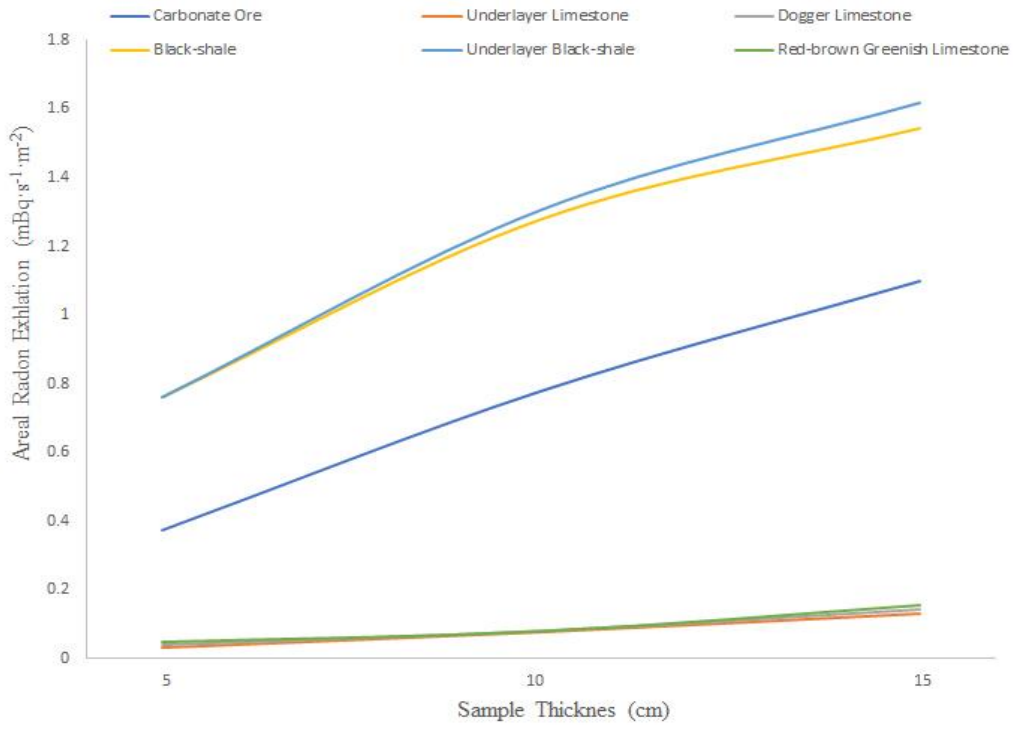

Figure 33- areal radon exhalation from the rock samples in terms of thickness

The radon exhalation rate is going to reach a constant value by increasing the thickness of samples. The high moisture content of the samples can be a reason for this behaviour as water in the sample could stop the radon diffusion, however in dry sample, radon exhalation can reach to the constant rate from 1 to several meters of sample thickness depends on the sample material. Várhegyi, et al. found radon exhalation can reach to a constant rate after a specific thickness of sand depending on the moisture (Várhegyi, et al., 2012). In the other words, moisture can influence on the radon exhalation. The soil moisture content as a deterrent factor influence on the radon emanation coefficient directly by filling the pores and space between material's grains resulting a temporary blockage of emanated radon from grains to pores space (radon is soluble water may also aid in the release of radon trapped in pores) and/or radon diffusion from pores to surface. However, it found the small amount of moisture can increase the radon emanation but by increasing the moisture rapidly reduce the emanation (Schumann & Gundersen, 1996; Barton & Ziemer, 1986).

3.2. Radon Concentration in Air

In order to investigate the radon distribution, two techniques used: a passive integrated method using NRPB track detectors were located in 12 different locations including old and new galleries, to indicate the sources of entry of radon at a height of 1–2 meters from the ground; The detectors changed in a consecutive period of three months (seasonal changes) between 2013 to 2016 and results evaluated as integrated average radon concentration per cubic meters in each season. As integrated measurements giving an overall view of radon concentration in mine e.g. measured radon concentrations during working hours can be differ from the whole-day averages due to the ventilation system that just worked only during the working hours, especially in this case when the work was organized with one shift per day, therefore, active radon monitoring carried out using AlphaGUARD PQ 2000Pro (specified to measure only radon concentration) and TESLA radon monitors (a newly marketed device to measure radon and humidity with the function of automatic smart central controller) saving the hourly values of radon activity concentrations for 5 days in each month. A comparison between results of duplicate measurements obtained with both techniques carried out concurrently in the same locations and conditions is in reasonably good agreement, with variations within 4.5% to 6.0%.

3.2.1. Radon in Air Passive Monitoring

The annual integrated averages radon concentration in whole mine area measured 824±42 $Bq \cdot m^{-3}$, 874±45 $Bq \cdot m^{-3}$ and 1050±85 $Bq \cdot m^{-3}$ in 2014, 2015 and 2016, respectively. The differences between the three consecutive years were just some percent 10-21%; The three-years averages radon concentration calculated as 916±54 $Bq \cdot m^{-3}$. It's important to note that these values represent the wholetime periods including the hours when there was no activity in the mine and the ventilation was off. Figures 34., 35., 36. and 37. are shown the seasonal average radon concentrations based on the measurement locations.

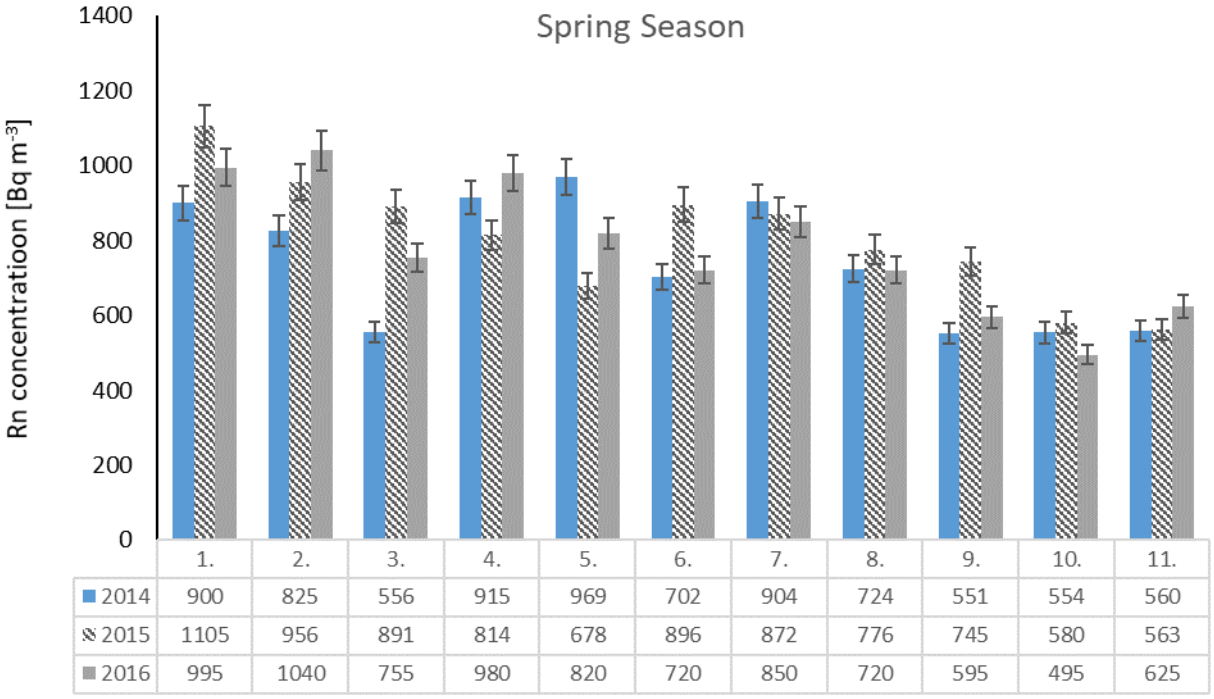

	1.	2.	3.	4.	5.	6.	7.	8.	9.	10.	11.
2014	900	825	556	915	969	702	904	724	551	554	560
2015	1105	956	891	814	678	896	872	776	745	580	563
2016	995	1040	755	980	820	720	850	720	595	495	625

Figure 34- Integrated seasonal average radon concentrations the mine (Spring)

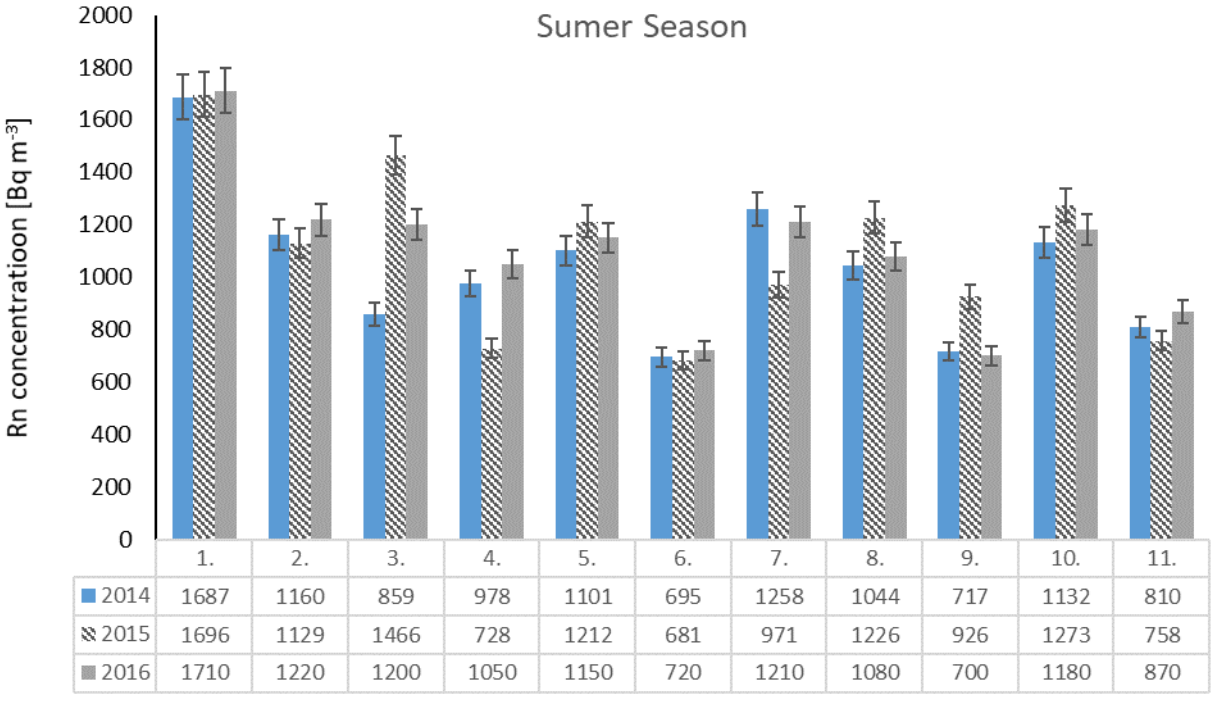

	1.	2.	3.	4.	5.	6.	7.	8.	9.	10.	11.
2014	1687	1160	859	978	1101	695	1258	1044	717	1132	810
2015	1696	1129	1466	728	1212	681	971	1226	926	1273	758
2016	1710	1220	1200	1050	1150	720	1210	1080	700	1180	870

Figure 35- Integrated seasonal average radon concentrations in the mine (Summer)

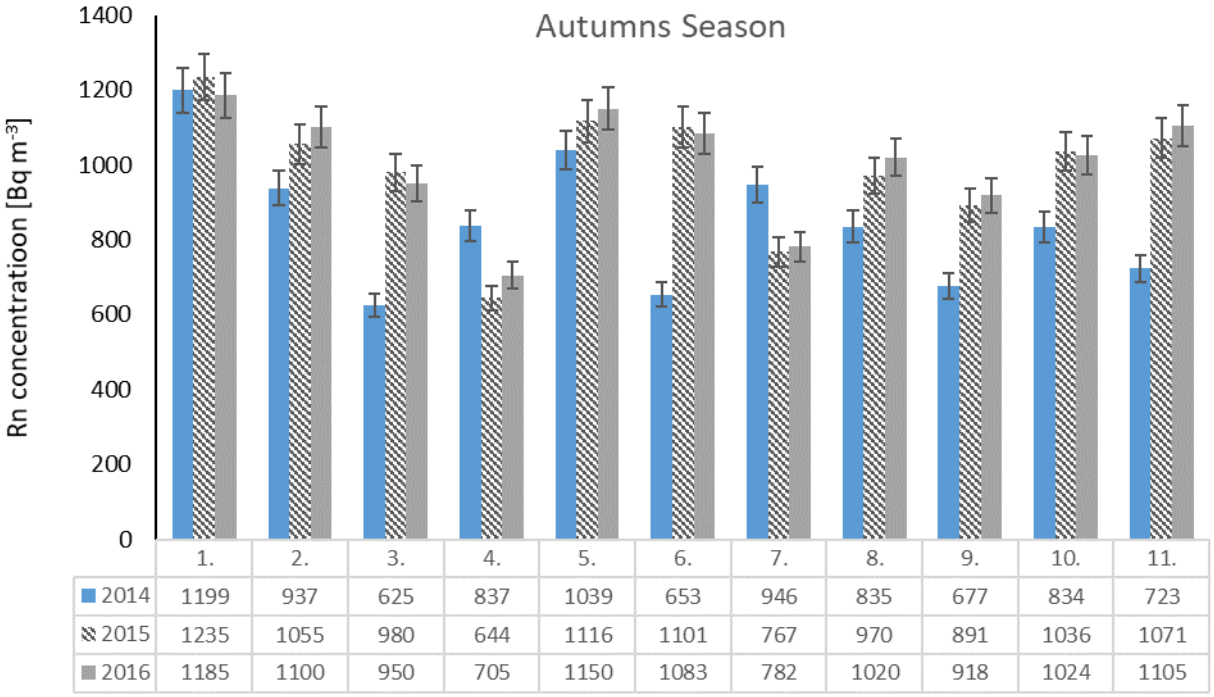

	1.	2.	3.	4.	5.	6.	7.	8.	9.	10.	11.
2014	1199	937	625	837	1039	653	946	835	677	834	723
2015	1235	1055	980	644	1116	1101	767	970	891	1036	1071
2016	1185	1100	950	705	1150	1083	782	1020	918	1024	1105

Figure 36- Integrated seasonal average radon concentrations the mine (Autumns)

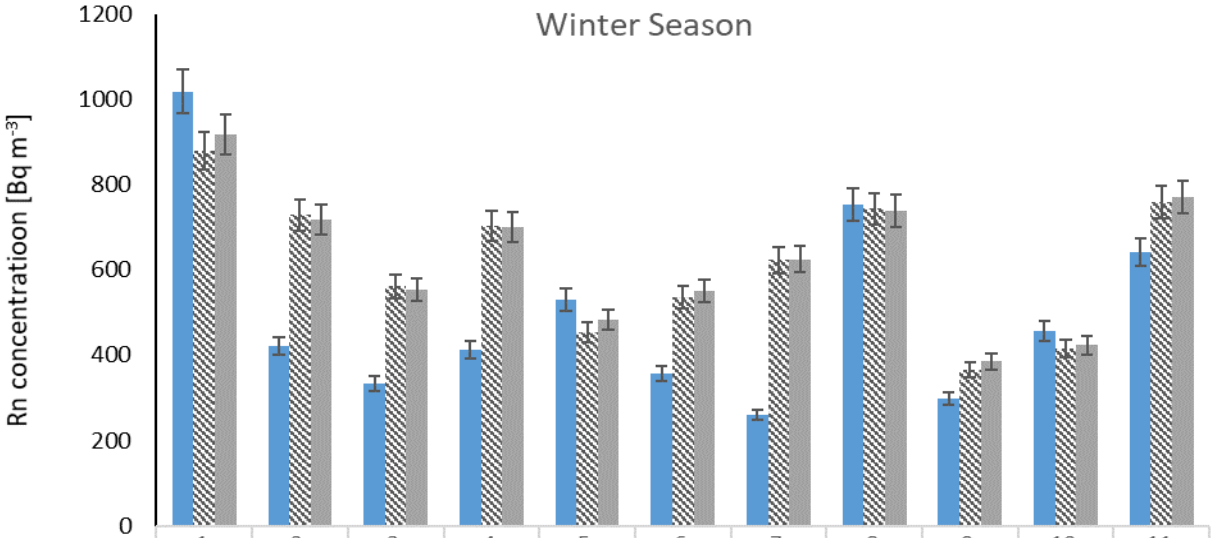

	1.	2.	3.	4.	5.	6.	7.	8.	9.	10.	11.
2014	1018	422	333	411	531	356	260	753	299	456	641
2015	880	728	561	704	453	536	623	743	365	416	758
2016	917	717	553	700	483	550	625	738	385	423	770

Figure 37- Integrated seasonal average radon concentrations the Úrkút mine (Winter)

Table 19. are summarised seasonal and annual average radon concentration in the all environment of the mine in each measurement year.

Table 19- Seasonal & annual Rn-222 concentration in mine environment

	Radon Concentration ($Bq \cdot m^{-3}$)				
	Spring	Summer	Autumns	Winter	Annual
2014	742±35	1040±43	846±41	498±24	867±45
2015	807±39	1207±49	988±43	615±29	1000±52
2016	781±33	1099±43	1002±40	624±29	960±48
$\sum$ **Average**			946±39		

As shown on the above figures, seasonal variations observed as: highest radon concentrations during summers, the lowest radon concentration during winters, during springs and autumns intermediate but higher in autumn than in spring. Outside temperature was measured during the study. The seasonal variation of outside temperature may be pointed as the main external factor that affected seasonal changes of radon concentrations, however, precipitation could be other reason. Figure 38. shows the seasonal average radon concentration in each year in function of average atmospheric temperature; As outside temperature raised the radon concentration inside the mine area increased.

Thermal diffusion due to difference temperature between outside and inside resulting natural air mass exchange between these two phases; While, in summer the average mine temperature is in range of surface atmospheric temperature resulting low mass air exchange, however.

This process in winter, when the greatest difference in temperature occurs between the inside and outside environment, is quite the opposite, the natural exchange rate of air between inside and outside phases reaches the maximum following indoor radon concentration reduction; Additionally, air pressure can influence on this exchange process, but as the air pressure was stable most of the times, it can be negligible as an influencing factor.

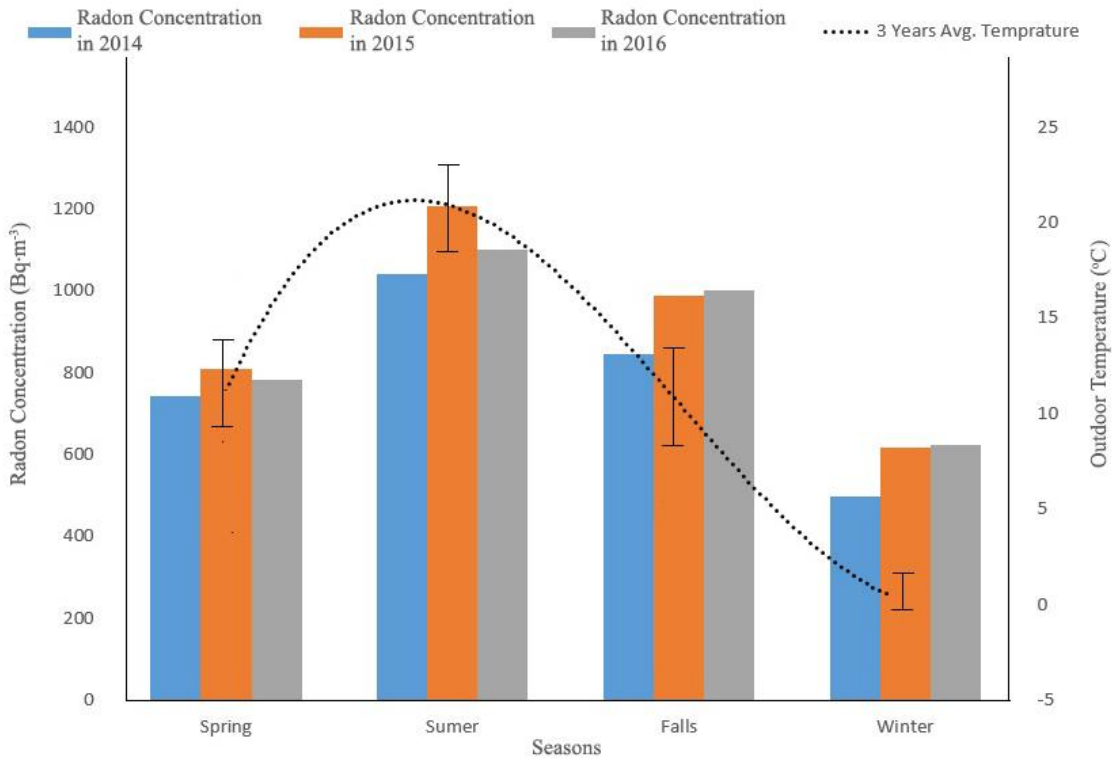

Figure 38- Seasonal average radon concentration and outdoor temperature

It is necessary to mention that these do not represent the average radon concentrations during the working periods which is the concern in the radiation protection point of view; however, it is important in point of view of regulation.

According to the obtained results, the annual average radon concentration inside the mine was along with the Hungarian legislation (with the action level of 1000 $Bq \cdot m^{-3}$ for workplace such as underground mines), but it could not meet the reference level suggested by the recently issued European Basic Safety Standard as "Member States shall establish national reference levels for indoor radon concentrations in workplaces. The reference level for the annual average activity concentration in air shall not be higher than 300 $Bq \cdot m^{-3}$" with no exception of workplace features.

3.2.2. Radon in Air Active Monitoring

As it was discussed, the overall annual average radon concentration in the mine air was below 1000 $Bq \cdot m^{-3}$; but still far from EU-BSS reference level (300 $Bq \cdot m^{-3}$). Meanwhile, this value represents the radon activity concentration in the whole year including working period and when mine was closed and no mining activity was in process. The high value can be due to accumulated radon concentration during off time when the ventilation system was not working. Therefore, short-time continuous radon measurements using different devices carried out to get an overview of radon concentration behaviour during working hours and closing hours.

Four locations in the active mining area (where mostly miners worked on that area) were selected for continues radon measurements. Two radon monitor devices namely AlphaGUARD, and TESLA used for this study.

Figure 39. is shown 5 days radon monitoring results in terms of measurement locations. As it can see, radon concentration in the mine area rapidly decreased by starting ventilation system and a sudden increase at the end of the working time (in the range of 700 to 3300 $Bq \cdot m^{-3}$) when the ventilation system changed to its low velocity rate.

Overall average radon concentration in measurement location during working hours (when ventilation system as a mitigation system worked) observed to be between 450 and 650 $Bq \cdot m^{-3}$; However, the overall average value for working time and off time was in range of passive integral measurement by 978 $Bq \cdot m^{-3}$. Radon concentration mitigated under 300 $Bq \cdot m^{-3}$ by using obtained results on the chapter 3.2.3. at the current study. As it was discussed and according to obtained results, fresh broken wall (ore) marked as the potential source of entry radon to manganese mine air (due to releasing the trapped radon in the rock pores, in addition to the increased exposed surface area); Therefore, a functionally developed air injection system based on existing ventilation system adopted. In this development a mobile tube has been designed and connected to ventilation system, and at the same time of the mining process it was moved to mining area and start mitigation from the origin. Results obtained after this method shows a huge improvement and success in radon reduction.

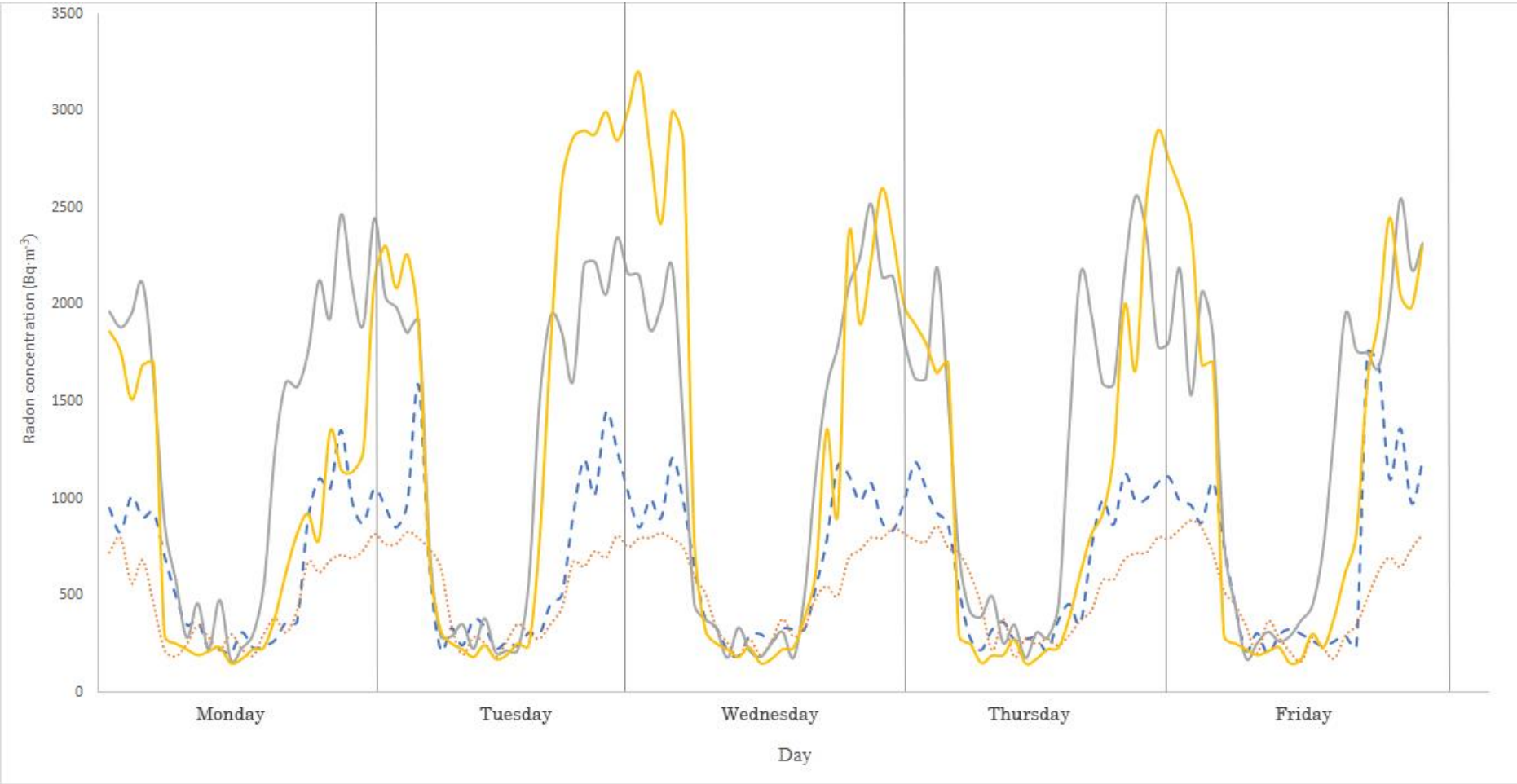

Figure 39- 5 days continues radon monitoring in measurement locations

Comparing the values obtained from this study with other study in Iran on the same type of mine shows on Table 20. However, in Iranian study one value was reported as 10 $Bq \cdot m^{-3}$ in working area with forced ventilation which is supposed to be a typo or a mistake during measurement as this value is in range of radon concentration in fresh air.

Table 20- Compare the data obtained from this study with other studies

Country	**Mine**	**Radon Concentration ($Bq \cdot m^{-3}$)**	**Reference**
Iran	Robat-Karim (Manganese mine)	1332±236 (no ventilation)	(Ghiassi-Nejad, et al., 2002)
	Venarge-Qom (Manganese mine)	10±2.6 (forced ventilation)	
Hungary	Úrkút mine (Manganese mine)	946±39 (integrated) 450 and 650 $Bq \cdot m^{-3}$ (working hours/ forced ventilation) 250 $Bq \cdot m^{-3}$ (working hours using optimized mitigation)	Present Study

3.2.3. Performance of New Developed Mitigation System

Using obtained result in previous sections of the current study (finding the potential rocks with high radon exhalation and identifying the main radon entry route) to achieve the EU-BSS recommendation level (300 $Bq \cdot m^{-3}$), it was tried to develop and optimize a mitigation system based on the existing ventilation system; With a combination of two different systems, a new optimized mitigation system applied for a short period to examine the new mitigation system under the same condition to figure out the difference between radon concentration before and after using new system.

Regarding the obtained result (the main route of entry radon to the mine air identified to be the freshly broken rocks), applying the idea of a system to inject fresh air directly to the specific area might be an option to reach low radon level in the mine. In this system a mobile tube was used to be able to adjust the location of the head, then the tube was connected to the primary ventilation system. Exactly after mining activity, the head of mobile tube was moved as close as to the freshly broken wall, not only to purify the dust and particles, but also to reduce the radon concentration immediately; Additionally, the mobile tube could remain in the same location for a period time till radon concentration drop down to its lowest value.

Basically, the forced ventilation system was used in the galleries by every 200 m and in the galleries longer than 15 m, and for the new galleries where already mining activity occurred or was occurring, the natural diffusion was responsible of radon mitigation. Regarding the author results, a new developed mitigation system was designed by close collaboration between manganese mine team (the manager of the mine as manganese mine representative) and our research team (the head of institute as representative) in the institute of Radiochemistry and Radioecology at the university of Pannonia. In this system, a flexible plastic tube as shown in Figure 40. with length of several centimetres (when it was compressed) up to 200 meters (when it was extended) with diameter about 460 mm was used to plug in to the last connector of the forced ventilation. Therefore, it was possible to extend the tube to the new galleries as near as possible to the freshly extracted walls and by injected fresh air (with flow rate in range of 50 up to 100 $m^3 \cdot min^{-1}$) diluted reach radon air, resulting immediate radon reduction.

Figure 41. shows the performance of the new application of the system by comparing 5 days radon concentration in the measurement location. Plot A shows the radon

concentration with regular mitigation system and plot B shows the radon concentration in the air after using new optimized mitigation system.

Figure 40- Image of optimized mobile mitigation system at Úrkút mine

Using developed mitigation system dramatically reduced the radon concentration by injecting fresh air directly to the high potential radon route source (fresh broken rocks). In regular mitigation system, the average radon concentrations during working hours measured between 400±55 $Bq \cdot m^{-3}$ and 650±81 $Bq \cdot m^{-3}$.

Optimized mitigation system was just used during working hours and when there was mining activity such as exploring or digging. During closing time, the regular ventilator was blowing fresh air to the mine galleries with low velocity.

Using the optimized mitigation system successfully reduced the radon concentration on that specific area to below 300 $Bq \cdot m^{-3}$ with an average of 250±41 $Bq \cdot m^{-3}$.

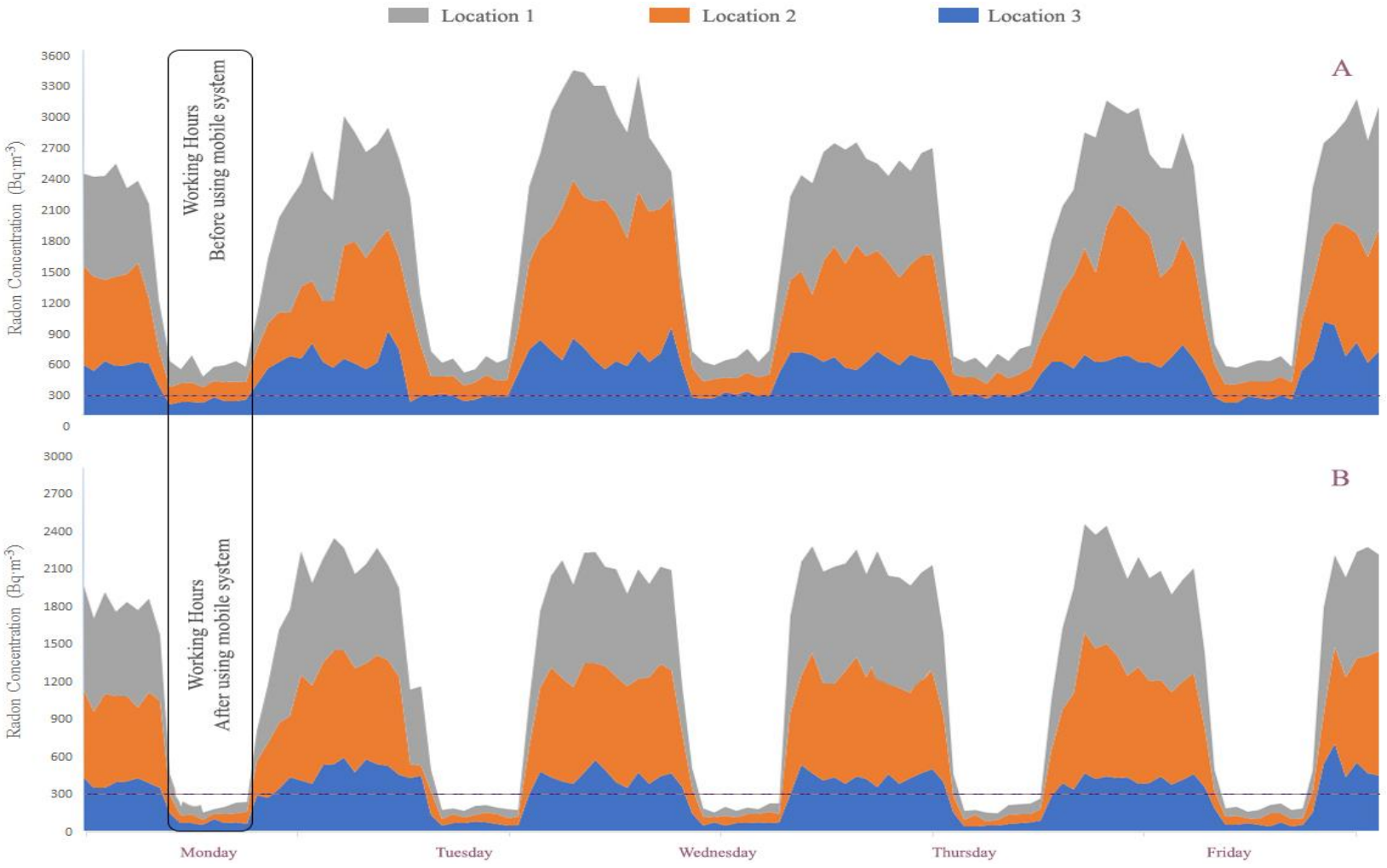

Figure 41- Performance of using mobile radon mitigation system;
A) Radon concentration in three locations when regular ventilation was used;
B) Radon concentration in the same locations when mobile mitigation system was tested.

By using the optimized mitigation system, radon concentration can reduce, not only by setting it up in the mine active faces, but also by mitigating directly before releasing radon to the mine air.

The measured radon concentration during working hours when the mobile system was applied are shown in Table 21. The geometric mean of the three locations calculated in the range of 150±40 $Bq \cdot m^{-3}$ to 216±53 $Bq \cdot m^{-3}$ with an average of 205±49 $Bq \cdot m^{-3}$.

Table 21- Radon concentration after using optimised mitigation system ($Bq \cdot m^{-3}$)

	M 1 **Min.-Max. (Mean)**	**M 2** **Min.-Max. (Mean)**	**M 3** **Min.-Max. (Mean)**	**Three Locations (Ave.)**
Monday	79±34 - 415±54 (166±44)	91±48 - 334±77 (166±43)	170±44 - 389±95 (216±53)	196±53
Tuesday	103±32 - 405±89 (161±44)	113±30 - 463±101 (173±44)	148±41 - 350±82 (199±49)	191±54
Wednesday	91±32 - 391±88 (150±40)	91±30 - 473±103 (176±48)	145±38 - 383±84 (201±53)	159±44
Thursday	90±30 - 415±97 (174±47)	91±35 - 313±77 (160±43)	129±37 -402±93 (180±49)	185±49
Friday	126±32 - 405±92 (182±49)	90±35 - 331±81 (166±43)	130±35 - 472±97 (186±50)	192±53
Average	166±45	209±44	196±51	
$\sum$ **Average**		205±49		

3.3. Radon Exposure & Personal Dosimetry

In this section of the study, the author tried to find out if the success of reducing radon to below to the reference level (300 $Bq \cdot m^{-3}$) can address concerns about underground miners in radiation and dosimetric point of view; Accordingly, after radon concentration reduce successfully to below 300 $Bq \cdot m^{-3}$, the author carried out a long-term radon dosimetry based on the resulted obtained from field measurements (including unattached factor, equilibrium factor and calculated dose conversion factor based on the field data), to figure out: (1) the effectiveness of radon reduction from radioecology point of view; (2) finding the effects of the difference between the actual and recommended parameters on dose estimation.

There are several studies about dose estimation on the same mine, however, previous studies were based on measured radon concentration in the mine area during integrated working hours. In this study for the first time, personal radon dosimeters used to get a precise results; As a matter, the miners exposure to the radon monitored based on working behaviour of each miner and for the specific working place and working activity e.g. in the break time, lunchtime or during the off-hour dosimeters were stored to prevent any extra radon exposure.

The exposure of miners to the radon measured using the personal dosimeters which were attached to the clothes of the workers; Table 22. is shown the radon concentration that miners exposed in terms of each miner per month. This could serve information about the radon levels during the effective working hours. The annual average radon concentration of each miner used to calculate the dose conversion factor and estimate the effective dose.

Using personal dosimeters had its own difficulty, in some cases, the detector was forgotten to be attached, was attached for some days or simply it was missing during miner's activity, but it was the only option for a precise dose assessment. As a solution, regarding to measurement period (15 days in per month), and possibility, when there was problem with detectors, new detectors were given to the miners for the other 15 days of the current month, however it could not always happen due to etching time, weathered condition, distance and other limitations. The missing results or the results that suspected as wrong values ignored from getting the average value. The relative error of each measurement calculated by getting a standard deviation from the 3 times counted tracks and then converted to radon concentration.

Table 22- The radon concentration that miners were exposed in terms of months ($Bq \cdot m^{-3}$)

	Jan	Feb	Mar	Apr	May	Jun	Jul	Aug	Sep	Oct	Nov	Dec	Annual Average
Miner 1	280±37	253±29	68±35	241±31	275±37	238±31	237±32	258±33	246±30	-	243±29	269±36	254±33
Miner 2	-	264±32	231±29	225±27	240±30	273±36	236±33	273±32	264±33	163±25	29±15	238±33	249±32
Miner 3	295±44	248±33	-	267±33	266±36	292±42	109±15	264±31	243±29	278±34	261±31	269±35	266±34
Miner 4	245±32	264±34	274±32	49±29	272±35	-	272±34	257±32	274±38	248±29	82±38	282±37	265±34
Miner 5	233±27	44±29	251±31	254±34	273±36	246±32	282±37	151±32	246±29	244±30	266±32	246±29	254±31
Miner 6	256±33	245±31	224±25	248±32	223±24	256±34	254±32	-	267±36	268±36	233±29	142±17	247±31
Miner 7	253±28	287±40	255±34	-	290±43	140±18	251±32	257±30	285±37	87±27	254±28	258±29	266±33
Miner 8	65±30	275±37	243±30	265±32	259±34	244±29	255±32	270±32	249±27	159±20	274±35	254±28	259±31
Miner 9	-	106±20	272±36	281±39	-	265±34	280±37	285±36	57±29	274±35	281±39	60±34	277±36
Miner 10	247±31	127±22	269±34	258±33	292±48	281±41	293±45	295±45	27±35	265±34	252±31	296±47	276±39
$\sum$ Average	**261±33**												

*Yellow colour cells are the missing results or the results that suspected as wrong values

Annual Working Hours									
Miner 1	**Miner 2**	**Miner 3**	**Miner 4**	**Miner 5**	**Miner 6**	**Miner 7**	**Miner 8**	**Miner 9**	**Miner 10**
1960±24	1976±16	1944±32	2000±40	1928±24	1984±32	1992±32	1960±24	1944±32	1912±16

In continues of radon measurement, the PAEC of the unattached and attached radon progenies measured using the SARAD EQF3220 and the unattached factors calculated based on the results. Table 23. is summarized the calculated unattached factor at the 3 measurement locations where selected miners for personal dosimetry mainly worked there. During working hours, the annual average unattached factor measured as 0.15, 0.3 and 0.2, at for workplaces 1, 2 and 3, respectively. The values of f_{un} show the same trend, while values from locations 2 and 3 are slightly higher than location 1. As the fact, the annual average of three locations used for dose assessment, however, the author separately calculated and estimated the DCF and effective dose for each group of miners based on their working place, working hours and measured parameters at their working places.

Table 23- The Annual average of unattached factor in three working locations

	Minimum	**Maximum**	**Annual Mean**
Location 1	0.07±0.01	0.24±0.03	0.15±0.04
Location 2	0. 21±0.04	0.38±0.05	0.3±0.05
Location 3	0.18±0.03	0.28±0.05	0.21±0.04
$\sum$ **Average**		0.21±0.04	

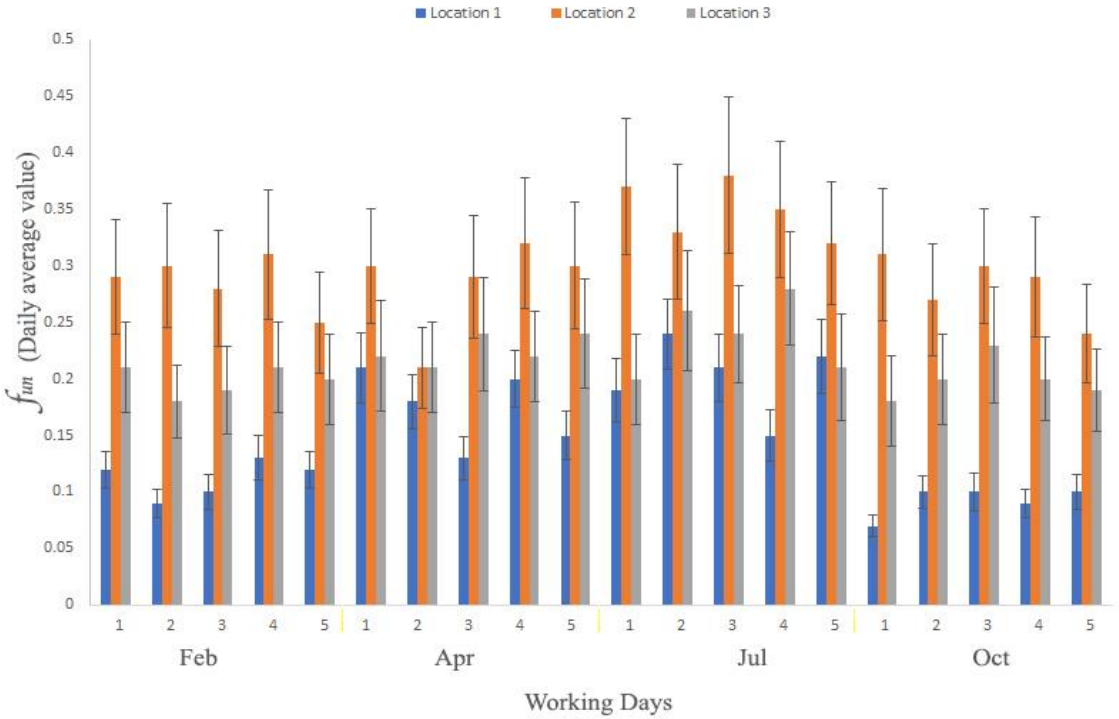

Figure 42- A plot of 5 days unattached factor at three working locations

As it is shown in Figure 42., the unattached factor changed in the same location during a year, therefore in dosimetry point of view, the unattached progenies of radon must be measured at least every 3 months. Additionally, a slight correlation between each season and unattached factor found (as in the spring and summer the f_{un} is slightly higher than other seasons), however, summer shows higher variation compared to other seasons and it might be due to the difference temperature between the outside and inside of the mine resulting a naturally air exchange and/or it could be due to the mining activity at the time of measurement.

More measurements carried out to determine the equilibrium equivalent concentration and equilibrium factor using Pylon WLx in the same locations (3 times in one year, every 4 months, 5 days monitoring) during working hours. According to the obtained results, the average equilibrium factor calculated as 0.35±0.1, 0.36±0.1 and 0.55±0.2 depending on location during working hours, Table 24.

Table 24- The annual average of equilibrium factor (F) at three working locations

	Minimum	**Maximum**	**Mean**
Location 1	0.23±0.12	0.79±0.24	0.55±0.2
Location 2	0.22±0.1	0.58±0.18	0.36±0.1
Location 3	0. 21±0.1	0.57±0.19	0.35±0.1
$\sum$ **Average**		0.42±0.13	

The total mean of radon concentration at location 1 was 235 $Bq \cdot m^{-3}$ with minimum and maximum values about of 125 $Bq \cdot m^{-3}$ and 425 $Bq \cdot m^{-3}$, respectively; While the measured average EEC was 106 $Bq \cdot m^{-3}$ (29 $Bq \cdot m^{-3}$ – 336 $Bq \cdot m^{-3}$); In location 2 the values were calculated as average radon concentration 293 $Bq \cdot m^{-3}$ (155 $Bq \cdot m^{-3}$ – 610 $Bq \cdot m^{-3}$) and EEC about 102 $Bq \cdot m^{-3}$ (34 $Bq \cdot m^{-3}$ – 353 $Bq \cdot m^{-3}$), and similar to location 3, radon concentration 270 $Bq \cdot m^{-3}$ (145 $Bq \cdot m^{-3}$ – 545 $Bq \cdot m^{-3}$) with EEC around 122 $Bq \cdot m^{-3}$ (30 $Bq \cdot m^{-3}$ – 310 $Bq \cdot m^{-3}$).

To complete the dose assessment, the author calculated the DCF based on the data obtained from field measurements; Table 25. is summarized the calculated DCF by this study comparing with DCF given by ICRP and WHO/EPA.

As explained in the section 2.5.3. of current study, the author calculated the dose conversion factors based on different breath behaviour and based on obtained data during working hours; As the breath behaviour of the miners in this study was not observed, the published recommended values (Porstendörfer, 1996) used to calculate the CDF (refer to section 2.5.3. of current study); Figure 43. is shown the DCF values based on the breathing behaviour (Porstendörfer, 1996) and the unattached factor obtained from this study.

First, the DCF separately calculated for each working location based on the average radon exposure using the average unattached factor of the same location; In the other words, the DCF calculated based on each miners group; Then, the total average of radon exposures and the unattached factors used to calculate the general DCF for the whole mine.

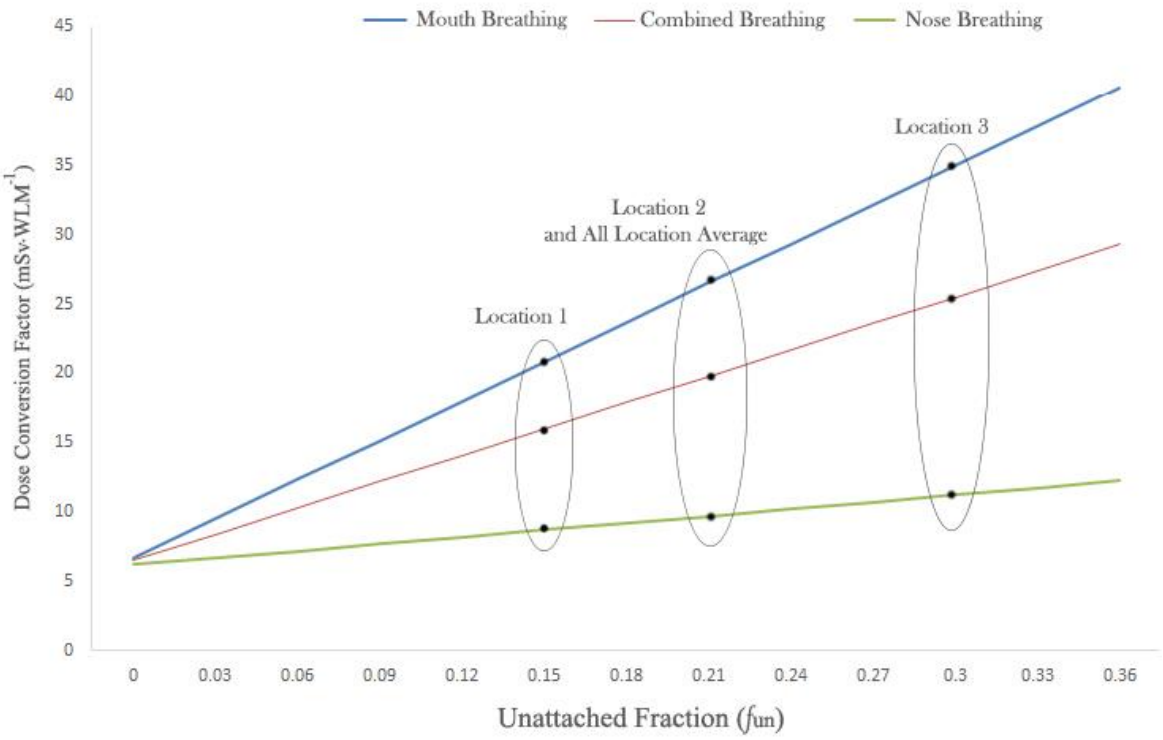

Figure 43- DCF values based on breathing behaviour and calculated the f_{un}

Table 25- The calculated DCF compared to the value given by ICRP (mSv·WLM^{-1})

	Location 1	**Location 2**	**Location 3**
f_{un}	0.15±0.04	0.3±0.05	0.21±0.04
DCF_m	21±10	35±11	26±10
DCF_n	9±7	11±7	10±7
$DCF_{m,n}$	**16±9**	**25±10**	**20±9**
$\sum$ **Average**		20±**9**	
ICRP-137		**10**	

However, the DCF in the ICRP-65 were suggested as 5 mSv·WLM^{-1} for workers and 4 mSv·WLM^{-1} for the public, in the new publication (ICRP-137, Part 3), this value changed to 3 mSv per mJ·h·m^{-3} (approximately 10 mSv per WLM), same for both group (workers and public, excluded the workers in the caves where DCF suggested as 20 mSv per WLM); In most circumstances the recommended dose is useful for official reports, but as shown in Table 25., this value is different by the calculated DCF based on the dosimetric model calculations of this study.

Regarding the result of this section, it can be stated that in view of radiation protection, DCF must be calculated individually as it depends on several environment parameters and the breath behaviour, e.g. the DCF increased almost 1.5 times greater when unattached fraction value changed from 0.15 to 0.3; Therefore, using pre-calculated value is not a useful tool in all situation (at least in underground mines) and it was confirmed by this study. The average dose conversion factor value (including three locations) is at least 2 times greater than the recommended value 10 mSv·WLM^{-1}. The author estimated the effective dose from radon and its short-lived decay products based on the observed data from field measurements and comparing with the effective dose estimated based on the DCF recommended by ICRP and EPA/WHO as shown in Table 26. The estimated effective dose, based on the observed data from field measurements, was in the range of 5.6±0.7 mSv·y^{-1} to 7.5±0.9 mSv·y^{-1} (geometric mean: 6.7±0.9 mSv·y^{-1}) as results of the ICRP-137 modelling equation; And between 5.6±0.9 and 7.6±0.9 mSv·y^{-1} with geometric mean of 7±0.8 mSv·y^{-1} when EPA modelling equation used for calculation; However, the estimated doses were cut to half when the recommended data used for effective dose estimation.

Table 26- The effects of actual and recommended parameters on dose estimation

		Working (h)	C_{Rn} (Bq·m^{-3})	(mSv·y^{-1})					
				E (ICRP)	E (EPA/WHO)	E(ICRP)	E(EPA/WHO)		
				F=0.4, DCF=10		F and DCF from this study ►		F	DCF
Location 1	Miner 1	1960	254±32	3.3±0.4	3.2±0.4	6.9±0.9	7.0±0.9	0.55±0.2	16±9
	Miner 2	1976	249±32	3.3±0.4	3.1±0.4	6.8±0.9	6.9±0.9		
	Miner 3	1944	266±34	3.5±0.4	3.3±0.4	7.1±0.9	7.2±0.9		
	Miner 4	2000	265±34	3.6±0.4	3.4±0.4	7.3±0.9	7.4±0.9		
Location 2	Miner 5	1928	254±32	3.3±0.4	3.1±0.4	6.9±0.9	7.0±0.9	0.36±0.1	25±10
	Miner 6	1984	247±31	3.3±0.4	3.1±0.4	6.9±0.9	7.0±0.9		
	Miner 7	1992	266±33	3.5±0.4	3.4±0.4	7.5±0.9	7.6±0.9		
Location 3	Miner 8	1960	259±31	3.4±0.4	3.2±0.4	5.6±0.7	5.6±0.9	0.35±0.1	20±9
	Miner 9	1944	277±36	3.6±0.5	3.4±0.4	5.9±0.8	6.0±0.7		
	Miner 10	1912	276±39	3.5±0.5	3.3±0.5	5.8±0.8	5.9±0.8		
$\sum$ Average		**1960**	**261±33**	**3.4±0.4**	**3.3±0.4**	**6.7±0.9**	**7±0.8**	**0.42±0.13**	**20±9**

It observed that the estimated effective dose based on the long-term radon dosimetry and the field measured parameters, e.g. unattached factor an equilibrium factor, is much higher (almost 2 times) than values when using ICRP-137 or EPA epidemiological modelling calculation and recommended data. The estimated effective doses using EPA modelling calculation are slightly higher than the values obtained using ICRP equation, in both cases when realistic or recommended data used to estimate the effective dose.

The EU-BSS recommends annual average radon concentration at 300 $Bq \cdot m^{-3}$ for in workplaces such as underground mines, while based on the results of this study, even when miners were exposed to radon concentration below 300 $Bq \cdot m^{-3}$ they could receive high doses from radon and its short-live progenies; It might be true that in the legislation systems point of view, the easiest way to express the limits in radon concentration is $Bq \cdot m^{-3}$, as it is much simple to measure in compare to dose calculations that involves additional measurements (such as working level, the attached and unattached fractions, particle size distributions, equilibrium factors, dose conversion factors, etc.); but in aim of dosimetric investigations, measuring only radon concentrations is not satisfactory.

3.4. Manganese Ore Mining Residue

The concentration of K-40, Ra-226 and Th-232 in the manganese mining residue determined in $Bq \cdot kg^{-1}$ as 607±34, 52±6 and 40±5, respectively. The concentrations of K-40 and Ra-226 with the exception of Th-232 were higher than the world average mean radionuclide concentration of soils reported in UNSCEAR 2008 Annex B (Ra-226: 32 $Bq \cdot kg^{-1}$, Th-232: 45 $Bq \cdot kg^{-1}$ and K-40: 412 $Bq \cdot kg^{-1}$) and Radiation Protection 112, 1999 (Ra-226: 40 $Bq \cdot kg^{-1}$, Th-232: 40 $Bq \cdot kg^{-1}$ and K-40: $Bq \cdot kg^{-1}$). Based on the radioactivity of K-40, Ra-226 and Th-232, the radioactivity index of manganese clay using European Basic Safety Standard (EU-BSS) was calculated (to be under 1) and the result could be stated that manganese ore mining residue can be used as building material.

The morphological attributes of the clay are related to the firing temperature except for pore volume. Increasing the firing temperature resulted in gradual decreases of the specific surface area and density decreased except at 550 °C; The effects of firing on the samples in terms of different temperatures are shown in Figure 44.

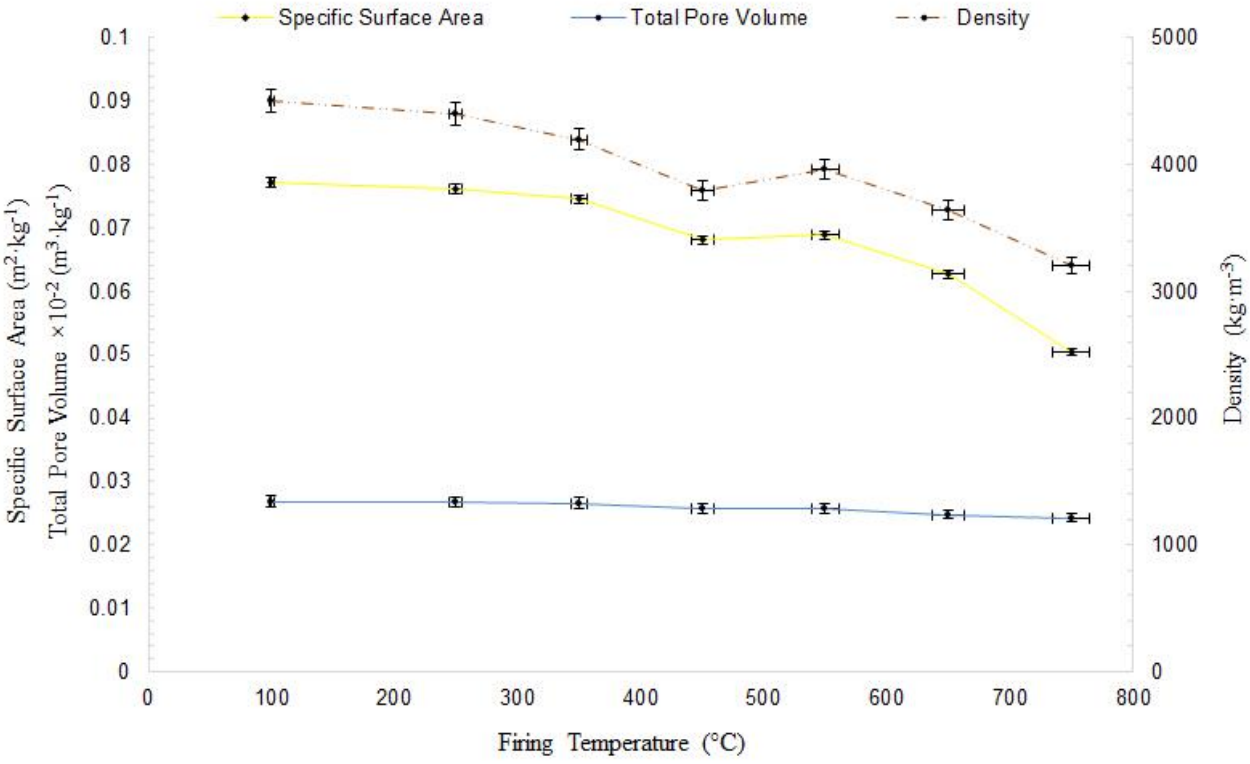

Figure 44- Morphological attributes as a function of firing temperature

A significant difference among firing temperatures observed for Rn-222 exhalation and emanation and temperature (Table 27.).

Table 27- Radon exhalation and emanation in terms of firing temperatures

Temperature (°C)	**100**	**250**	**350**	**450**	**550**	**650**	**750**
Massic exhalation ($Bq \cdot kg^{-1} \cdot h^{-1}$)	76	67	74	30	51	46	3
Emanation factor	0.25	0.22	0.24	0.11	0.17	0.16	0.01

The relationship between cumulative pore volume, radon exhalation and the emanation factor are shown in Figure 45.

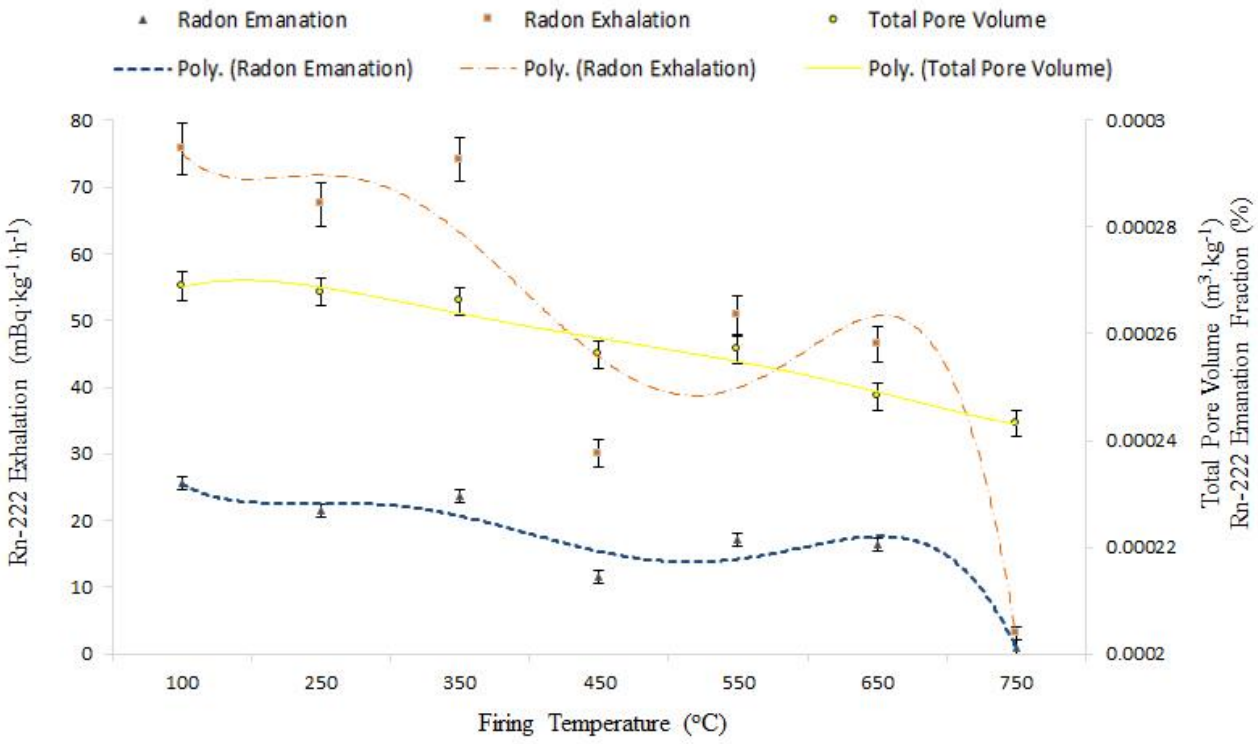

Figure 45- Plot of cumulative pore volume and radon exhalation and emanation

Figure 46. shows Cumulative pore volume distribution of fired manganese clay. The obtained results clearly proved that in the case of high temperature range the pore size

distribution significantly shifted towards bigger pore diameter compared with at low temperatures. The density, specific surface area and total pore volumes decreased as heat treatment temperature increased. The massic radon exhalation reduced by 97% from 75.7 to 2.4 $mBq \cdot kg^{-1} \cdot h^{-1}$.

As a result, it can be stated that low radon emanation and exhalation at high temperatures can be caused by the modified porosity features. Furthermore, it can be concluded that by firing, the radon emanation and exhalation features can be significantly reduced, which can ensure safer building material production from manganese clay in terms of a radiological point of view.

It can be stated that reusing manganese mine residue clay in the building and ceramic industries can be considered without any pre-treatment because of: 1) Following EU-BSS, the radioactivity index of manganese mine residue estimated to be under 1; 2) Usually the range of then the range of firing temperatures are between 700 and 1100 $^{\circ}C$, and based on obtained data, the high temperature treatment (above 750 $^{\circ}C$) has a beneficial effect on the internal structure of the clay, which is favourable from building material production point.

On the basis of presented results, the possibility of the application of manganese clay as additive material is considerable, which justifies further experiments of their clay-based mixtures focusing on mechanical and radiological properties.

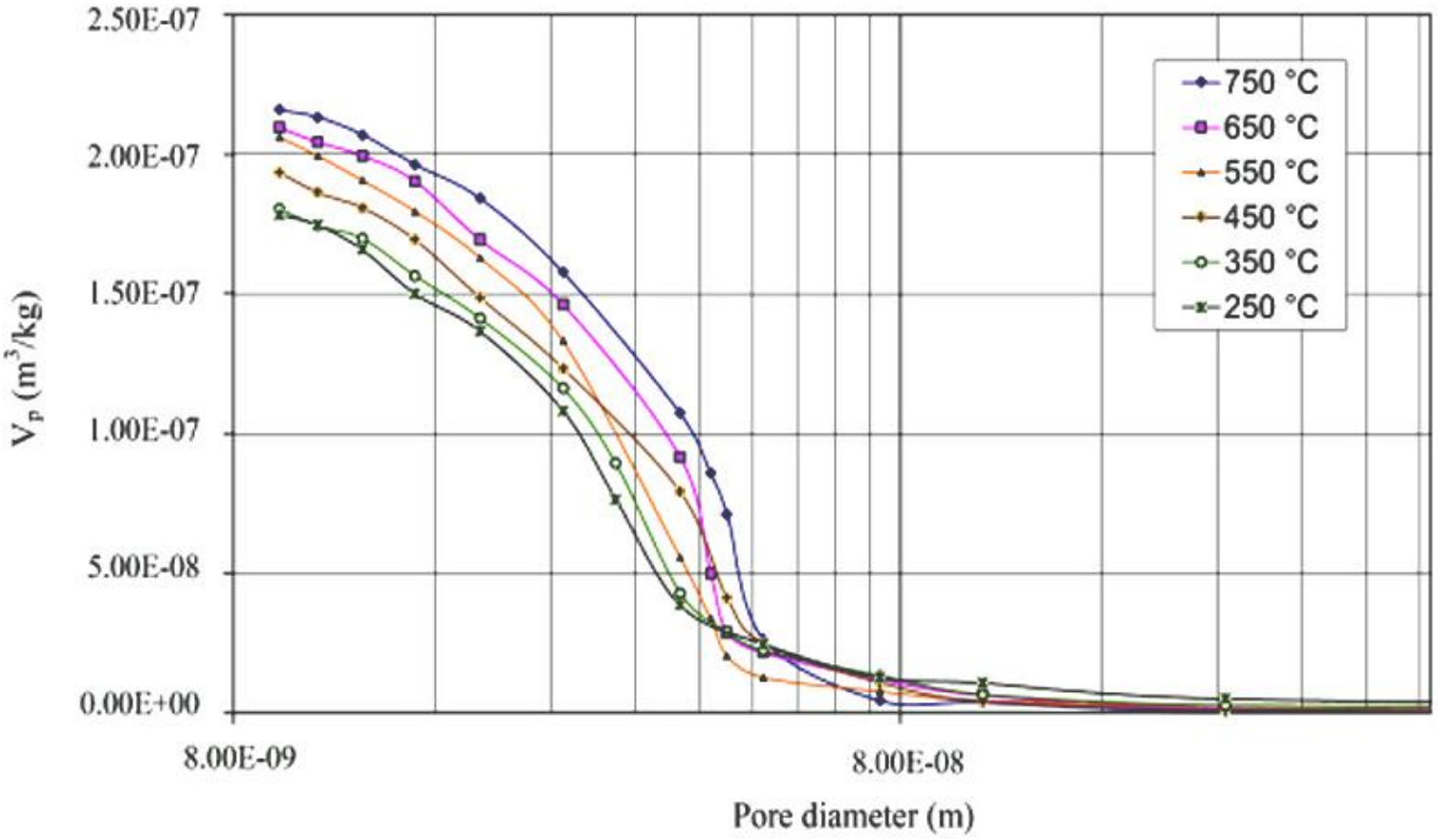

Figure 46- Cumulative pore volume distribution of fired manganese clay

SUMMARY

The recent changes, in regulation based on the EU-BSS and the ICRP dose conversion coefficient recommendations, make the revaluation of many previously compliant work-places necessary; Therefore, it made the candidate to selected current thesis topic, finding the effects of the difference between the actual and recommended parameters on dose estimation. The author conducted a long-term comprehensive radioecology survey in an underground mine (Úrkút manganese mine) in Hungary to identify the potential routes of radon exhalation and its measurement in the mine to control the radiation levels within safe limits and protect miners from radiation hazards. A long-term radon monitoring was conducted using CR-39 based NRPB detector, AlphaGUARD PQ2000 and TESLA TSR2 in mainly active locations of the mine. A two and half years measurement carried out using RAD7 and RAD H2O for drain water samples from 8 sampling point to estimate the contribution of the dissolved radon in water to the radon concentration in the mine air. In-situ radon exhalation measurement from mine walls using accumulation chamber based on CR-39 was used in 5 locations in mine galleries; In addition, a total of 36 rock samples from 6 different most abundant rock types were conducted for ex-situ radon exhalation with concerning the activity concentration of natural radioactive materials using a HPGe gamma spectrometry. The author applied a developed mitigation system to test the performance on radon reduction. The attached and unattached radon progenies and also the radon equilibrium factor was measured using SARAD EQF3220 and Pylon WLx. To complete dose assessment, 10 miners (all male, with an average age of 44 years old, with recording working hours) were monitored for radon exposure using a CR-39 based personal dosimetry for one year. Using author obtained data from field measurement the dose conversion factor and following that the effective dose from radon inhalation were estimated and compare with the values calculate using ICRP recommended parameters. Following EU-BSS, the manganese mining residue (mud) were investigated to confirm the ability of reusing in the building material industries.

The annual integrated averages radon concentration in whole mine area was measured 824±42 $Bq \cdot m^{-3}$, 874±45 $Bq \cdot m^{-3}$ and 1050±85 $Bq \cdot m^{-3}$ for years 2014, 2015 and 2016, respectively. The differences between the three consecutive years were just some percent; The three-years averages radon concentration was measured as 916±54 $Bq \cdot m^{-3}$. Seasonal variations observed as: highest radon concentrations during the summer, the lowest

radon concentration during the winter, during the spring and the autumn intermediate but higher in autumn than in spring. Radon concentration in the mine area during working hours was measured between 450±65 and 650±83 $Bq \cdot m^{-3}$. It has been found that the dissolved radon concentration in mine water varies in the range of 0.2±0.1 to 5.5±0.7 $Bq \cdot L^{-1}$. The geometric mean of dissolved radon concentration in the mine water was determined around 3±0.4 $Bq \cdot L^{-1}$; The contribution of exhalation of radon from water to the mine air was estimated in the worst case scenario, as 7 $mBq \cdot s^{-1} \cdot m^{-3}$, that regarding to the low contact surface and forced ventilation capacity this value is negligible. The radon exhalation from mine wall was measured in the range of 0.7±0.1 $mBq \cdot s^{-1} \cdot m^{-2}$ and 1.5±0.2 $mBq \cdot s^{-1} \cdot m^{-2}$, with an average of 1.1±0.1 $mBq \cdot s^{-1} \cdot m^{-2}$. Underlayer black shale shows the highest concentration of Ra-226 and Th-232 among the other samples with an average of 16±4 and 19±5 $Bq \cdot kg^{-1}$, respectively. Additionally, the underlayer black shale, black shale and carbonate ore determined to content higher concentration of Ra-226 compared to other samples. After several attempts finding the main route of entry of the radon to the mine atmosphere, it was found that, the ore, fragmented during the course of mining operations, provides a source of higher radon exhalation due to the increased exposed surface area; Exactly after mining activity the released radon from same the wall with fresh broken wall increase dramatically with an average of about 5900±420 $Bq \cdot m^{-3}$. Therefore, by identifying the main route of radon in to the mine's air, using optimized mitigation system could successfully reduce the radon concentration to below 300 $Bq \cdot m^{-3}$ with an average of 250 $Bq \cdot m^{-3}$. During working hours, the annual average of unattached factor in the three workplaces, where the selected miners for personal dosimetry were mainly worked (it was difficult to monitor all miner workplaces as they were active, and it could happen some miners change workplace for some days), was measured and calculated between 0.15±0.04, 0.3±0.05 (with an average of 0.21±0.04). Using the f_{un} and the EEC values measured by Pylon WLx, the average equilibrium factor calculated to be varied between 0.35±0.1 and 0.55±0.2 depending on location with the average of 0.42±0.13 in the whole representative measurement locations during working hours. Following the dose assessment, the annual exposures of miners to the radon was measured between 247±31 and 277±36 $Bq \cdot m^{-3}$ with an average of 261±33 $Bq \cdot m^{-3}$; Then, the author calculated the dose conversion factor, based on realistic data obtained from this study, between 16±9 and 25±10 $mSv \cdot WLM^{-1}$ with the average of 20±9 $mSv \cdot WLM^{-1}$; The dose conversion factor increased 1.5 times greater when unattached fraction value changed from 0.15 to 0.3. Even the average dose conversion factor of three locations is at least 2 times greater than the ICRP recommended value 10 $mSv \cdot WLM^{-1}$. The

effective dose, which estimated based on DCF, found: (A) In case of using ICRP modelling equation, in the range of 5.6±0.7 $mSv \cdot y^{-1}$ and 7.5±0.9 $mSv \cdot y^{-1}$ (with a geometric mean of 6.7±0.9 $mSv \cdot y^{-1}$); (B) Between 5.6±0.9 and 7.6±0.9 $mSv \cdot y^{-1}$ (with a geometric mean of 7±0.8 $mSv \cdot y^{-1}$) in case of using EPA modelling equation. The radioactivity index of manganese mine residue estimated to be under 1 and it found that the high temperature firing (above 750 $^{\circ}C$) has a beneficial effect on the internal structure of the clay resulting a huge reduction on radon exhalation. Therefore, according to these results, the author found that from radioecology point of view, reusing the manganese mining residue without any pre-treatment can be considered in the building material industries which is favourable from building material production point.

BIBLIOGRAPH

Anjos, R. M. et al., 2010. Occupational exposure to radon and natural gamma radiation in the La Carolina, a former gold mine in San Luis Province, Argentina. *Journal of Environmental Radioactivity,* 101(2), pp. 153-158.

Australian Uranium Association and Australia. Department of Resources, Energy and Tourism, 2009. *Radiation Workers' Handbook. Radiation Control in the Mining & Mineral Processing Industry.* Melbourne and Canberra: Melbourne and Canberra : Australian Uranium Association and Dept. of Resources, Energy and Tourism.

Axelsson, G., Andersson, E. M. & Barregard, L., 2015. Lung cancer risk from radon exposure in dwellings in Sweden: how many cases can be prevented if radon levels are lowered?. *Cancer Causes Control,* 26(4), pp. 541-547.

Barton, T. P. & Ziemer, P. L., 1986. The effects of particle size and moisture content on the emanation of Rn from coal ash. *Health Physics,* 50(5), pp. 581-588.

Baskaran, M., 2016. Chapter 2: Radon Measurement Techniques. In: *Radon: A Tracer for Geological, Geophysical and Geochemical Studies.* 1st ed. s.l.:Springer International Publishing, pp. 15-35.

Bátor, G. et al., 2015. A comparison of a track shape analysis-based automated slide scanner system with traditional methods. *Journal of Radioanalytical and Nuclear Chemistry,* 306(1), pp. 333-339.

BEIR, 1999. *Biological Effects of Ionizing Radiation IV Report. Health risks of radon and other internally deposited Alpha-emitters.* Washington D.C.: National Academy Press.

Bing, S., 1993. CR-39 RADON DETECTOR. *Nuclear Tracks and Radiation Measurements,* 22(1-4), pp. 451-454.

Bíró, L. et al., 2015. Terrestrial radioisotopes as paleoenvironmental proxies in sedimentary formations. *Journal of Radioanalytical and Nuclear Chemistry*, 306(1), pp. 289-293.

Council National Research, 1999. *Health Effects of Exposure to Radon: BEIR VI.* Washington, DC: The National Academies Press.

Council of the European Union, 2014. Council Directive 2013/59/Euratom of 5 December 2013 laying down basic safety standards for protection against the dangers arising from exposure to ionising radiation, and repealing Directives 89/618/Euratom, 90/641/Euratom, 96/29/Euratom, 97/43/Euratom. *Official Journal of the European Union,* 57(L 13), pp. 1-73.

Darby, S. C. et al., 1995. Radon and cancers other than lung cancer in underground miners: a collaborative analysis of 11 studies. *Journal of the National Cancer Institute,* 87(5), pp. 378-384.

Darby, S. et al., 2005. Radon in homes and risk of lung cancer: collaborative analysis of individual data from 13 European case-control studies.. *BMJ,* 330(7485), p. 223.

Darby, S. et al., 2006. Residential radon and lung cancer--detailed results of a collaborative analysis of individual data on 7148 persons with lung cancer and 14,208 persons without lung cancer from 13 epidemiologic studies in Europe. *Scandinavian Journal of Work, Environment & Health,* 32(1), pp. 1-83.

De Simone, G., Lucchetti, C., Galli, G. & Tuccimei, P., 2016. Correcting for H2O interference using a RAD7 electrostatic collection-based silicon detector. *J. Environ. Radioact.,* Volume 162-163, pp. 146-153.

Duggan, M. J., Howell, D. M. & Soilleux, P. J., 1968. Concentration of radon-222 in coal mines in England and Scotland. *Nature,* Volume 219, p. 1149.

DURRIDGE Company Inc., 2018. *BIG BOTTLE SYSTEM - High Sensitivity Radon in Water Accessory for the RAD7 With Aerator Cap Revision C: User Manual.* [Online] Available at: https://bit.ly/2JhSSut

DURRIDGE Company Inc., n.d. *Pylon Radioactive Sources.* [Online] Available at: www.bit.do/2000a

Editorials, 1932. Primary carcinoma of the lung in the miners of joachimstal. *Annals of Internal Medicine,* 6(4), pp. 585-586.

El-Sersy, A., Mansy, M. & Hussein, A., 2004. Effect of environmental conditions on radon concentration-track density calibration factor of solid-state nuclear track detectors. *Pramana,* 62(4), pp. 861-867.

EPA, 2016. *A Citizen's Guide to Radon: The Guide to Protecting Yourself and Your Family from Radon,*. Revised 2016 ed. Washington, D.C.: U.S. Environmental Protection Agency.

Ghiassi-Nejad, M., Beitollahi, M. M., Fathabadi, N. & Nasiree, P., 2002. EXPOSURE TO 222Rn IN TEN UNDERGROUND MINES IN IRAN. *Radiation Protection Dosimetry,* 98(2), p. 223–225.

Gutiérrez, J., Mungaray, A. & Hallack, M., 2015. Reuse of Hydraulic Concrete Waste as a New Material in Construction Procedures: a Sustainable Alternative in Northwest Mexico. *Journal of Construction,* 14(2), pp. 51-57.

Harb, S., Ahmed, N. K. & Elnobi, S., 2016. Effect of grain size on the radon exhalation rate and emanation coefficient of soil, phosphate and building material samples. *Journal of Nuclear and Particle Physics,* 6(4), pp. 80-87.

Harley, N. H. & Robbins, E. S., 2009. Radon and leukemia in the Danish study: another source of dose. *Health Physics,* 97(4), pp. 343-347.

Hewson, G. S. & Ralph, M. I., 1994. An investigation into radiation exposures in underground non-uranium mines in Western Australia. *Journal of Radiological Protection,* 14(4), pp. 359-370.

Hodolli, G. et al., 2015. Radon concentration and gamma exposure in some Kosovo underground mines. *International Journal of Radiation Research,* 13(4), pp. 369-372.

Homer, J. B. & Miles, J. C. H., 1986. The effects of heat and humidity before, during and after exposure on the response of PADC (CR-39) to alpha particles. *Nuclear Tracks and Radiation Measurements,* 12(1-6), pp. 133-136.

IAEA, 2007. *Update of X Ray and Gamma Ray Decay Data Standards for Detector Calibration and Other Application: Data Selection, Assessment and Evaluation Procedures.* Vienna: International Atomic Energy Agency.

ICRP, 1994. Human Respiratory Tract Model for Radiological Protection: ICRP Publication 66. *Ann. ICRP,* 24(1-3).

ICRP, 2007. ICRP Publication 103: The 2007 recommendations of the international commission on radiological protection. *Annals of the ICRP,* 37(2-4).

ICRP, 2010. ICRP Publication 115: Lung Cancer Risk from Radon and Progeny. *Annals of the ICRP,* 40(1), pp. 1-64.

ICRP, 2017. Occupational intakes of radionuclides: Part 3. ICRP Publication 137. *Annals of the ICRP,* 46(3/4).

International Atomic Energy Agency, 2004. *Radiation, people and the environment.* Vienna: IAEA.

International Atomic Energy Agency, 2014. *Radiation protection and safety of radiation sources : international basic safety.* Vienna: IAEA.

International Atomic Energy Agency, 2014. *Radiation protection and safety of radiation sources : international basic safety,* Vienna: IAEA.

Jobbágy, V. et al., 2017. A brief overview on radon measurements in drinking water. *Journal of Environmental Radioactivity,* Volume 173, pp. 18-24.

Kávási, N. et al., 2014. In situ comparison of passive radon-thoron discriminative monitors at subsurface workplaces in Hungary. *Review of Scientific Instruments,* 85(022002).

Kávási, N. et al., 2009. Difficulties in the dose estimate of workers originated from radon and radon progeny in a manganese mine. *Radiation Measurements,* 44(3), pp. 300-305.

Kávási, N. et al., 2011. Dose estimation and radon action level problems due to nanosize radon progeny. *Journal of Environmental Radioactivity,* 102(9), pp. 806-812.

Kávási, N. et al., 2012. *Natural radioactivity of manganese clay in Hungary.* Veszprém, Pannon Egyetemi Kiadó, pp. 135-138.

Kávási, N. et al., 2010. Effective dose of miners due to natural radioactivity in a manganese mine in Hungary. *Radiation Protection Dosimetry,* 141(4), pp. 432-435.

Khan, A. H., 1979. A study on the factors affecting the build-up of radon-222 and its progeny in uranium mines. In: *M.Sc. Thesis.* Mumbai, India: University of Bombay.

Korpás, L. et al., 1999. Evaluation of the prospected areas and formatations. *Geologica Hungarica Series Geologica,* Volume Tomus 24, pp. 197-293.

Kovács, T. et al., 2017. Radon exhalation study of manganese clay residue and usability in brick production. *Journal of Environmental Radioactivity,* Volume 168, pp. 15-20.

Kreuzer, M. et al., 2010. Radon and risk of death from cancer and cardiovascular diseases in the German uranium miners cohort study: follow-up 1946-2003. *Radiation and Environmental Biophysics,* 49(2), pp. 177-185.

Krewski, D. et al., 2005. Residential radon and risk of lung cancer: a combined analysis of 7 North American case-control studies. *Epidemiology,* 16(2), pp. 137-145.

Krewski, D. et al., 2006. A combined analysis of North American case-control studies of residential radon and lung cancer. *Journal of Toxicology and Environmental Health,* 69(7), pp. 533-597.

Lecomte, J.-F.et al., 2014. ICRP Publication 126: Radiological protection against radon exposure. *Annals of the ICRP,* 43(3).

Leenhouts, H. P., 1998. Radon-induced lung cancer in smokers and non-smokers: risk implications using a two-mutation carcinogenesis model. *Radiation and Environmental Biophysics,* 38(1), pp. 57-71.

Li, X., 2008. Recycling and reuse of waste concrete in China: Part I. Material behaviour of recycled aggregate concrete. *Resources, Conservation and Recycling,* 53(1-2), pp. 36-44.

Lubin, J. H. et al., 1995. Lung cancer in radon-exposed miners and estimation of risk from indoor exposure. *Journal of the National Cancer Institute,* 7(87), pp. 817-827.

Mansy, A. et al., 2000. *Calibration of radon monitors and its associated uncertainties in NIS Egypt radon calibration chamber.* Cairo, Cairo University, pp. 569-575.

Marsh, J. W., Laurier, D. & Tirmarche, M., 2017. Radon dosimetry for workers: ICRP's approach. *Radiation Protection Dosimetry,* 177(4), pp. 466-474.

Masahiro, H. et al., 2007. Effect of soil moisture content on radon and thoron exhalation. *Journal of Nuclear Science and Technology,* 44(4), pp. 664-672.

Mattsson, S. & Söderberg, M., 2013. Chapter 2 - Dose Quantities and Units for Radiation Protection. In: S. Mattsson & C. Hoeschen, eds. *Radiation Protection in Nuclear Medicine.* s.l.:Springer-Verlag Berlin Heidelberg, pp. 7-18.

Moreno, V., Baixeras, C. & Font, L. I., 2013. Experimental study on the effect of high humidity environments on the response of long-term exposed nuclear track detectors. *Radiation Measurements,* Volume 50, pp. 207-211.

Műllerová, M. et al., 2016. Indoor radon activity concentration in thermal spas: the comparison of three types of passive radon detectors. *Journal of Radioanalytical and Nuclear Chemistry,* 310(3), pp. 1077-1084.

Műllerová, M. et al., 2016. Preliminary results of radon survey in thermal spas in V4 countries. *NUKLEONIKA,* 61(3), pp. 303-306.

Müller, W. et al., 2016. Current knowledge on radon risk: implications for practical radiation protection? radon workshop, 1/2 December 2015, Bonn, BMUB (Bundesministerium für

Umwelt, Naturschutz, Bau und Reaktorsicherheit; Federal Ministry for the Environment, Nature Conservatio. *Radiation and Environmental Biophysics*, 55(3), pp. 267-280.

National Research Council, 1999. *Evaluation of Guidelines for Exposures to Technologically Enhanced Naturally Occurring Radioactive Materials.* Washington, DC: The National Academies Press.

Nazaroff, W. W., 1992. Radon transport from soil to air. *Reviews of Geophysics,* 30(2), pp. 137-160.

Nazaroff, W. W., Moed, B. A. & Sextro, R. G., 1998. Soil as a source of indoor radon: generation, migration, and entry. In: W. W. Nazaroff & A. V. Nero, eds. *Radon and its decay products in indoor air.* NewYork: John Wiley & Sons, Inc., pp. 57-112.

Nobuyuki , H. & Yuki, F., 2014. Classification of radiation effects for dose limitation purposes: history,current situation and future prospects. *Journal of Radiation Research,* Volume 55, pp. 629-640.

Orabi, M., 2017a. Estimation of the radon surface exhalation rate from a wall as related to that from its building material sample. *Canadian Journal of Physics,* 96(3), pp. 353-357.

Orabi, M., 2017b. Radon Release and Its Simulated Effect on Radiation Doses. *Health Physics,* 12(3), pp. 294-299.

Polgári, M., 1993. *Manganese Geochemistry Reflected by Black Shale Formation and Diagenetic Processes: Model of Formation of the Carbonatic Manganese Ore of Úrkút.* Ushgorod: Karpati Publish House.

Polgári, M. et al., 2013. Celadonite and smectite formation in the Úrkút Mn-carbonate ore. *Sedimentary Geology,* Volume 294, pp. 157-163.

Polgári, M., Szabó-Drubina, M. & Szabó, Z., 2004. Theoretical model for Jurassic manganese mineralization in Central Europe, Úrkút, Hungary. *Bulletin of Geosciences,* 79(1), pp. 53-61.

Porstendörfer, J., 1996. Radon: measurement related to dose. *Environment International,* 22(1), pp. 563-583.

PYLON, 2018 . *Radiation monitors - model WLx Portable Working Level Radiation Monitor,* Ottawa: PYLON ELECTRONICS INC..

Qureshi, A. A. et al., 2000. Radon concentrations in coal mines of Baluchistan, Pakistan. *Journal of Environmental Radioactivity,* 48(2), pp. 203-209.

Rabi, R. & Oufni, L., 2018. Evaluation of indoor radon equilibrium factor using CFD modeling and resulting annual effective dose. *Radiation Physics and Chemistry,* Volume 145, pp. 213-221.

Ramola, R. C. et al., 2016. Dose estimation derived from the exposure to radon, thoron and their progeny in the indoor environment. *Scientific Reports,* Volume 6.

Rao, V. K. et al., 2001. Airborne radon and its progeny levels in the coal mines of Godavarikhani, Andhra Pradesh, India. *JOURNAL OF RADIOLOGICAL PROTECTION,* Volume 21, pp. 259-268.

Reddy, N. K. & Bhutani, M. S., 2009. Racial disparities in pancreatic cancer and radon exposure: a correlation study. *Pancreas,* 38(4), pp. 391-395.

Řeřicha, V. et al., 2006. Incidence of leukemia, lymphoma, and multiple myeloma in czech uranium miners: a case–cohort study. *Environ Health Perspect,* 114(6), pp. 818-822.

Roessler, F., Buerkin, W. & Villert, J., 2016. *AlphaGUARD, the new reference for continuous radon monitoring in air, soil, gas, water and material*. Germany, Radiation protection for humans and environment 50 years competence in the professional association, p. 468.

Ruzer, L. S., 2011. Exposure and Dose: Health Effect Studies Associated with Nanometer Aerosols. *Journal of Nanomedicine and Nanotechnology,* 2(7), pp. 2-9.

Saccomanno, G. et al., 1996. A comparison between the localization of lung tumors in uranium miners and in nonminers from 1947 to 1991. *Cancer.,* 77(7), pp. 1278-1283.

Sakoda, A., Ishimori, Y. & Yamaoka, K., 2011. A comprehensive review of radon emanation measurements for mineral, rock, soil, mill tailing and fly ash. *Applied Radiation and Isotopes,* Volume 69, pp. 1422-1435.

Saphymo, 2016. *lphaGUARD: professional Radon monitor from Saphymo.* [Online] Available at: http://bit.do/alphaguard

SARAD GmbH, 2013. *EQF3220 - SARAD Radon Thoron Gas Monitoring.* [Online] Available at: www.bit.do/eqf3220

SARAD GmbH, 2016. *Manual RTM2200 - RPM2200 - EQF3200 - EQF3220 - A²M4000.* [Online]
Available at: https://bit.ly/2xNWjaJ

Sas, Z., Somlai, J., Szeiler, G. & Kovacs, T., 2015a. Usability of clay mixed red mud in Hungarian building material production industry. *Journal of Radioanalytical and Nuclear Chemistry,* Volume 306, pp. 271-275.

Sas, Z. et al., 2015b. Influencing effect of heat-treatment on radon emanation and exhalation characteristic of red mud. *Journal of Environmental Radioactivity,* Volume 148, pp. 27-32.

Schroeder, G. L. & Evans, R. D., 1969. Some basic concepts in uranium mine ventilation. *AIME Transactions,* 244(301-307).

Schumann, R. R. & Gundersen, L. C., 1996. Geologic and climatic controls on the radon emanation coefficient. *Environment International,* 22(1), pp. 439-446.

Seil, G. E. & Heiligman, H. A., 1928. Use of Manganese in the manufacture of face brick. *Journal of the American Ceramic Society,* Volume 11, pp. 241-248.

Sethi, T. K., El-Ghamry, M. N. & Kloecker, G. H., 2012. Radon and lung cancer. *Clinical Advances in Hematology & Oncology,* 10(3), pp. 157-164.

Shahrokhi, A., Burghele, B. D., Fábián, F. & Kovács, T., 2015. New study on the correlation between carbon dioxide concentration in the environment and radon monitor devices. *Journal of Environmental Radioactivity,* Volume 150, pp. 57-61.

Shahrokhi, A. et al., 2016. Distribution of indoor radon concentrations between selected Hungarian thermal baths. *Nukleonika,* 61(3), pp. 333-336.

Shahrokhi, A. et al., 2017. Radon measurements and dose estimate of workers in a manganese ore mine. *Applied Radiation and Isotopes,* Volume 127, pp. 32-37.

Smith, B. J., Zhang, L. & Field, W. R., 2007. Iowa radon leukaemia study: a hierarchical population risk model for spatially correlated exposure measured with error. *Statistics in Medicine,* 26(25), pp. 4619-4642.

Somlai, J. et al., 2008. Radiological aspects of the usability of red mud as building material additive. *Journal of Hazardous Materials,* 150(3), pp. 541-545.

Somlai, J. et al., 2006. Radiation dose from coal slag used as building material in the Transdanubian region of Hungary. *Radiation Protection Dosimetry,* Volume 118, pp. 82-87.

Somlai, J., Németh, C., Lendvai, Z. & Bodnár, R., 1997. Dose contribution from school buildings containing coal slag insulation with elevated concentrations of natural radionuclides. *Journal of Radioanalytical and Nuclear Chemistry,* Volume 218, pp. 1-63.

Szabó, Z., Grasselly, G. & Cseh Németh, J., 1981. Some conceptual questions regarding the origin of manganese in the Úrkút deposit, Hungary. *Chemical Geology,* Volume 34, pp. 19-29.

TESLA, 2016. *TSR2 Wireless Radon Probe: Technical Specifications & Operation Manual,* Prague: TESLA.

Tirmarche, M. et al., 2010. ICRP publication 115: Lung cancer risk from radon and progeny and statement on radon. *Annals of the ICRP,* 40(1).

Tirmarche, M. et al., 2012. Risk of lung cancer from radon exposure: contribution of recently published studies of uranium miners.. *Annals of the ICRP,* 41(3-4), pp. 368-377.

Tomásek, L. et al., 1994. Patterns of lung cancer mortality among uranium miners in West Bohemia with varying rates of exposure to radon and its progeny. *Radiation Research,* 137(2), pp. 251-261.

U.S. Environmental Protection Agency, 1993. *Protocols for radon and radon decay produc measurements in homes: EPA402-R-92-003.* [Online] Available at: https://bit.ly/2HoXhdg

U.S. Environmental Protection Agency, 2003. *EPA assessment of risks from radon in homes.* Washington, DC: U.S. EPA.

UNSCEAR, 2010. *Sources and effects of ionizing radiation: UNSCEAR 2008 report to the general assembly with scientific annexes.* New York: United Nations.

UNSCEAR, 2012. *Biological mechanisms of radiation actions at low doses*, New York: United Nations.

Vanmarcke, H., Janssens, A. & Raes, F., 1985. The equilibrium of attached and unattached radon daughters in the domestic environment. *Science of the Total Environment*, Volume 45, pp. 251-260.

Várhegyi, A., Somlai, J. & Sas, Z., 2012. RADON MIGRATION MODEL FOR COVERING U MINE AND ORE PROCESSING TAILINGS. *Romanian Journal of Physics*, Volume 58, pp. 298-310.

Vigh, T. et al., 2013. Terrestrial radioisotopes in black shale hosted Mn-carbonate deposit (Úrkút, Hungary). *Acta Geophysica*, 61(4), pp. 831-847.

Weigel, F., 1978. Radon. *Chemiker Zeitung*, 102(9), pp. 287-299.

WHO, 2009. *WHO handbook on indoor radon: a public health perspective.* Geneva: WHO.

Yener, G. & Küçüktas, E., 1998. Concentrations of radon and decay products in various underground mines in western Turkey and total effective dose equivalents. *Analyst*, Volume 123, pp. 31-34.

Yonggang, H., Peng, X., Chunlin, Z. & Feng, Y., 2009. Effect of environment humidity to radon measurement with SSNTD. *Nuclear Science and Techniques*, 20(4), pp. 228-230.

THESES

(1) The recent changes in the European Basic Safety Standard, introducing a new reference level of radon concentration (300 $Bq \cdot m^{-3}$), makes the author to carry out a new comprehensive radiological survey to identify the potential route of entry radon to the mine air in the Úrkút manganese mine where radon concentration exceeded the EU-BSS reference level.

i. Monthly measurements conducted monitoring radon concentration in the mine water samples from 8 sampling point for two and half years. The dissolved radon concentration in water samples varied between 0.2±0.1 and 5.5±0.7 $Bq \cdot L^{-1}$. The contribution of the released radon from water to the mine air estimated in the worst-case scenario, as 7 $mBq \cdot s^{-1} \cdot m^{-3}$, therefore, taking into the consideration of the other parameters (contact surface, water amount and ventilation capacity) this flux is negligible, and it cannot be the main route of entry radon.

ii. The surface radon exhalation from the wall in the 5 mostly active mining areas measured in the range of 0.7±0.1 and 1.5±0.2 $mBq \cdot s^{-1} \cdot m^{-2}$. While by paying attention to the performance of the mine ventilation in connection with the surface area of the active workplaces, this could not be the main source causing high radon concentration in the mine atmosphere.

iii. Additionally, a total of 36 samples from the 6 most abundant different rocks examined for gamma spectrometry and ex-situ radon exhalation to find out the contribution of the mullock and ore rocks in radon exhalation. The author found that the mullock rocks, the geological structure of the mine walls, contained a small amount of Ra-226 (underlayer limestone: 4 $Bq \cdot kg^{-1}$, dogger limestone: 2 $Bq \cdot kg^{-1}$, Puce greenish marl: 4 $Bq \cdot kg^{-1}$); however, black shale, underlayer black shale and carbonate ore, extracted as the manganese ores, showed the highest concentration of Ra-226 (12, 16 and 16 $Bq \cdot kg^{-1}$, respectively) and the highest areal radon exhalation (the average areal exhalation at 15 cm thickness sample: 1.5, 1.6 and 1.2 $mBq \cdot s^{-1} \cdot m^{-2}$, respectively).

iv. The author found that the ore, fragmented during the course of mining operations, provided a source of higher radon exhalation due to the increased exposed surface area. Exactly after mining activity the radon concentration near the freshly broken wall increased dramatically (average 6 $kBq \cdot m^{-3}$). According to author's results, it was indicated that the main source of radon in the mine can be the freshly broken wall.

(2) After identifying the potential route of entry radon to the mine air, an effective developed mitigation system used to fulfil the European Basic Safety Standard requirement; New developed mobile mitigation system was introduced using a mobile tube connected to the enforced ventilation to adjust the mitigation as close as possible to the wall of new galleries. The author using the new mitigation reduced the radon concentration to below 300 $Bq \cdot m^{-3}$ with an average of 250±41 $Bq \cdot m^{-3}$.

(3) Long-term personal dosimetry conducted to find out: first, if this reduction could address the concerns in dosimetry point of view; second, the effects of the difference between the actual and recommended parameters (equilibrium factor and dose conversion factor) on dose estimation. However the radon concentration in the mine air reduced to below 300 $Bq \cdot m^{-3}$, applying the calculated dose conversion factors based on the field measurements (average of 20 $mSv \cdot WLM^{-1}$) result higher effective dose (with an average of 7 $mSv \cdot y^{-1}$, at least two times greater) compared to the ICRP estimation (with an average of 3 $mSv \cdot y^{-1}$). Therefore, expressing the limits of radon concentration in $Bq \cdot m^{-3}$ might not be satisfactory in point of dosimetric view.

(4) Following the EU-BSS regarding the supervision of building materials, the possibility of reusing manganese mining residue, in addition to considering the manganese mud as a source of accumulated radon in the mine, investigate by determining the radioactivity index and radon exhalation in terms of surface area and total pore volumes. Considering the calculated radioactivity index ($I<1$) and measuring radon exhalation, it concluded that these residues not cause any radiation risk and in point of radioecological view, manganese mining residue can be reused in brick and ceramic productions.

TÉZISPONTOK

(1) Az Európai Uniós irányelvben a radon koncentrációra bevezetett új vonatkoztatási szint (300 $Bq \cdot m^{-3}$) miatt egy átfogó radiológiai felmérést végeztem el az úrkúti mangánbányában, ahol korábbi mérések alapján a radonkoncentráció meghaladta az irányelvben megadott szintet. A felmérés célja az volt, hogy meghatározzam a bányában lévő radon származási helyét.

i. A felmérés keretén belül havonta 8 pontról gyűjtöttem bányavíz mintákat és meghatároztam a radon aktivitáskoncentrációját, ami 0,2±0,1 és 5,5±0,7 $Bq \cdot L^{-1}$ között változott. A vízből a levegőbe kiáramló radon – konzervatív becslés alapján – legfeljebb 7 $mBq \cdot s^{-1} \cdot m^{-3}$. Figyelembe véve a többi paramétert (érintkezési felület, bányavíz mennyiség, szállított levegő mennyiség) a bányavíz légköri radon szint hozzájárulása elhanyagolható.

ii. Meghatároztam a felületi radon exhaláció értékét 5 olyan területen, ahol bányászati tevékenység folyik. A kapott eredmények 0,7±0,1 $mBq \cdot s^{-1} \cdot m^{-2}$ és 1,5±0,2 $mBq \cdot s^{-1} \cdot m^{-2}$ között változtak. Figyelembe véve a szellőzőrendszer teljesítményét, ezt a lehetőséget is elvetettem, mint a radon származási helyét.

iii. A 6 leggyakoribb kőzetből, összesen 36 mintának laboratóriumban meghatároztam a radionuklid koncentrációját és radonexhalációját. A meddőkőzet (ami a bánya geológiai struktúráját adó kőzet), csak kis mennyiségben tartalmaznak Ra-226 izotópot (fekü mészkő: 4 $Bq \cdot kg^{-1}$, dogger mészkő: 2 $Bq \cdot kg^{-1}$, vörösbarna-zöldfoltos mészmárga: 4 $Bq \cdot kg^{-1}$). A fekete pala, fekürétegi fekete pala és a karbonátos érc esetén, amelyeket mangánércként nyernek ki, kicsit magasabb volt a Ra-226 koncentráció (12, 16 és 16 $Bq \cdot kg^{-1}$) és az exhalációs értékek is magasabbak voltak (átlagosan 15 cm-es vastagságú minta: 1,5, 1,6 és 1,2 $mBq \cdot s^{-1} \cdot m^{-2}$).

iv. A mangánérc bányászata során az aprózódás miatt a kőzetek felülete, a radonemanáció, így a radon kiáramlás mértéke is megnő. A robbantásokat követően jelentősen megnövekedett radon koncentrációkat mértem (átlagosan 6 $kBq \cdot m^{-3}$). Ezek alapján igazoltam, hogy a bányában lévő radon fő származási helye a fejtés.

(2) A radon származási helyének azonosítása után a magasabb radonkoncentrációt egy mobil, az új vágatokban elhelyezhető, friss levegő befúvással sikerült az EU által javasolt 300 $Bq \cdot m^{-3}$ alá (mért értékek átlaga: 250±41 $Bq \cdot m^{-3}$) csökkenteni.

(3) Személyi radon detektorokkal végzett mérésekkel meghatároztam a munkaidő alatti átlagos radonkoncentrációt, és az ICRP által javasolt dóziskonverziós tényezővel meghatároztam a várható sugárterhelést (átlagosan 3 $mSv \cdot év^{-1}$). Ugyanakkor helyszíni mérésekkel meghatároztam a tényleges sugárterhelést lényegesen befolyásoló paramétereket (tapadt-nem tapadt frakció, egyensúlyi faktor) is. Az utóbbiak alapján számolt sugárterhelés közel kétszer nagyobb értéknek adódott (átlagosan 7 $mSv \cdot év^{-1}$). Ezek alapján kijelenthetjük, hogy ilyen és ehhez hasonló jellegű munkahelyeken nem elegendő az ICRP által javasolt, csak a radonkoncentráción alapuló korlátozás. Hosszú-távú személyi dozimetriai becslést végeztem a referenciaérték csökkentésének dozimetriai szempontból történő vizsgálatára. Ezen kívül összevetettem a mért értékek alapján számított és ajánlott paraméterek (egyensúlyi faktor, dózis konverziós tényező) alapján végzett becslés közti különbséget az ICRP legújabb javaslatát figyelembe véve. Bár a radon koncentrációt sikerült a referencia érték alá csökkenteni, az általam meghatározott dózis konverziós tényezőt (átlagosan 20 $mSv \cdot WLM^{-1}$) használva az éves effektív dózis kétszer nagyobb (átlagosan 7 $mSv \cdot év^{-1}$), mint az ICRP által ajánlott értékkel számolva (átlagosan 3 $mSv \cdot év^{-1}$). Ezzel igazoltam, hogy a radon koncentráció korlátozása $Bq \cdot m^{-3}$ egységben nem mindig kielégítő: ebben az esetben is az éves dózis mértéke meghaladja a javasolt 6 $mSv \cdot év^{-1}$ értéket**.**

(4) A bányászat során nagy mennyiségben felhalmozódott mangános agyag radionuklid koncentrációjából számolt I index ($I \leq 1$) alapján megállapítottam, hogy (az EU előírásainak megfelelően) az építőanyag gyártás során radiológiai szempontból korlátlan mennyiségben felhasználható.